2023-08-10

Physics-Guided Modeling of Acoustic Environments Using Limited Spatio-Spectro-Temporal Data

Mylan Ray Cook
Brigham Young University

Physics-Guided Modeling of Acoustic Environments

Using Limited Spatio-Spectro-Temporal Data

Mylan Ray Cook

A dissertation submitted to the faculty of
Brigham Young University
in partial fulfillment of the requirements for the degree of

Doctor of Philosophy

Kent L. Gee, Chair
Mark K. Transtrum
Shane V. Lympany
Gregory S. Macfarlane
Tracianne B. Neilsen

Department of Physics and Astronomy

Brigham Young University

ABSTRACT

Physics-Guided Modeling of Acoustic Environments
Using Limited Spatio-Spectro-Temporal Data

Mylan Ray Cook
Department of Physics and Astronomy, BYU
Doctor of Philosophy

When creating data-based models it is important to include the underlying physical characteristics and constraints of the data. If physical characteristics are not properly included in the model, results may be infeasible or physically impossible. Acoustic environments are better characterized by ensuring that models include the fundamental spatial, spectral, and temporal characteristics of noise sources, or how they change based on location, frequency, and time. When model data are limited, in availability or in reliability, additional care must be taken to ensure models predict feasible results. This dissertation focuses on physics-guided modeling of acoustic environments using limited data, taking into consideration spatial, spectral, and temporal characteristics of noise sources, specifically focused on wind noise and traffic noise.

Wind noise contamination in spectral data can be significant, even when using a windscreen. By modeling spectral characteristics of temporally varying wind noise contamination, a method for automatically detecting and reducing wind noise was developed. Reducing non-acoustic wind noise contamination allows for better characterization of outdoor acoustic environments and is useful for accurately measuring other noise sources.

Traffic noise varies spatially, spectrally, and temporally, and depends on traffic volume (the number of vehicles per unit time) and traffic class mix (e.g., the relative number of small vehicles compared to large trucks). Using the temporal variation found in reported traffic volume at thousands of locations, a model was developed to represent and predict the spatio-temporal variability of traffic volume nationwide. Further models were created to include dynamic changes in traffic class mix and to predict spectral source traffic noise. The resulting model for predicting source traffic noise is known as VROOM, the Vehicular Reduced-Order Observation-based Model.

The physics-guided modeling techniques presented in this dissertation are intended for characterizing acoustic environments, which has applications for such diverse areas as human health and wellness, bioacoustics, wildlife conservation, urban and roadway planning, land development and conservation, noise ordinance legislation, homebuying, and more.

Keywords: noise, modeling, wind noise, traffic noise, traffic modeling, physics-guided modeling

TABLE OF CONTENTS

Chapter 1

Introduction

When taking outdoor acoustic measurements, measured data can contain multiple types of noise, including non-acoustic noise signals, such as wind noise contamination, as well as acoustic noise signals, such as noise from vehicular traffic. To characterize an acoustic environment, noise signals must be understood and accounted for. Modeling these noise signals properly so as to allow for accurate noise predictions of acoustic environments requires a physics-based modeling approach.

Noise can show many types of variation. First, noise can vary spatially. This means that the noise can change from one location to another. Second, noise can vary spectrally. This means that it changes based on frequency. Third, noise can vary temporally. This means that the noise can change from one time period to another. Noise does not have to change in only one of these ways, but can change spatially, spectrally, and temporally. Measuring noise that changes in these three ways produces spatio-spectro-temporal data.

In modeling data, determinations must be made as to which mathematical methods are used to represent the underlying system. Methods with the smallest errors may not properly represent the physical processes and can ignore relationships within data. Special considerations must be taken in modeling spatio-spectro-temporal data so that data representation and predictions are physically meaningful and can accurately represent the acoustic environment, which fully data-driven models may fail to do. A physics-based modeling approach ensures that non-physical

effects are not allowed. In particular for this research, physics-based models are used to represent an acoustic environment to preserve spatial, spectral, and temporal relations of noise.

Using limited data further complicates modeling of acoustic environments. Data may be limited to relatively few locations, to a specific frequency range, to a relatively short time period, or may be limited in availability or even reliability. Data weighting methods and other signal processing techniques may be used so that limited data does not disproportionately negative impact models.

1.1 Part I: Spectro-temporal data modeling

Part I of this dissertation focuses on spectro-temporal data modeling, specifically applied to detecting and reducing wind noise in outdoor acoustic measurements. Wind noise is a non-acoustic signal caused by atmospheric conditions [1-2]. Many methods have been used to mitigate wind noise contamination, including the use of microphone windscreens, signal processing techniques involving multiple microphones, and removing data when the measured wind speed is high [3-7]. Even with a windscreen, contamination is only partially reduced. However, wind noise produces contamination with specific spectral characteristics, even though the amount of contamination can vary with time [8]. By modeling the spectral characteristics of temporally varying wind noise, a model was created to automatically detect and remove wind noise in spectral data obtained with a screened microphone so that non-acoustic wind noise contamination does not erroneously contribute to the characterization of the acoustic environment.

1.2 Part II: Spatio-temporal data modeling

Part II of this dissertation focuses spatio-temporal data modeling, specifically applied to modeling traffic volume on a national scale, which is prerequisite to characterizing traffic noise

on a national scale. Traffic volume—or the number of vehicles per time period—changes based on location and time period, with especially pronounced diurnal (day/night) patterns which can differ in urban and rural locations. Day-of-week and month-of-year patterns, along with yearly variation, are also commonly seen, and many models have been created that characterize traffic volume at particular, targeted spatial locations [9-17]. Using reported traffic counts from the Federal Highway Administration, which are limited in both amount and in reliability, a traffic volume model has been created using physically meaningful temporal traffic volume cycles which can represent and predict the spatio-temporal variation of road traffic across the continental United States. This traffic volume model is part of a larger model called VROOM, the Vehicular Reduced-Order Observation-based Model, which can predict traffic noise nationwide with hourly resolution.

1.3 Part III: Spatio-spectro-temporal data modeling

Part III of this dissertation focuses on modeling spatio-spectro-temporal data modeling, specifically applied to modeling road traffic noise on a national scale. The Federal Highway Administration uses traffic volume data in the production of the National Transportation Noise Map [18-19]. Despite road traffic noise being one of the most widespread sources of anthropogenic noise across the country, this map lacks temporal and spectral variability, and acoustic signals taken at a particular time can often differ from the average levels reported [20].

In addition to the traffic volume model, a traffic class mix model was created to predict not just total traffic volume, but traffic volume by traffic class type, which includes combination trucks, single-unit trucks, and other vehicles. The class mix model uses reported traffic volume of different traffic class types from Hallenbeck et. al. (1997) [21]. Then, a traffic noise source model was created to predict source traffic noise near roads using vehicle source emission equations from

the Federal Highway Administration's Traffic Noise Model 3.0 Technical Manual [22]. Together these three models comprise VROOM, the Vehicular Reduced-Order Observation-based Model, which is used to predict traffic noise nationwide with spatial, spectral, and temporal variability.

1.4 Additional notes on chapters and organization

This dissertation includes six papers, including conference proceedings as well as journal publications. This introduction comprises Chapter 1, and Chapter 8 contains conclusions and final remarks. The body of the dissertation is divided into three parts, which were described above, with two papers in each section. Chapters 2-7 each contain one paper, with titles and publication status as follows:

- PART I: SPECTRO-TEMPORAL DATA MODELING
  - Chapter 2: "Automatic classification and reduction of wind noise in spectral data," published in the Journal of the Acoustical Society of America Express Letters 1 (6), 063602 (2021).
  - Chapter 3: "Application of a spectral-based wind noise reduction method to acoustical measurements," published in Proceedings of Meetings on Acoustics, Vol. 45, 045002 (2022).
- PART II: SPATIO-TEMPORAL DATA MODELING
  - Chapter 4: "Toward improving road traffic noise characterization: A reduced-order model for representing hourly traffic volume dynamics," published in Proceedings of Meetings on Acoustics, Vol. 45, 045002 (2022).

- Chapter 5: “Toward a dynamic national transportation noise map: Modeling temporal variability of traffic volume,” submitted to the Journal of the Acoustical Society of America on 23 May 2023.

- PART III: SPATIO-SPECTRO-TEMPORAL DATA MODELING
  - Chapter 6: “Toward a dynamic national transportation noise map: Modeling spectral traffic noise emission levels,” being prepared for submission to the Journal of the Acoustical Society of America.
  - Chapter 7: “An app for nationwide dynamic traffic noise prediction,” accepted to INTER-NOISE and NOISE-CON Congress and Conference Proceedings in May 2023, publication forthcoming.

REFERENCES

[1] H. F. Boersma, Characterization of the natural ambient sound environment: Measurements in open agricultural grassland, The Journal of the Acoustical Society of America 101, 2104 (1997).

[2] R. Raspet, J. Yu, and J. Webster, Low frequency wind noise contributions in measurement microphones, The Journal of the Acoustical Society of America 123, 1260 (2008).

[3] S. Zhao, M. Dabin, E. Cheng, X. Qiu, I. Burnett, and J. C. Liu, Mitigating wind noise with a spherical microphone array, The Journal of the Acoustical Society of America 142, 2454 (2017).

[4] J. P. Abbott, R. Raspet, and J. Webster, Wind fence enclosures for infrasonic wind noise reduction, The Journal of the Acoustical Society of America 137, 12650 (2015).

[5] M. R. Shust and J. C. Rogers, Active removal of wind noise from outdoor microphones using local velocity measurements, The Journal of the Acoustical Society of America 104, 1781 (1998).

[6] Jinuk Park, Jihoon Park, S. Lee, J. Kim, and M. Hahn, Coherence-based Dual Microphone Wind Noise Reduction by Wiener Filtering, ICSPS, November 2016, pp. 170-172.

[7] Z. C. Zheng and B. K. Tan, Reynolds number effects on volume/acoustic mechanisms in spherical windscreens, The Journal of the Acoustical Society of America 113, 161 (2003).

[8] G. P. van den Berg, Wind-induced noise in a screened microphone, The Journal of the Acoustical Society of America 119, 824 (2006).

[9] A. D. May, Traffic volume Fundamentals, Prentice-Hall Incorporated, 1990.

[10] F. Kessels, Introduction to Traffic volume Modelling, Springer Link, 2018.

[11] H. Xiao, H. Sun, B. Ran, and Y. Oh, Fuzzy-Neural Network Traffic Prediction Framework with Wavelet Decomposition, Transportation Research Record 1836, no.1 (2003), pp. 16-20.

[12] D. S. Dendrinos, Urban Traffic volumes and Fourier Transforms, Geographical analysis, Volume 26, Issue 3, July 1994, pp. 261-281.

[13] Y. Xie, Y. Zhang, and Z. Ye, Short-Term Traffic Volume Forecasting Using Kalman Filter with Discrete Wavelet Decomposition, Computer-aided Civil and Infrastructure Engineering, Volume 22, Issue 5, July 2007, pp. 326-334.

[14] W. Min and L. Wynter, Real-time road traffic prediction with spatio-temporal correlations, Transportation Research Part C: Emerging Technologies, Volume 19, Issue 4, August 2011, pp. 606-616.

[15] L. Li, S. He, J. Zhang, and B. Ran, Short-term highway traffic volume prediction based on a hybrid strategy considering temporal-spatial information, Journal of Advanced Transportation, Volume 50, Issue 8, December 2016, pp. 2029-2040.

[16] P. Sun, N. AlJeri and A. Boukerche, A Fast Vehicular Traffic volume Prediction Scheme Based on Fourier and Wavelet Analysis, 2018 IEEE Global Communications Conference (GLOBECOM), 2018, pp. 1-6.

[17] M. Fu, J. A. Kelly, and J. P. Clinch, Estimating annual average daily traffic and transport emissions for a national road network: A bottom-up methodology for both nationally-aggregated and spatially-disaggregated results, Journal of Transport Geography, Vol 58, 2017, pp. 186-195.

[18] Website https://maps.dot.gov/BTS/NationalTransportationNoiseMap/, accessed April 2023.

[19] Website https://www.bts.gov/geospatial/national-transportation-noise-map, accessed April 2023.

[20] U.S. Department of Transportation, Bureau of Transportation Statistics, National Transportation Noise Map Documentation, 2020.

[21] M. E. Hallenbeck, M. Rice, and B. Smith, Vehicle Volume Distributions by Classifications, FHWA-PL-97-025, 1997.

[22] Federal Highway Administration's Traffic Noise Model 3.0 Technical Manual. See details at <https://highways.dot.gov/research/projects/traffic-noise-model-30-implementation-and-future-development> or download at <https://rosap.ntl.bts.gov/view/dot/10000/dot_10000_DS1.pdf?>.

*Note: References for the papers included in this dissertation may be found at the end of each individual paper.

PART I: SPECTRO-TEMPORAL DATA MODELING

Chapter 2

Automatic classification and reduction of wind noise in spectral data

2.1 Introduction

This article focuses on a spectral-based method of automatically detecting and removing wind noise for a screened microphone. It was selected as an editor's pick article, and within a few months of publication received thousands of views and hundreds of downloads.

2.2 Required Copyright Notice

Citation: Mylan R. Cook, Kent L. Gee, Mark K. Transtrum, Shane V. Lympany, Matt Calton; Automatic classification and reduction of wind noise in spectral data. *JASA Express Lett* 1 June 2021; 1 (6): 063602. https://doi.org/10.1121/10.0005308

2.3 Published Article

JASA EXPRESS LETTERS ARTICLE asa.scitation.org/journal/jel

Automatic classification and reduction of wind noise in spectral data

Mylan R. Cook,[1] Kent L. Gee,[1,a)] Mark K. Transtrum,[1] Shane V. Lympany,[2] and Matt Calton[2]
[1]Department of Physics and Astronomy, Brigham Young University, Provo, Utah 84602, USA
[2]Blue Ridge Research and Consulting, LLC, Asheville, North Carolina 28801, USA
mylanray@byu.edu, kentgee@byu.edu, mkt24@byu.edu, shane.lympany@blueridgeresearch.com, matt.calton@blueridgeresearch.com

Abstract: Outdoor acoustic data often include non-acoustic pressures caused by atmospheric turbulence, particularly below a few hundred Hz in frequency, even when using microphone windscreens. This paper describes a method for automatic wind-noise classification and reduction in spectral data without requiring measured wind speeds. The method finds individual frequency bands matching the characteristic decreasing spectral slope of wind noise. Uncontaminated data from several short-timescale spectra can be used to obtain a decontaminated long-timescale spectrum. This method is validated with field-test data and can be applied to large datasets to efficiently find and reduce the negative impact of wind noise contamination.

[Editor: Tracianne B. Neilsen] https://doi.org/10.1121/10.0005308

Received: 31 March 2021 **Accepted:** 28 May 2021 **Published Online:** 18 June 2021

1. Introduction

When collecting acoustic data in uncontrolled environments, extraneous noise signals can contaminate or even invalidate measurements. Contaminating noise can be caused by both acoustic sources and by non-acoustic signals, and therefore correctly measuring a source signal alone can be difficult. Contamination can be more pronounced in outdoor measurements due to non-acoustic contamination caused by atmospheric and weather conditions. One particularly challenging source of outdoor contamination is wind, which not only creates additional acoustic sources—such as the rustling of leaves—but also introduces non-acoustic pressures, known as wind-induced microphone self-noise or hydrodynamic noise, that contaminate data.

Acoustic signals like the rustling of leaves caused by wind are a part of the acoustic environment and are not addressed in this paper. Conversely, wind-induced microphone self-noise—hereafter referred to simply as "wind noise"—is a non-acoustic signal which should not be considered as indicative of the acoustic environment.[1] For outdoor acoustic measurements in the audible frequency range, the dominant source of wind noise is the stagnation pressure fluctuations caused by atmospheric turbulence interacting with the microphone diaphragm or windscreen.[2,3] While microphone windscreens can reduce the overall amount of contamination measured by a microphone, they do not eliminate all wind contamination.

Various methods are used to mitigate the excess pressures resulting from wind noise,[4–7] such as using multiple microphone coherence to eliminate uncorrelated noise.[8] Another possible solution relies on measuring wind speeds along with acoustic data so that data taken during times of increased wind can be removed. For example, the National Park Service (NPS) Natural Sounds and Night Skies Division typically removes any data that were collected when the measured wind speed exceeds 5 m/s.[9] However, when considering data sets that contain only a single-channel recording and that do not include measured wind speeds, or even for relatively low but still relevant wind speeds, it can be more difficult to determine which data are the result of acoustic sources and which are wind-contaminated data.

This paper describes the development of a wind contamination identification and reduction method for one-third-octave band data taken with unobstructed, outdoor, screened microphones and is based on known spectral characteristics of wind noise contamination. The method uses the characteristic spectral slope of wind noise to classify individual spectral frequencies as either contaminated or uncontaminated. When several short-timescale measurements (e.g., several two-second spectra) are available, a decontaminated long-timescale average spectrum can be calculated (e.g., a spectrum composed of one-hour median spectral levels at each frequency, also known as an L_{50}). This method allows for automatic calculation of wind-noise-reduced or decontaminated spectra—and thus decontaminated overall sound pressure levels—for single-microphone data where wind speeds were not measured. By removing the wind-noise-contaminated data, the method can automatically estimate decontaminated acoustic levels for a wind-noise-contaminated sound field.

a)ORCID: 0000-0002-5768-6483.

2. Characteristic slope of wind-contaminated spectral data

2.1 Theory

Wind noise is caused by non-acoustic turbulent pressure fluctuations on a microphone diaphragm. The sources of these pressure fluctuations may include turbulence that occurs naturally in the atmosphere or wake turbulence generated by the microphone and windscreen. In outdoor measurements, atmospheric turbulence is the dominant source of wind noise.[3] The magnitude of the pressure fluctuations produced by atmospheric turbulence depends on the wind speed, height above the ground, stability of the atmosphere, and frequency.

The frequency spectrum of atmospheric turbulent pressure fluctuations can be grouped into three frequency ranges: the energy-containing range, the inertial subrange, and the dissipation range. The energy-containing range occurs at low infrasonic frequencies (often less than a few Hz), which are below the frequencies of interest for the outdoor acoustic measurements considered in this paper. In the dissipation range, turbulent fluctuations rapidly dissipate into heat, so wind noise is typically negligible compared with the acoustic sources or instrumentation noise. The frequency of the dissipation range increases with wind speed and typically occurs above 100–1000 Hz.

For most outdoor acoustic measurements, contaminating wind noise in the inertial subrange is of primary importance. The inertial subrange lies between the energy-containing range and the dissipation range and can occur between high infrasonic and mid-range audible frequencies. In the inertial subrange, the stagnation pressure fluctuations caused by atmospheric turbulence interacting with the microphone diaphragm or windscreen are proportional to $f^{-5/3}$, where f is the frequency. Turbulent-turbulent pressure fluctuations, which are proportional to $f^{-7/3}$, are negligible compared with the stagnation pressure fluctuations.[3] Thus, the magnitude frequency spectrum of wind noise varies linearly with logarithmic frequency, i.e., $SPL \propto \log(f)$, where SPL is the sound pressure level created by wind noise.

Windscreens are often used in an attempt to reduce wind noise in outdoor acoustic measurements. The pressure measured by a microphone at the center of a windscreen is a combination of the acoustic pressure and the turbulent pressure fluctuations as mitigated by the windscreen. Within the inertial subrange, the turbulent pressure fluctuations vary linearly with the fractional-octave band, which produces a characteristic spectral slope indicative of wind noise. However, the characteristic spectral slope changes at a crossover frequency of $f_c = V/(3D)$, where V is the mean wind speed and D is the windscreen diameter.[10] At frequencies below f_c in the inertial subrange, the turbulent pressure fluctuations are coherent over the entire surface of the windscreen, and the characteristic spectral slope is −6.7 dB per decade.[3] At frequencies above f_c in the inertial subrange, the turbulent pressure fluctuations are incoherent over the surface of the windscreen, and the characteristic spectral slope is −26.7 dB per decade.[3,11] This result implies that a windscreen reduces wind noise by "averaging out" incoherent turbulent pressure fluctuations over its surface.[2,3]

For many outdoor acoustic measurements with reasonably low wind speeds compared to the size of the windscreen, the crossover frequency occurs at infrasonic frequencies, and the characteristic spectral slope is −26.7 dB per decade at audible frequencies. For example, for a windscreen with a diameter of 9 cm at a wind speed of 5.4 m/s, the crossover frequency is $f_c = 20$ Hz. Although an increase in wind speed results in higher measured sound pressure levels, the characteristic spectral slope is independent of wind speed above the crossover frequency. Thus, if the crossover frequency is not greater than the lowest frequencies of interest, the characteristic spectral slope can be used to detect the presence of wind noise in acoustic measurements without requiring knowledge of the wind speed.

2.2 Current work

Data for this paper were collected in a remote, barren location in a Utah desert with few ambient acoustic sources, while a powered SOUNDBOKS speaker was used to generate a brown noise signal. The low-frequency roll-off of the speaker occurs around 50 Hz, below which there was no dominant acoustic source, and so measured levels are primarily the result of wind noise. Brown noise was chosen as the source signal because its characteristic slope—approximately −32 dB per decade for the type of brown noise used here—is similar to that of wind noise, and so the limitations of correctly classifying wind noise-contaminated data could be investigated. A GRAS 40-AE 12.7 mm diameter microphone with a GRAS AM0069 9-cm diameter porous foam ball windscreen was placed on a tripod at a height of approximately 1.5 m. Recorded data totaled approximately 75 min after removing time intervals where data were contaminated by airplanes flying overhead. Wind speeds were measured using a Kestrel 5500 weather meter at the sound measurement height with a two-second temporal resolution. Short-timescale spectra were likewise calculated for each two-second interval so that each spectrum has an associated measured wind speed.

Figure 1(a) shows the short-timescale one-third octave band spectra collected, each colored by its respective measured wind speed. Levels increase at low frequencies for higher wind speeds. Greater wind speeds also cause contamination to reach higher in frequency—at 0.7 m/s the contamination reaches only to about 25 Hz, while for a wind speed of 4.3 m/s the contamination reaches up to around 40 Hz. Figure 1(b) shows a few representative spectra, and how each spectral slope at low frequencies, regardless of measured wind speed, follows the characteristic slope of wind noise in the inertial subrange; the increase in wind speed correlates with an increase in overall levels, while the slope of −26.7 dB per decade remains unchanged.

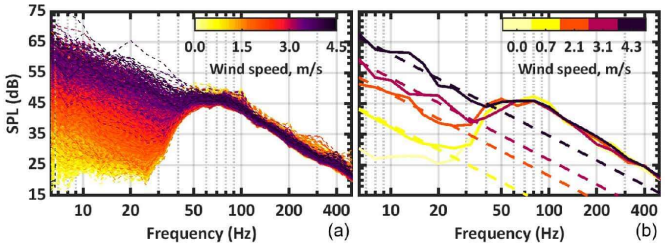

Fig. 1. Two-second spectra colored by measured wind speed (a). As wind speed increases, levels at low frequencies increase. The acoustic signal consisted of brown noise, while other measured levels, particularly at low frequencies, are primarily the result of wind noise contamination. A few selected spectra are shown (b), along with dashed lines showing the characteristic slope of wind noise, which is seen to fit the data.

3. Classifying contamination

Identifying contamination in screened microphone data processed using one-third-octave bands is accomplished by finding data which approximates the characteristic wind noise slope of −26.7 dB per decade. However, measured spectra typically include contributions from both acoustic signals and wind noise, so the measured data will rarely fit the characteristic wind noise slope precisely. Therefore, it is necessary to find data which *approximately* match the characteristic slope.

3.1 Data transformation

The complexity of finding points that fall along the same line can be greatly reduced by transforming the data. Spectral data consist of several two-dimensional data points, each giving the sound pressure level in decibels for a particular logarithmic fractional-octave band frequency. By using the characteristic wind-noise slope, these data are transformed into single-dimensional, linear data to find points that approximately match the characteristic slope.

The transformation can be considered as a projection of each data point along a line with the characteristic slope onto a vertical axis, similar to finding a y-intercept value for data points in a two-dimensional, linear space. As any two points can be connected by a straight line, we can use the analytic slope to find the point on the vertical axis that connects with each data point. For an illustration of the transformation method see Fig. 2(a). Note that the intercept need not be calculated at a vertical line going through the origin (i.e., $10^0 = 1$ Hz in logarithmic frequency space); the absolute *difference* between any two intercept values will be equal when projecting onto *any* vertical—or even horizontal (in this case logarithmic)—axis. Points that yield the same intercept value necessarily lie along the same line, and points with similar intercept values lie approximately on the same line. The differences between intercept values are then used to find points that approximate the characteristic wind noise slope.

3.2 Classifying contamination

Ideally, all contaminated data for a particular spectrum would yield the same intercept value; in practice, however, there will be some standard deviation between intercept values, depending on the particular data used. Some maximum standard

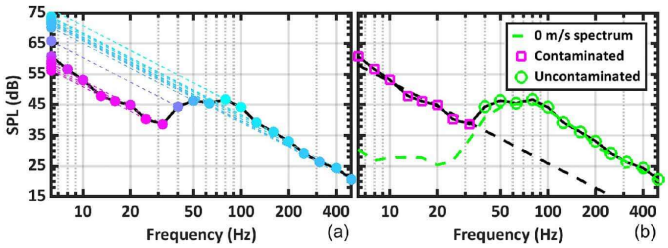

Fig. 2. For a particular wind noise contaminated spectrum, the process of finding contaminated data is shown. Plot (a) shows the point projection onto the vertical axis using the characteristic wind noise slope. Points have been colored based on their intercept values, meaning that similar colored points are approximately on the same line, as seen for all frequencies below 40 Hz. Plot (b) shows how these points are all labeled as contaminated and shows the best fit line with the characteristic wind noise slope fitting these data points. The measured wind speed for this spectrum was 2.3 m/s. A spectrum measured with no contaminating wind noise is shown for reference in plot (b).

deviation needs to be chosen—a default of 2 dB will generally suffice—so that intercept values near one another can be considered as fitting the characteristic slope.

In the inertial subrange, data points with wind contamination will give the lowest intercept values. Any acoustic signal will increase overall levels, and therefore intercept values. While this is not generally true for frequencies in the dissipation range, in practice the acoustic noise floor and/or acoustic signal will generally be louder than the dissipation range wind-contaminated levels, and so inertial subrange wind-contaminated frequencies will still give the lowest intercept values. However, it is still important to account for potential low outliers in intercept values.

The classification algorithm finds a tight grouping of points among the lowest intercept values, allowing for possible low outliers. By iteratively adding points with similar intercept values, the average intercept value is calculated, along with the standard deviation of the differences. The absolute differences of intercept values are used as they are invariant to the vertical axis location, unlike intercept values themselves. Additional points are added until the standard deviation of intercept differences exceeds the determined maximum standard deviation; the default standard deviation of 2 dB requires the grouping of intercept values have a standard deviation of no more than 2 dB. This process yields a group of points with similar intercept values. This is shown in Fig. 2(b), where all frequencies below 40 Hz were found to be contaminated.

The data giving the grouped intercept values all lie along a line with the characteristic slope of −26.7 dB per decade. These points can therefore all be classified as contaminated data. If determined necessary, data points that are low outliers among the intercept values can also be classified as contaminated. In addition to finding contaminated points, this process also finds a best-fit intercept value, which determines the line that the data approximate. This is shown in Fig. 2(b).

This method for classifying wind noise contamination assumes a constant characteristic spectral slope of −26.7 dB per decade for wind noise contamination, so the lower frequency limit is determined by the crossover frequency f_c, but makes no further assumptions about the frequency range of contamination. Contaminated frequencies need not be adjacent to one another, and no cutoff frequency must be specified. Additionally, no assumptions are made about the frequency output of the source signal. Thus, the method can classify wind noise contamination in measured signals that contain acoustic spectra and wind noise spectra in overlapping frequency ranges, even when the source signal—which could be broadband, band limited, tonal, or even more complex—is unknown.

3.3 Experimental validation

The data considered previously are used to validate the classification method. Each frequency band from every two-second spectrum is individually classified as either contaminated or uncontaminated. Figure 3(a) shows the results for all of the spectra together, while Fig. 3(b) shows the results for a few particular spectra. While there are some data points labeled as uncontaminated at lower frequencies with high levels, the classification is accurate for most spectra. Between 12% and 30% of the data below 25 Hz were classified as uncontaminated, corresponding to the amount of time the measured wind speed was below 1.1 m/s, showing that the algorithm is successfully able to find wind contamination. More than 99% of the data above 50 Hz were classified as uncontaminated, and so very little of the acoustic signal was incorrectly classified as contaminated.

One limitation of the method is that some acoustic data can be misclassified as wind noise. A single two-second brown noise spectrum, with a wind speed of 4.1 m/s, was classified as contaminated up to 1 kHz, showing that the classifier can mistake brown noise for wind-noise contamination. However, this only occurred for a single two-second spectrum (where the lower frequencies were indeed contaminated), meaning that less than 0.05% of the brown-noise spectra, despite having a similar characteristic slope as wind noise, were classified as contaminated.

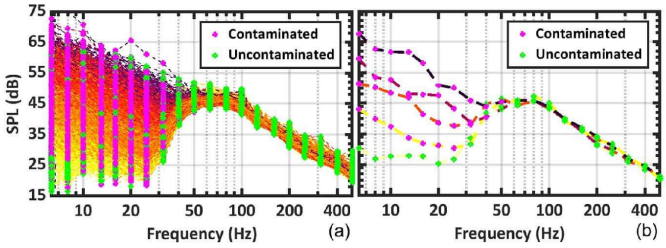

Fig. 3. Two-second spectra classification results for the same data shown in Fig. 1. While there are some high-level, low-frequency data classified as uncontaminated, seen in (a), much of the wind-contaminated data have been classified correctly. The low-level, low-frequency data are seen to be classified as uncontaminated, as are nearly all data at frequencies above 50 Hz. For clarity, a few distinct spectral classification results are shown in (b), where contamination is correctly classified below the low-frequency roll-off of the source.

Further validation of the classification algorithm's success can be obtained by calculating the correlation coefficient between the measured wind speed and the best-fit intercept value for each spectrum. Higher wind speeds should result in larger best-fit intercept values, and perfect correlation would yield a value of 1. The correlation value calculated is 0.9, which indicates that this is indeed the case—an increase in wind speed results in a higher intercept value. The contamination found is a result of wind noise.

4. Removing contamination

In addition to classifying data, a decontaminated average spectrum for a longer timescale can be calculated by using the results of the contamination classification method on short-timescale spectra. As frequency bands are classified as contaminated or uncontaminated individually, the average spectrum is calculated for each frequency independently. Figure 4 shows three different versions of an L_{50} (median level): (1) using only the data with a measured wind speed of 0 m/s, (2) using all of the data, and (3) using only the data classified as uncontaminated. The 0 m/s L_{50} represents the sought-after result where the signal is a result of the acoustic sources in the absence of wind noise. All three types of L_{50} correctly measure the speaker signal above 50 Hz, but below the speaker roll-off the 0 m/s L_{50} represents the acoustic noise floor. The spectral slope at low frequencies of the all-data L_{50} is about −26.7 dB per decade, as there were no relevant acoustic sources in this low frequency range, and so the data is a result of wind noise alone. The decontaminated L_{50} is similar to the 0 m/s L_{50} in both spectral slope and overall levels.

It should be noted that removing several contaminated data can overemphasize short-timescale acoustic signals: if a low-frequency source of similar level as the wind noise were emitting sound for only 20 min during an hour, but 50 min of data were contaminated at a particular frequency, the level at this frequency would not represent the true average non-wind-contaminated sound level for the entire hour; the source signal may be entirely removed, present in every non-contaminated spectra, or anything in between the two. This is a risk of removing data, though if the data discarded were contaminated, keeping them will also result in inaccurate sound levels.

These results show that by removing wind-contaminated data, the average spectrum calculated is much more representative of what would be measured in the absence of wind noise. While the 0 m/s L_{50} was obtained by using the measured wind speed, the decontaminated L_{50} was found using *only* spectral data and does *not* require having a measured wind speed. This method has myriad applications—while some measurements contain short-timescale measured wind speeds, many others do not, and the recorded spectra may contain high levels of wind contamination. This method can be applied to experimental data, past and future, that do not have measured wind speed, and can automatically detect and remove the effects of wind noise.

5. Conclusion and broader applications

The wind noise contamination classification and reduction algorithm described herein has broad application for validating and removing non-acoustic noise from experimental data. Computationally efficient and simple to apply, the method requires only spectral levels, and thus can be applied to data whether or not wind speeds were recorded. Whether using the highest quality recording equipment or a simple hand-held device, this method can improve measured spectra by removing non-acoustic pressures.

Finding wind noise contamination in acoustic data is not a simple endeavor. While not without the possibility of error, this method has proven useful in simply and elegantly identifying and removing wind noise from spectral data. For data taken with a windscreen (and for frequencies within the inertial subrange), wind noise creates a characteristic slope of −26.7 dB per decade. By using this characteristic spectral slope, this method can determine which frequencies in a spectrum are likely contaminated by wind noise.

Detection of wind noise is performed automatically, and so the method can quickly indicate which frequencies in a spectrum are probably contaminated. Beyond classification, when multiple short-timescale spectra are available, a

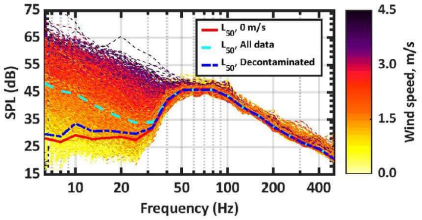

Fig. 4. Average spectra for the duration of the measurement using data measured with no wind, using all of the data, and using only the data classified as uncontaminated. Using the uncontaminated data alone results in a decontaminated average spectrum much nearer to the average spectrum seen with no wind but does not require having a measured wind speed.

decontaminated average spectrum can be calculated by removing contaminated data so that the non-acoustic wind noise pressures do not erroneously increase average levels. Possible applications are extensive because the method does not require measured wind speeds, and so can be performed on spectra for which other information is not readily available. This wind noise contamination detection and reduction method allows for a simple yet efficient way to identify and remove contaminated data.

Acknowledgments

This work was supported by a U.S. Army Small Business Innovation Research contract to Blue Ridge Research and Consulting, LLC, with Dr. James Stephenson as the technical monitor.

References and links

[1]H. F. Boersma, "Characterization of the natural ambient sound environment: Measurements in open agricultural grassland," J. Acoust. Soc. Am. **101**, 2104 (1997).
[2]R. Raspet, J. Yu, and J. Webster, "Low frequency wind noise contributions in measurement microphones," J. Acoust. Soc. Am. **123**, 1260 (2008).
[3]G. P. van den Berg, "Wind-induced noise in a screened microphone," J. Acoust. Soc. Am. **119**, 824 (2006).
[4]S. Zhao, M. Dabin, E. Cheng, X. Qiu, I. Burnett, and J. C. Liu, "Mitigating wind noise with a spherical microphone array," J. Acoust. Soc. Am. **144**, 3211 (2018).
[5]S. Zhao, M. Dabin, E. Cheng, X. Qiu, I. Burnett, and J. C. Liu, "On the wind noise reduction mechanism of porous microphone windscreens," J. Acoust. Soc. Am. **142**, 2454 (2017).
[6]J. P. Abbott, R. Raspet, and J. Webster, "Wind fence enclosures for infrasonic wind noise reduction," J. Acoust. Soc. Am. **137**, 1265 (2015).
[7]M. R. Shust and J. C. Rogers, "Active removal of wind noise from outdoor microphones using local velocity measurements," J. Acoust. Soc. Am. **104**, 1781 (1998).
[8]J. Park, J. Park, S. Lee, J. Kim, and, and M. Hahn, "Coherence-based dual microphone wind noise reduction by Wiener filtering," in *ICSPS 2016: Proceedings of the 8th International Conference on Signal Processing Systems* (2016). pp. 170–172.
[9]National Park Service, *Acoustical Monitoring Training Manual* (Natural Sounds and Night Skies Division, Fort Collings, CO, 2013).
[10]Z. C. Zheng and B. K. Tan, "Reynolds number effects on flow/acoustic mechanisms in spherical windscreens," J. Acoust. Soc. Am. **113**, 161 (2003).
[11]Z. T. Jones, M. R. Cook, A. M. Gunther, T. S. Kimball, K. L. Gee, M. K. Transtrum, S. V. Lympany, M. Calton, and M. M. James, "Examining wind noise reduction effects of windscreens and microphone elevation in outdoor acoustical measurements," J. Acoust. Soc. Am. **148**, 2617 (2020).

Chapter 3

Application of a spectral-based wind noise reduction method to acoustical measurements

3.1 Introduction

This article focuses on applications of the spectral-based wind noise reduction method described in Chapter 2. It was selected for first place in the Physical Acoustics Student Paper Competition 2021 (Seattle, WA).

3.2 Required Copyright Notice

Citation: Mylan R. Cook, Kent L. Gee, Mark K. Transtrum, Shane V. Lympany, Matt Calton; Application of a spectral-based wind noise reduction method to acoustical measurements. Proc. Mtgs. Acoust. 29 November 2021; 45 (1): 045002. https://doi.org/10.1121/2.0001526

I hereby confirm that the use of this article is compliant with all publishing agreements.

3.3 Published Article

Proceedings of Meetings on Acoustics

Volume 45 http://acousticalsociety.org/

181st Meeting of the Acoustical Society of America

Seattle, Washington

29 November - 3 December 2021

*Physical Acoustics: Paper 2aPA8

Application of a spectral-based wind noise reduction method to acoustical measurements

Mylan R. Cook, Kent L. Gee and Mark K. Transtrum
Department of Physics and Astronomy, Brigham Young University, Provo, Utah, 84602; mylan.cook@gmail.com; kentgee@byu.edu; mkt24@byu.edu

Shane V. Lympany and Matt Calton
Blue Ridge Research and Consulting LLC, Asheville, NC, 28801; shane.lympany@blueridgeresearch.com; matt.calton@blueridgeresearch.com

Wind-induced microphone self-noise is a non-acoustic signal that may contaminate outdoor acoustical measurements, particularly at low frequencies, even when using a windscreen. A recently developed method [Cook *et al.*, JASA Express Lett. 1, 063602 (2021)] uses the characteristic spectral slope of wind noise in the inertial subrange for screened microphones to automatically classify and reduce wind noise in acoustical measurements in the lower to middling frequency range of human hearing. To explore its uses and limitations, this method is applied to acoustical measurements which include both natural and anthropogenic noise sources. The method can be applied to one-third octave band spectral data with different frequency ranges and sampling intervals. By removing the shorter timescale data at frequencies where wind noise dominates the signal, the longer timescale acoustical environment can be more accurately represented. While considerations should be made about the specific applicability of the method to particular datasets, the wind reduction method allows for simple classification and reduction of wind-noise-contaminated data in large, diverse datasets.

**1st Place in the Physical Acoustics Student Paper Competition 2021 (Seattle, WA)*

Published by the Acoustical Society of America

 https://doi.org/10.1121/2.0001526
Proceedings of Meetings on Acoustics, Vol. 45, 045002 (2022)

1. INTRODUCTION

Extraneous noise can contaminate or invalidate outdoor acoustical measurements. Contaminating noise can be caused by both acoustic sources and by non-acoustic signals, and therefore correctly measuring a source signal can be difficult. One particularly challenging source of outdoor contamination is wind, which not only creates additional acoustic sources—such as the rustling of leaves—but also introduces non-acoustic pressures, known as wind-induced microphone self-noise or hydrodynamic noise, that corrupt data.

Acoustic signals like the rustling of leaves caused by wind are a part of the acoustic environment and are not addressed in this paper. Conversely, wind-induced microphone self-noise—hereafter referred to simply as "wind noise"—is a non-acoustic signal which should not be considered as indicative of the acoustic environment.[1] For outdoor acoustic measurements in the audible frequency range, the dominant source of wind noise is the stagnation pressure fluctuations caused by atmospheric turbulence interacting with the microphone diaphragm or windscreen.[2,3] While microphone windscreens can reduce the overall amount of contamination measured by a microphone, they do not eliminate all wind contamination.

Various methods are used to mitigate the excess pressures resulting from wind noise,[4–7] such as using multiple microphone coherence to eliminate uncorrelated noise.[8] Another possible solution relies on measuring wind speeds along with acoustic data so that data taken during times of increased wind can be removed. For example, the National Park Service (NPS) Natural Sounds and Night Skies Division typically removes any data that were collected when the measured wind speed exceeds 5 m/s.[9] However, when considering datasets that contain only a single-channel recording and that do not include measured wind speeds, or even for relatively low but still relevant wind speeds, it is more difficult to determine which data are the result of acoustic sources and which are wind-contaminated data.

A recent paper was published to describe the development of a wind contamination identification and reduction method for one-third-octave band data taken with unobstructed, outdoor, screened microphones, based on known spectral characteristics of wind noise contamination.[10] The method uses the characteristic spectral slope of wind noise to classify individual spectral frequencies as either contaminated or uncontaminated. When several short-timescale measurements (e.g., several two-second spectra) are available, a decontaminated long-timescale average spectrum can be calculated (e.g., a spectrum composed of one-hour median spectral levels at each frequency, also known as an L_{50}). This method allows for automatic calculation of wind-noise-reduced or decontaminated spectra—and thus decontaminated overall sound pressure levels—for single-microphone data where wind speeds were not measured. By removing the wind-noise-contaminated data, the method can automatically estimate clean or decontaminated acoustic levels for a wind-noise-contaminated sound field.

This paper further explores the usefulness and limitations of the classification and reduction method by applying the method to spectral datasets where exact acoustic source characteristics and wind speeds are unknown. Different sized windscreens are used, and both natural and anthropogenic sources are considered. The method is able to remove not just high levels of low frequency wind noise contamination, but also lower-level contamination and wind noise at frequencies between multiple band-limited acoustic sources.

2. WIND NOISE THEORY

Wind noise is caused by non-acoustic turbulent pressure fluctuations on a microphone diaphragm. The sources of these pressure fluctuations may include turbulence that occurs naturally in the atmosphere or wake turbulence generated by the microphone and windscreen. In outdoor measurements, atmospheric turbulence is the dominant source of wind noise.[3] The magnitude of the pressure fluctuations produced by atmospheric turbulence depends on the wind speed, height above the ground, stability of the atmosphere, and frequency.

The frequency spectrum of atmospheric turbulent pressure fluctuations can be grouped into three frequency ranges: the energy-containing range, the inertial subrange, and the dissipation range. The energy-containing range occurs at low infrasonic frequencies (often less that a few hertz), which are below the frequencies of interest for the outdoor acoustic measurements considered in this paper. In the dissipation range, turbulent fluctuations rapidly dissipate into heat, so wind noise is typically negligible compared with the acoustic sources or instrumentation noise. The frequency of the dissipation range increases with wind speed and typically occurs above 100-1000 Hz.

For most outdoor acoustic measurements, contaminating wind noise in the inertial subrange is of primary importance. The inertial subrange lies between the energy-containing range and the dissipation range and can occur between high infrasonic and mid-range audible frequencies. In the inertial subrange, the stagnation pressure fluctuations caused by atmospheric turbulence interacting with the microphone diaphragm or windscreen are proportional to $f^{-5/3}$, where f is the frequency. Turbulent-turbulent pressure fluctuations, which are proportional to $f^{-7/3}$, are negligible compared with the stagnation pressure fluctuations.[311] Thus, the magnitude frequency spectrum of wind noise varies linearly with logarithmic frequency, i.e., SPL $\propto \log(f)$, where SPL is the sound pressure level created by wind noise.

Windscreens are often used in an attempt to reduce wind noise in outdoor acoustic measurements. The pressure measured by a microphone at the center of a windscreen is a combination of the acoustic pressure and the turbulent pressure fluctuations as mitigated by the windscreen. Within the inertial subrange, the turbulent pressure fluctuations vary linearly with the fractional-octave band, which produces a characteristic spectral slope indicative of wind noise. However, the characteristic spectral slope changes at a crossover frequency of $f_c = V/(3D)$, where V is the mean wind speed and D is the windscreen diameter.[12] At frequencies below f_c in the inertial subrange, the turbulent pressure fluctuations are coherent over the entire surface of the windscreen, and the characteristic spectral slope is -6.7 dB per decade.[3] At frequencies above f_c in the inertial subrange, the turbulent pressure fluctuations are incoherent over the surface of the windscreen, and the characteristic spectral slope is -26.7 dB per decade, shown in Figure 1.[3,13] This result implies that a windscreen reduces wind noise at these frequencies by "averaging out" incoherent turbulent pressure fluctuations over its surface.[2,3]

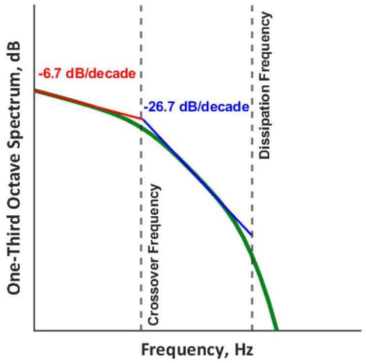

Figure 1. Visualization of spectral wind noise characteristics in the inertial subrange. Above the crossover frequency and before the dissipation range, the characteristic slope of wind noise is -26.7 dB per decade.

For many outdoor acoustic measurements with reasonably low wind speeds compared to the size of the windscreen, the crossover frequency occurs at infrasonic frequencies, and so the characteristic spectral slope is -26.7 dB per decade at audible frequencies. For example, for a windscreen with a diameter of 9 cm at a wind speed of 5.4 m/s, the crossover frequency is f_c= 20 Hz. Although an increase in wind speed results in higher measured sound pressure levels, the characteristic spectral slope is independent of wind speed above the crossover frequency. Thus, if the crossover frequency is generally below the lowest frequencies of interest, the characteristic spectral slope can be used to detect the presence of wind noise in acoustic measurements without requiring knowledge of the wind speed.

3. WIND NOISE CLASSIFIER

An implementation of the wind noise classification and reduction method is described in detail by Cook et al.[10] Given a particular spectrum, the algorithm seeks to find frequencies whose levels align with the characteristic spectral slope of wind noise of -26.7 dB per decade. Frequency data that match this spectral slope within a couple of decibels are classified as contaminated, while the other frequencies, which can be between contaminated frequencies, are classified as clean. No knowledge of microphone and windscreen setup, acoustic sources, suspected frequency range of wind contamination, or wind speed is necessary. By

classifying multiple short timescale spectral data, longer timescale average spectra can then be calculated using only clean data. The automatic classification and reduction of wind noise can give a more accurate representation of the acoustic environment than that calculated using all the data.

To illustrate the effectiveness of this method, the variable wind speed was measured while recording a constant acoustic source, as described in Cook et al.[10]. Each 1-second spectrum is shown in Figure 2, colored by wind speed. At lower frequencies, increase in wind speed causes an increase in amplitude, though the spectral slope remains the same. The maximum crossover frequency during the data collection, based on windscreen size and maximum measured wind speed, was approximately 18 Hz, while on average was closer to 4 Hz, which is below the lowest 1/3 octave band used of 6.3 Hz. While it is not necessary for the crossover frequency of all 1-second spectra to be below the lowest frequency of interest, default algorithm parameters should be changed if thre crossover frequency is too high due to high wind speeds.

The method is able to correctly classify the contamination, and remove contaminated data when calculating the average spectrum. For comparison, two other average spectra are shown: one using all of the data, where the high levels at lower frequencies are the result of wind noise, and a second using only spectra where the measured wind speed was 0 m/s. The spectrum calculated using only the clean data approximates the no-wind spectrum, which is a more accurate representation of the acoustic environment than the average spectrum calculated from all of the data, as much of the data were contaminated by wind noise.

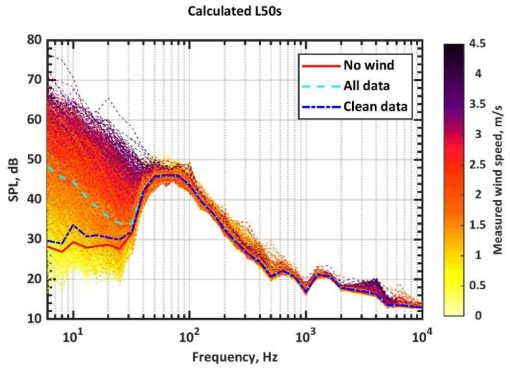

Figure 2. Wind contamination reduction results for a constant brown noise source. Below 50 Hz measured levels are primarily caused by wind contamination. The reduction method median level approximates the median level when wind speeds of 0 m/s were measured, indicating that the method is able to correctly classify frequencies where spectral data are a product of wind noise rather than acoustic noise.

In application, acoustic sources and wind speeds may not be known, and so while it has been shown that this method is effective with a known source and known wind speed, it is also instructive to show how the wind noise classification and reduction method works on spectral data of non-controlled sources with unknown wind speeds. Two different microphone setups are considered, which use different sizes of wind screens in different environments.

4. APPLICATION OF CLASSIFIER TO DATA

A. NATURAL AMBIENT ENVIRONMENT

Acoustic data were taken in the Bear River Migratory Bird Refuge using a ground-based microphone setup with a 30 cm windscreen.[14] While nearly 6 months of data were collected and run through the wind noise classifier, this paper focuses on a particular 90-minute period on the afternoon of May 10th, 2021, when there was evidence of variable amounts of wind noise contamination. Several natural and variable acoustic sources, both biotic and abiotic, were measured during this period. The wind noise classification and reduction method is applied to these spectral data and results are investigated.

The left plot in Figure 3 shows a spectrogram for the 90-minute period. The wind noise classification method is applied to each 1-second spectrum, and frequencies that show evidence of wind noise contamination are removed, resulting in the spectrogram in the right plot of Figure 3. Wind noise contamination is primarily found for frequencies below 160 Hz. While there appears to be higher-level wind noise after about 18:08, the classifier is able to not only classify these high levels of contamination, but also lower levels of wind noise contamination prior to this. With some exceptions, much of the visible wind noise in the spectrogram has been automatically removed successfully.

Something important to note is that there is additional noise in the 160-2500 Hz range after about 18:08, during periods of apparent high wind speed. This likely caused by the rustling of plants when there is wind, which itself is not wind noise contamination (wind-induced microphone self-noise) but is an actual acoustic source which is only present when there is wind. This noise is part of the acoustic environment, caused by physical sound sources, and should not be considered wind noise contamination. Because it is a physical noise source, it does not match the characteristic slope for wind noise and is not removed.

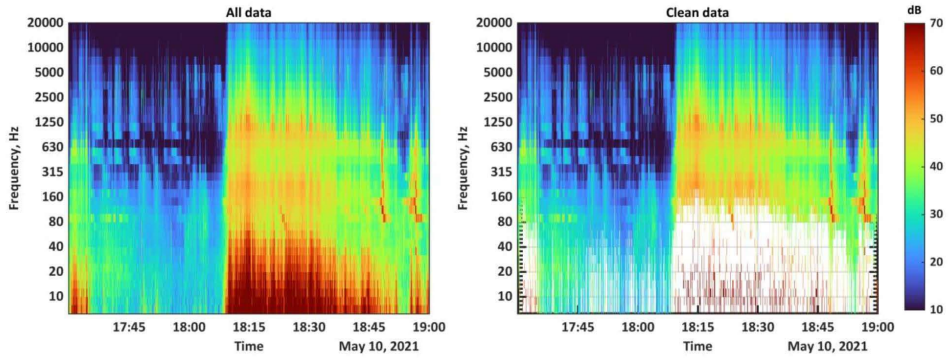

Figure 3. Wind noise classification applied to 90 minutes of ambient acoustic recordings at the Bear River Migratory Bird Refuge.

The classification alone, while useful in its own right, is further used to calculate median or $\boldsymbol{L_{50}}$ acoustic spectra. Median spectral levels are calculated for 15-minute intervals, as well as for the entire 90-minute duration. These can be compared to the median spectral levels for each corresponding time period when using all the data, and are shown in Figure 4. In each 15-minute period, it can be seen that the levels of the average spectrum of the clean data are less than or equal to the levels of the average spectrum of all the data. When applied to the entire 90-minute period, a reduction of up to 25 dB occurs at the lowest frequencies.

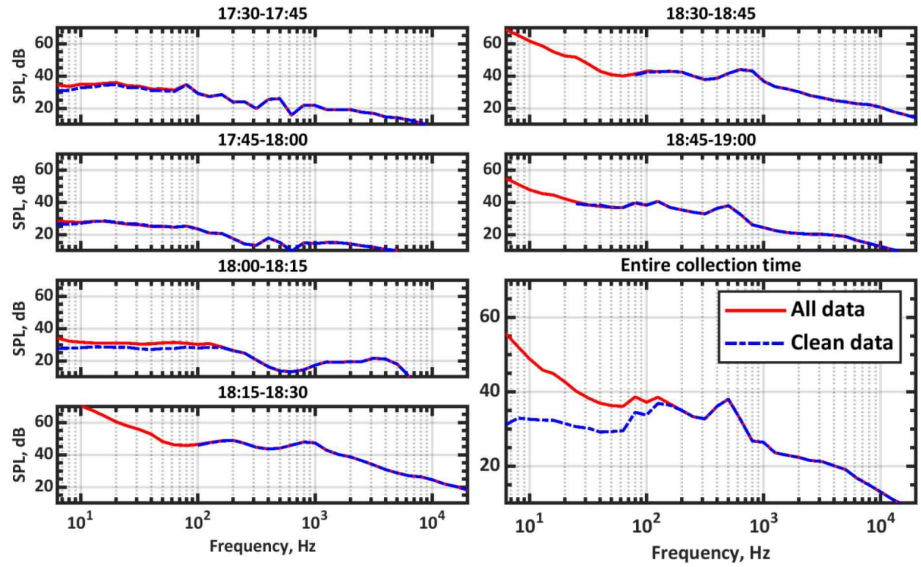

Figure 4. Wind noise reduction applied to the spectral data shown in Figure 3. Results are shown for 15-minute intervals, along with results for the entire collection period. For the clean data average, frequencies that were contaminated for more than 75% of the measurement period are omitted.

It is important to note than when calculating average levels using only the clean data, each frequency can be calculated using a different percentage of the total time period. Because wind noise contamination is not found at frequencies above 200 Hz in these data, the average spectrum at those frequencies represents 100% of the time duration; at lower frequencies, however, some of the data are contaminated. The exact amount of contaminated data depends on the particular frequency. If a high percentage of the data are contaminated, then it is possible that the 'average' spectrum at a particular frequency could be dominated by a very short time period. For this reason, frequenices where more than 75% of the data were classified as contaminated do not return an average level. For example, this is the case for frequencies below 100 Hz between 18:15-18:30.

Notably, if all spectral data had been removed when wind noise contamination was present instead of just the frequencies that were contaminated, the peak at 500 Hz—which is only present during time periods with higher wind—would also have been removed. This evidences that spectra calculated by the wind noise reduction method can give a more accurate representation of the acoustic environment than removing entire spectra that contain wind-contaminated data, all without having a measured wind speed.

In this natural ambient environment, the observed acoustic sources varied during data collection, and some acoustic sources were created by wind. Possible issues with too much of the data being contaminated by wind noise were seen, as well as how average spectra are calculated for a different percentage of the data collection time at different frequencies. The wind noise reduction method is able to preserve the acoustic sources while removing wind noise contamination, even though the wind speed during the collection was unknown.

B. ANTHROPOGENIC NOISE

To investigate other successes and limitations of the wind noise classification and reduction method, data containing anthropogenic noise is used. Acoustic data were taken on farmland using a microphone at a height of 1.5 m with a 9 cm diameter ball windscreen. This setup is more prone to wind noise contamination, due both to the microphone being higher off the ground, where wind speeds are greater, and to the smaller windscreen, where the crossover frequency is higher. However, for this particular time period, wind speeds were rather low, and so no more wind contamination is seen here than in the previous data set.

Figure 5 shows spectrograms for the two hours of data used, where the right plot removes data that were classified as contaminated. Sound sources observed include farm machinery, which exhibit some bandlimited or tonal behaviour, primarily at 13-16 Hz, and also at 31.5 Hz and 50 Hz. Acoustic data are consistent and of low level at higher frequencies, and so the frequency range shown is limited to below 315 Hz.

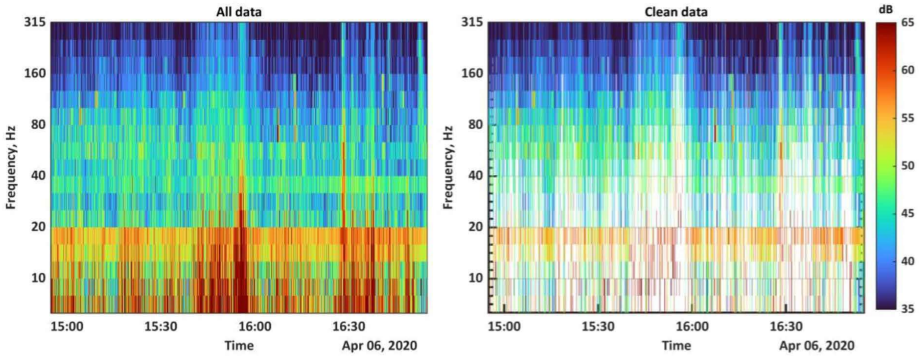

Figure 5. Wind noise classification applied to 2 hours of spectral data taken on farmland near machinery.

Median spectral levels are obtained for 20-minute intervals, and are shown in Figure 6. For each interval, the peaks at 13-16 Hz, 31.5 Hz, and 50 Hz are maintained, while wind noise at other frequencies—below, above, and also between the peaks—is removed. Note particularly 15:35-15:55, where all frequencies below 31.5 Hz except for 13-16 Hz are removed. These results show that source signals that are in the same frequency range as wind noise can be retained even when the wind noise is removed. This is significant, because even when there is wind noise, if the source levels are of higher than wind noise, the source signal is not removed with the wind noise.

In contrast to the previous data set, the average spectrum of the clean data is not always of equal or lesser level than the average spectrum of all the data. This is seen in the 31.5-80 Hz range for several of the time periods. This can happen in at least two possible situations: (1) when ambient sound levels are positively correlated with wind speed, e.g., a wind vane creaking when wind speeds pick up, or (2) when low levels of wind noise are removed but high levels of wind noise are not removed. In this case it is possible that the machinery was slightly louder when wind speeds were higher, as the higher levels of wind noise contamination appear to be removed successfully, though this is not certain. While results differ by less than 1 dB for this data set, this is an important limitation of the method.

Overall, sound levels at lower frequencies were reduced by up to 8 dB, while source levels were accurately maintained even during periods with high wind noise contamination. By removing the wind noise contamination, the peak at 13-16 Hz is seen to be more pronounced due to the reduction of wind noise at 10 Hz and below.

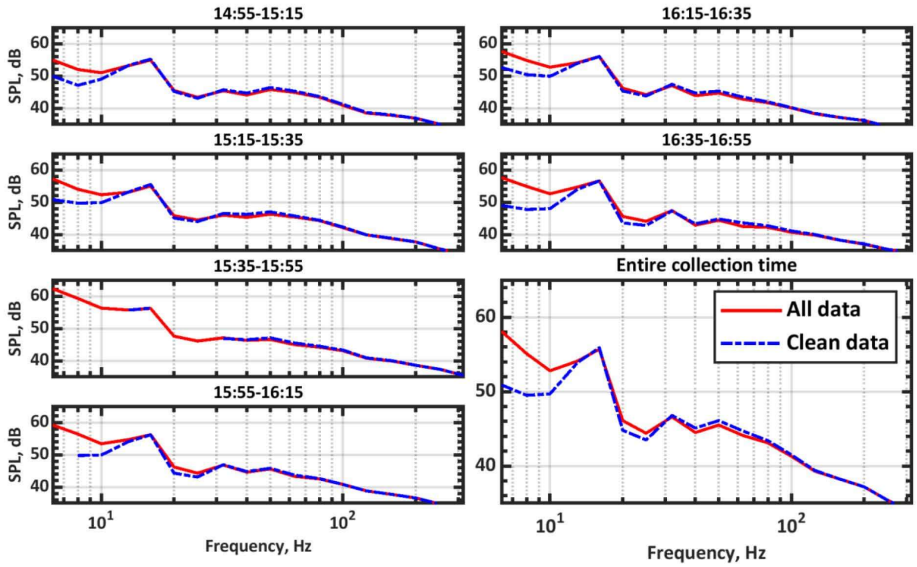

Figure 6. Wind noise reduction applied to the spectral data shown in Figure 5. Results are shown for 20-minute intervals, along with results for the entire collection period.

5. CONCLUSION

This paper has explored some application and limitations of the wind noise classification and reduction method published by Cook et al.[10] to spectral data where wind speed is unknown. The wind noise classification and reduction method is able to automatically detect and remove the negative effects of wind noise contamination in spectral data. While some care must be taken to ensure that spectral data are above the crossover frequency (when the windscreen is small compared to the wind speed), and while data must be taken using a windscreen, this method can be applied to many kinds of spectral data, even when specifics of data collection are unknown.

By using the characteristic slope of wind noise, levels at different frequency bands are independently classified so that acoustic data present during time periods with wind, and acoustic data in the same frequency range as wind noise contamination, is retained. This allows average spectra to be calculated that are better representative of the acoustic environment than those calculated by removing time periods of wind contamination and can be performed automatically without requiring a measured wind speed.

In practice, it may be infeasible to measure wind speeds while taking acoustic data. Even when wind speeds can be measured simultaneously, it is possible for wind speed measurement hardware to contaminate acoustic measurements. While the wind noise classification and reduction method is not applicable in every situation, it provides a simple, elegant way to classify and remove wind noise contamination in spectral data. It can be applied to spectra during data processing, and is performed automatically with minimal to no user input. This method can help anybody to improve outdoor measurements by removing wind noise from acoustic data.

ACKNOWLEDGMENTS

Development of the wind noise classification and reduction method was supported in part by a U.S. Army Small Business Innovation Research contract to Blue Ridge Research and Consulting, LLC, with Dr. James Stephenson as the technical monitor.

REFERENCES

[1] H. F. Boersma, "Characterization of the natural ambient sound environment: Measurements in open agricultural grassland," J. Acoust. Soc. Am. 101, 2104 (1997).

[2] 2 R. Raspet, J. Yu, and J. Webster, "Low frequency wind noise contributions in measurement microphones," J. Acoust. Soc. Am. 123, 1260 (2008).

[3] G. P. van den Berg, "Wind-induced noise in a screened microphone," J. Acoust. Soc. Am. 119, 824 (2006).

[4] S. Zhao, M. Dabin, E. Cheng, X. Qiu, I. Burnett, and J. C. Liu, "Mitigating wind noise with a spherical microphone array," J. Acoust. Soc. Am. 144, 3211 (2018).

[5] S. Zhao, M. Dabin, E. Cheng, X. Qiu, I. Burnett, and J. C. Liu, "On the wind noise reduction mechanism of porous microphone windscreens," J. Acoust. Soc. Am. 142, 2454 (2017).

[6] J. P. Abbott, R. Raspet, and J. Webster, "Wind fence enclosures for infrasonic wind noise reduction," J. Acoust. Soc. Am. 137, 1265 (2015).

[7] M. R. Shust and J. C. Rogers, "Active removal of wind noise from outdoor microphones using local velocity measurements," J. Acoust. Soc. Am. 104, 1781 (1998).

[8] J. Park, J. Park, S. Lee, J. Kim, and, and M. Hahn, "Coherence-based dual microphone wind noise reduction by Wiener filtering," in ICSPS 2016: Proceedings of the 8th International Conference on Signal Processing Systems (2016). pp. 170–172.

[9] National Park Service, Acoustical Monitoring Training Manual (Natural Sounds and Night Skies Division, Fort Collings, CO, 2013).

[10] M. R. Cook, K. L. Gee, M. K. Transtrum, S. V. Lympany, and M. Calton, "Automatic classification and reduction of wind noise in spectral data," JASA Express Letters 1, 063602 (2021).

[11] G. W. Lyons, C. R. Hart, and R. Raspet, "As the Wind Blows: Turbulent Noise on Outdoor Microphones", Acoustics Today, Volume 17, issue 4 (2021)

[12] Z. C. Zheng and B. K. Tan, "Reynolds number effects on flow/acoustic mechanisms in spherical windscreens," J. Acoust. Soc. Am. 113, 161 (2003)

[13] Z. T. Jones, M. R. Cook, A. M. Gunther, T. S. Kimball, K. L. Gee, M. K. Transtrum, S. V. Lympany, M. Calton, and M. M. James, "Examining wind noise reduction effects of windscreens and microphone elevation in outdoor acoustical measurements," Proc. Mtgs Acoust. 42, 045007 (2020).

[14] L. T. Moats, M. R. Cook, C. L. Teusch, L. K. Hall, K. L. Gee, and M. K. Transtrum, "Acoustical characteristics of avian choruses in a western migratory bird refuge," J. Acoust. Soc. Am. 150(4). A47 (2021).

PART II: SPATIO-TEMPORAL DATA MODELING

Chapter 4

Toward improving road traffic noise characterization: A reduced-order model for representing hourly traffic volume dynamics

4.1 Introduction

This article describes the development of the traffic volume model, which is the foundational model developed for VROOM, the Vehicular Reduced-Order Observation-based Model. This model gives a concise way to represent and predict traffic volume anywhere, requiring just nine principal components. This article describes the model itself, while model and prediction errors are explored in the article in Chapter 5.

4.2 Required Copyright Notice

Citation: Mylan R. Cook, Kent L. Gee, Mark K. Transtrum, Shane V. Lympany, Matthew F. Calton; Toward improving road traffic noise characterization: A reduced-order model for

representing hourly traffic volume dynamics. Proc. Mtgs. Acoust. 29 November 2021; 45 (1): 055001. https://doi.org/10.1121/2.0001636

I hereby confirm that the use of this article is compliant with all publishing agreements.

4.3 Published Article

Proceedings of Meetings on Acoustics

Volume 45 http://acousticalsociety.org/

181st Meeting of the Acoustical Society of America

Seattle, Washington

29 November -3 December 2021

Signal Processing in Acoustics: Paper 2aSP8

Toward improving road traffic noise characterization: A reduced-order model for representing hourly traffic volume dynamics

Mylan R. Cook, Kent L. Gee and Mark K. Transtrum
Department of Physics and Astronomy, Brigham Young University, Provo, Utah, 84602; mylan.cook@gmail.com; kentgee@byu.edu, mkt24@byu.edu

Shane V. Lympany and Matthew F. Calton
Blue Ridge Research and Consulting LLC, Asheville, NC, 28801; shane.lympany@blueridgeresearch.com; matt.calton@blueridgeresearch.com

The National Transportation Noise Map predicts time-averaged road traffic noise across the continental United States (CONUS) based on average annual daily traffic counts. However, traffic counts may vary significantly with time. Since traffic noise is correlated with traffic counts, a more detailed temporal representation of traffic noise requires knowledge of the time-varying traffic counts. Each year, the Federal Highway Administration tabulates the hourly traffic counts recorded at more than 5000 traffic monitoring sites across CONUS. Each site records up to 8760 traffic counts corresponding to each hour of the year. The hourly traffic counts can be treated as time-dependent signals upon which signal processing techniques can be applied. First, Fourier analysis is used to find the daily, weekly, and yearly temporal cycles present at each traffic monitoring site. Next, principal component analysis is applied to the peaks in the Fourier spectra. A reduced-order model using only nine principal components represents much of the temporal variability in traffic counts while requiring only 0.1% as many values as the original hourly traffic counts. This reduced-order model can be used in conjunction with sound mapping tools to predict traffic noise on hourly, rather than time-averaged, timescales. [Work supported by U.S. Army SBIR.]

Published by the Acoustical Society of America

 https://doi.org/10.1121/2.0001636
Proceedings of Meetings on Acoustics, Vol. 45, 055001 (2022)

1. INTRODUCTION

Road noise can be a significant component of total anthropogenic noise in many developed areas and can have a large impact on diverse acoustic environments. Not only humans are adversely affected by loud road noise,[1] but also other species.[2,3] Road noise cannot be effectively measured along every roadside, so accurate modeling of road noise is necessary for improving road noise characterization.

Because overall traffic noise is correlated with traffic volume rates, traffic noise characterization can depend heavily on characterization of traffic volume, along with other parameters such as vehicle speed, pavement type, road inclination, and land cover[4,5]. The National Transportation Noise Map published by the Bureau of Transportation Statistics uses annual average daily traffic (AADT) counts to predict an annually and daily averaged sound level near major roads across the continental United States (CONUS)[6]. While this map is useful for determining average sound levels, it lacks temporal variability, and so may not reflect the actual sound level for a particular time of the day or night.

Traffic volume can show large variation, not only diurnally but also from weekday to weekend and from summer to winter. A dynamically varying representation of traffic noise would be useful for determining hourly sound levels across CONUS. Characterizing the dynamic nature of traffic volume is not only useful for determining the changes in sound levels at locations where traffic counts are known but can also lead to a model for predicting variable traffic volume at other locations, and therefore predicting sound levels across CONUS for particular time periods.

Modeling traffic volume can be done in various ways, though a simple model can be made using vehicle counts at various locations[7,8]. Each year, the Federal Highway Administration tabulates hourly traffic counts recorded at thousands of traffic monitoring sites across the United States. Each site can record up to 8760 traffic counts corresponding to each hour of the year (or 8784 for leap years). While this gives a detailed representation of hourly traffic volume for individual sites, this representation requires thousands of individual hourly counts for each location, and using vehicle counts to predict counts at other times or at other locations is not straightforward. Methods such as wavelet decomposition[9] can be used to include temporal variability. In this paper, another possible method that can be used to predict hourly vehicle counts, hereafter used synonymously with traffic volume, at other locations is considered.

Treating the vehicle volume as a time-dependent signal enables signal processing techniques to be applied. The approach explained in this paper uses Fourier analysis and principal component analysis to give a reduced-order model to represent and predict vehicle counts[10]. This representation requires a total of only nine variables at a site to determine hourly traffic counts for any day of any year, a total of 0.1% as many variables as the hourly counts for a single year.

The approach for this paper uses hourly-resolution vehicle counts, and does not consider shorter-term traffic volume behavior, though it may be possible to adapt this approach for shorter timescales.[11-13] This approach also creates a method to predict hourly vehicle counts at other locations using geospatial or location-specific features. This reduced-order model can be used in conjunction with sound mapping tools to predict traffic noise across the continent on hourly, rather than time-averaged, timescales.[14]

2. DATA USED FOR ANALYSES

The Federal Highway Administration obtains hourly traffic counts from thousands of traffic monitoring sites across the United States. Data reported between 1 January 2015 and 31 December 2018 are used in this paper. However, not all stations report counts for each hour during this time period. Additionally, some of the data reported contain erroneous counts. Initial automatic checks found probable errors in data reported at several sites, which were entirely removed from the dataset. The remaining data come from 5695 sites across CONUS and are further analyzed for useability.

Within the remaining data set, some sites can still contain possible erroneous counts, and site-reported data are not equally reliable. For sites that report data consistently, reported values are more reliable, while sites that only report counts intermittently can contain dubious values. This can be seen in the data counts shown in Figure 1. The data pictured in Figure 1(a) contain values for every hour of the 4-year period and reported counts show high consistency. For the data pictured in Figure 1(b), however, shows several gaps where days, weeks, or even months of hourly counts were not reported; additionally, the reported counts for some months seem to be shifted

by up to a few hours. To mitigate doubts in data fidelity, and therefore in results, a further data validation step is necessary. A site data confidence weighting is therefore used.

Generally, weights can be assigned based on the percentage of data present for each site. Sites with half as many reported hourly counts could be given half the weight as sites where all four years of hourly counts were reported. However, for processing purposes explained further on, cyclically missing data, or data missing between times with reported data, can have a negative impact on analysis. Therefore, an adjusted weighting is made based not on the total number of hourly counts reported, but by the maximum number of *consecutive* hourly counts reported for each site. By weighting data in this manner, each site is given a relative weighting between zero and one.

Figure 1. Reported hourly traffic counts for two locations (top). The horizontal axis shows the day of the year, while the vertical axis shows the hours of each day, with the traffic count represented by the color. The normalized Fourier transform of the vehicle counts for both locations, explained in Section 3, is also shown (bottom). Amplitudes for integer multiples of daily cycles are marked in red, and amplitudes for integer multiples of weekly cycles are marked in black.

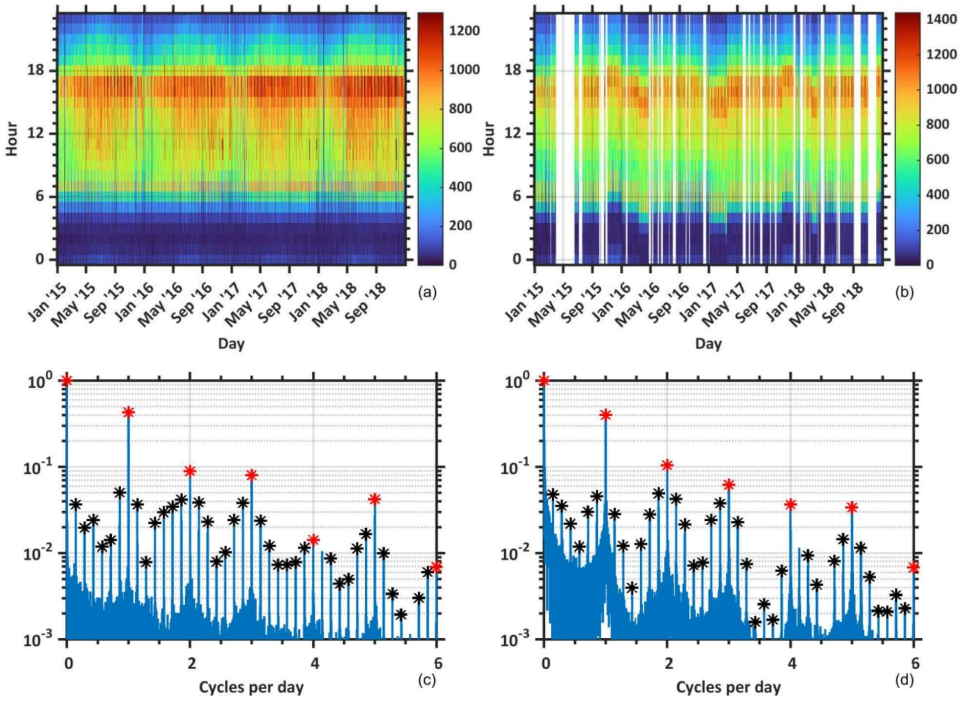

3. FOURIER ANALYSIS OF TRAFFIC VOLUME

While visual patterns are seen when viewing traffic volume in Figure 1(a-b) (such as the diurnal or day/night patterns), in order to make use of this information—such as to predict traffic volume at other locations, or to predict missing vehicle counts like the gaps seen in Figure 1(b)—it is necessary to characterize these traffic volume patterns. By treating hourly traffic counts as time-dependent signals, Fourier analysis is used to identify the temporal cycles present at each individual site[15]. However, because a fast or discrete Fourier transform

generally requires equally spaced and non-missing data, and because several sites contain some missing vehicle counts, a non-uniform Fourier transform must be used.

A. NON-UNIFORM FOURIER TRANSFORM

Fourier transforms usually require equally spaced temporal data, with the sampling frequency determining the maximum number of cycles that can be found for a time period. Most discrete Fourier transform algorithms are ill-equipped to handle missing data, and so instead the non-uniform discrete fast Fourier transform is used to analyze the traffic counts at each site[16]. This yields a two-sided, complex-valued Fourier spectrum. The magnitude of the single-sided spectrum for two sites is shown in Figure 1(c-d).

Clear peaks in the Fourier spectra appear at several relevant frequencies. One important peak is that seen at 0 cycles per day, which represents the average number of measured vehicles per hour (the AADT divided by 24), the value of which has been used to normalize the plotted spectra. Other strong peaks are seen at integer multiples of 1 cycle per day (marked in red), which together represent the daily-repeating traffic volume pattern. More peaks are seen at integer multiples of 1/7 cycle per day (marked in black), and together represent the weekly-repeating traffic volume pattern. Though not visible on this scale, there are also peaks at integer multiples of one cycle per year.

B. DENOISING FOURIER SPECTRA

Peaks in the Fourier spectra on integer multiples of daily, weekly, and yearly time periods are often quite pronounced, but the spectra can also contain non-zero amplitudes at other time period cycles. This is because the traffic pattern does not repeat exactly every day, week, or year. Because the present research is concerned with average hourly behaviors, rather than a precise representation of the traffic counts, the small but non-zero amplitudes are treated as noise in the Fourier spectra, and so are removed or zeroed out.

A representation of the average traffic volume pattern for a site is obtained using the Fourier amplitudes at frequencies that are integer multiples of weekly and yearly cycles (daily cycle frequencies are captured using integer multiples of weekly cycles). Due to missing data or machine precision errors, peaks in the Fourier spectra can sometimes be found at frequencies that are adjacent to multiples of weekly and yearly cycles; when this is the case, the peak amplitude at that frequency is used instead of the Fourier amplitude at the integer-multiple frequency. This representation serves to decompose hourly traffic counts into a combination of sinusoidal traffic patterns that repeat on weekly and yearly cycles. This representation has the benefit of removing noise in traffic counts and requires a few hundred values instead of thousands of individual hourly vehicle counts.

C. PEAK VALUES REPRESENTATION

A smoothed, average hourly traffic volume pattern for each site is obtained by using an inverse Fourier transform on the denoised Fourier spectrum peak values. For the reported traffic counts shown in Figure 2(a), this approach yields a reasonable approximation as shown in Figure 2(c). However, for the reported counts shown in Figure 2(b), the representation shown in Figure 2(d) is not especially accurate. Some of the main reasons for the errors in the representation are considered below.

One reason for inaccuracy in the representation is caused by missing hourly counts at individual sites. That is why Figure 2(d) is not an accurate representation of the data in Figure 2(b). Missing data causes noise in the Fourier spectrum, which can alter the amplitude of the Fourier peaks which typically occur on integer multiples of weekly and yearly time cycles. The site weighting discussed previously, while not altering the behavior at an individual location, is important when looking at trends across sites, and will be discussed further on.

Another reason for inaccuracy is because, while traffic patterns contain both weekly and yearly repeating patterns, the days of the week do not match the day of the year, e. g., the first day of 2015 was a Thursday while the first day of 2017 was a Sunday. For generality, and to allow for traffic volume prediction for any day of the week of any year, the weekly traffic pattern is separated from the yearly traffic pattern. This is done by separating each Fourier spectrum into two separate data sets, one containing peaks on integer multiples of one cycle per year (up to 12 cycles per year, as after this the peaks are effectively in the noise floor), and the other containing peaks on integer multiples of 1/7 cycle per day (including the peak at 0 cycles per day so the average vehicle count is not removed). This ensures that the former will result in a yearly-repeating traffic pattern, and the latter in a weekly-repeating traffic pattern. These two patterns can then be combined to represent the traffic volume for any specific day of the week and day of the year.

A third reason for inaccuracy is that peak amplitudes in the Fourier spectrum are not independent of one another, and so noise in the Fourier spectrum that affects a single peak value, even by a small amount, can

fundamentally change the overall temporal pattern found after performing an inverse Fourier transform. To state this in another way, a weekly-repeating traffic pattern is not determined solely by a single Fourier peak amplitude, and any irregularities in the data can cause changes in a single Fourier peak amplitude. For this reason, representing traffic volume solely as the sum of independent sinusoidal patterns is not the best representation. A better and more concise way to represent traffic volume is by using principal component coefficients of cyclic traffic patterns.

Figure 2. A comparison of the reported traffic volume for two sites (top) with the traffic volume calculated using the Fourier peak values representation (bottom).

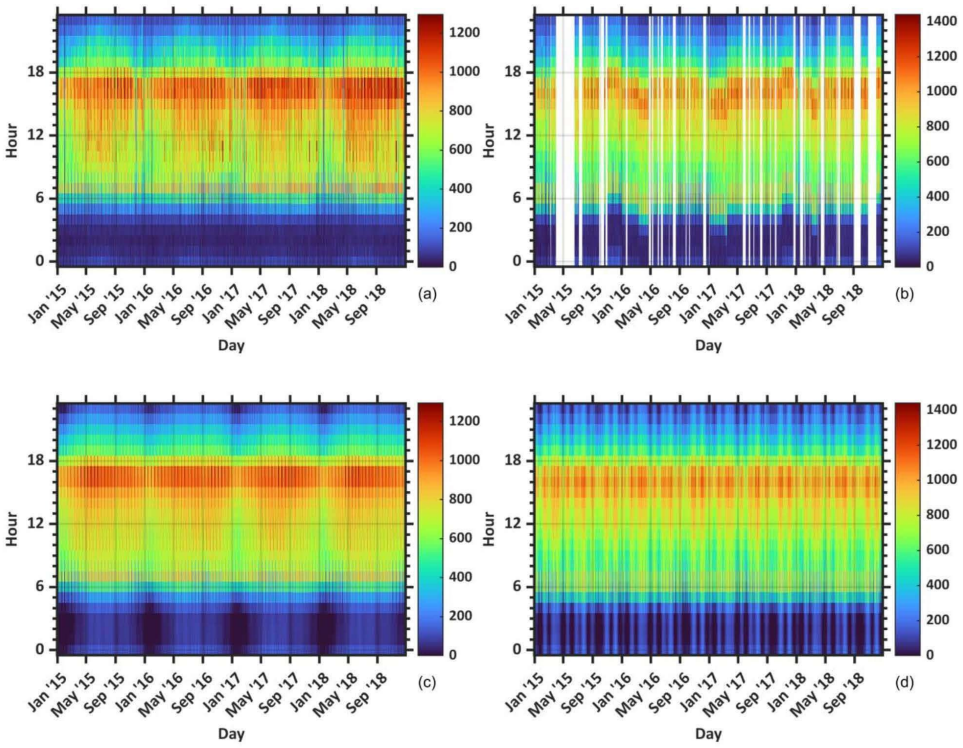

4. PRINCIPAL COMPONENT ALANYSIS OF FOURIER SPECTRA

Principal component analysis (PCA) is used to find a lower-dimensional basis which can represent the majority of multi-dimensional data points of a set. For the current research, each dimension of a data point consists of the Fourier amplitude at a particular frequency. By splitting the Fourier peaks into separate weekly and yearly cycles, we create two separate data sets, each containing a point in a high-dimensional space for each traffic measurement site. Because the Fourier peak amplitudes are interdependent, principal component analysis is used to find a simpler basis to represent the most common combinations of cyclic traffic patterns found across sites. This serves to reduce irregularities in the traffic pattern at a particular site by using the common traffic patterns seen across multiple sites. What this means is that by using this approach, the weekly or yearly traffic

pattern at any particular site can be represented as a combination of the most common cyclic weekly or yearly traffic patterns found across all sites.

As mentioned in Section 2, the hourly counts from all sites are not equally reliable, and therefore the Fourier peak amplitudes at one site are not as accurate as they are for another site. To avoid propagating these errors, a weighted PCA is used to improve the accuracy of results, where the weighting used is described in Section 2. The analysis is performed separately for the weekly and yearly cycles. The analysis returns principal components, which each represents a linear combination of Fourier amplitudes or, by using an inverse Fourier transform, a specific traffic volume pattern. The principal component coefficients, which are simply numeric values, give the linear combination of these traffic volume patterns.

The first principal component vectors, one for the weekly data and another for the yearly data, are shown in temporal space in Figure 3, and give the weighted average traffic volume pattern seen across sites. The yearly pattern shows little variation across the course of a year. The weekly pattern shows the average hourly traffic pattern found across CONUS, namely one where weekends show a smooth hourly variation during daytime hours, while the weekdays show an increase in morning and evening hours higher than that during the middle of the day, with less traffic activity during the nighttime hours. This type of traffic pattern is common for several urban locations, and in particular shows high similarity to data shown in Fu et al. (2017).[17]

To represent different traffic patterns seen at other sites, especially rural locations, a few more principal components. By using an elbow analysis on the eigenvalue of the principal components, it was determined that six principal components should be used to represent the weekly traffic pattern, and four principal components to represent the yearly traffic pattern. In this manner, 73% of the weekly data is represented, and 83% of the yearly data. The unique traffic pattern at a site can then be represented using just 10 principal component coefficients (PCCs).

The first weekly and yearly principal components, as mentioned before, give the weighted average traffic pattern seen across sites, and are shown in Figure 3. The coefficients for the first principal component, both weekly and yearly, show high linear correlation with the AADT. This leads to a normalization approach based on the first PCC. What this means is that rather than needing 10 PCCs to represent traffic volume at a site, five normalized weekly PCCs and three normalized yearly PCCs, along with the AADT, can represent the total vehicle counts for a site. This normalized approach is more useful, as representing traffic volume for any hour of the week at a site, relative to its normal average number of vehicles, requires only five values, and only three for any day of a year, and predictions can be made that match the overall AADT of a site when it is known. The final reduced-order model therefore requires just nine total coefficients to represent hourly traffic counts for any site, 0.1% as many variables as the total number of hourly counts for a single year.

Figure 3. Normalized principal components that represent the most common normalized traffic patterns found across CONUS.

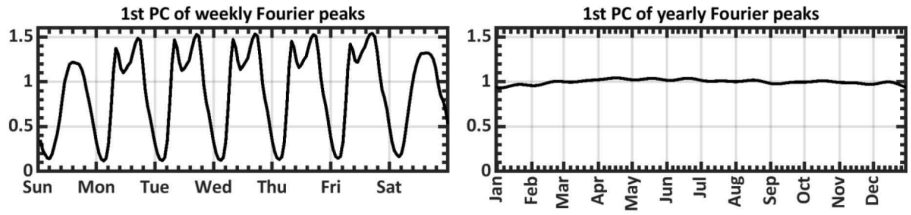

By using just these nine coefficients for a site, modeled traffic volumes are obtained, examples of which are shown in Figure 4(c-d) alongside the reported traffic counts in Figure 4(a-b). A comparison between the reported and modeled traffic counts shows that the PCA representation effectively smooths out inconsistencies in the raw data, while maintaining overall temporal trends. Additionally, because of the data weighting, missing data do not adversely affect the modeled traffic counts. By requiring only nine coefficients, the PCA representation allows for a simple way to both represent traffic volume data, which can not only be used to estimate traffic volume at sites when numbers are not reported, but also—by way of predicting PCCs—to predict traffic volume at other locations.

Figure 4. A comparison of the reported traffic volume for two sites (top) with the traffic volume calculated using the PCA representation (bottom).

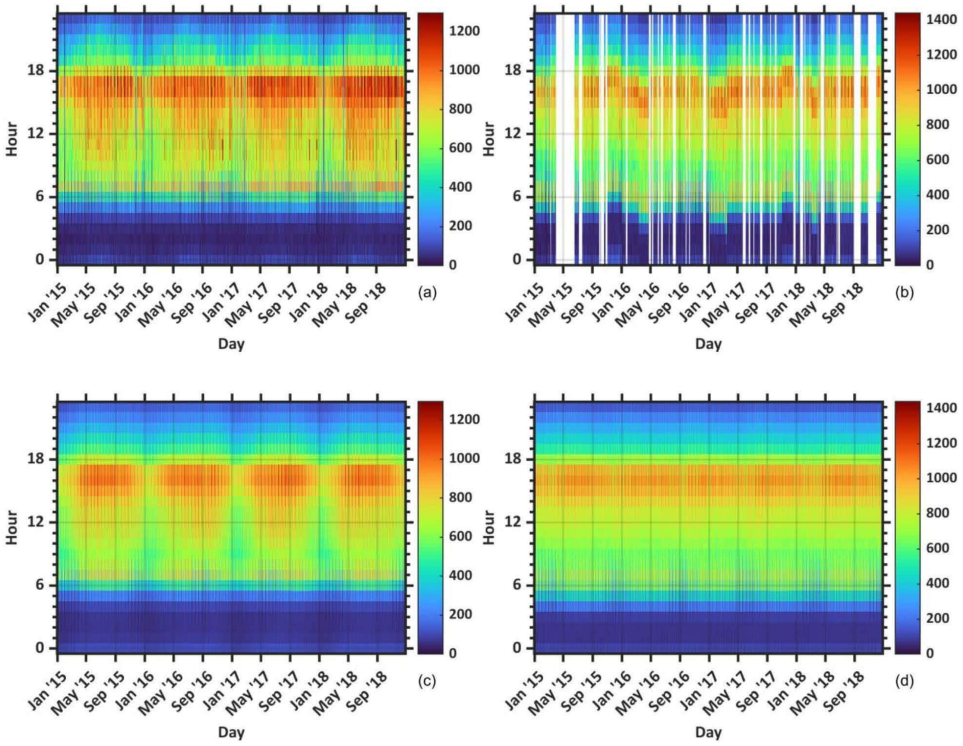

5. CONCLUSION

The number of vehicles on a road can change drastically from one time period to another. While knowing the average number of vehicles is necessary to predict average noise levels caused by road traffic, a temporally varying model of road traffic is more beneficial as it can be used to predict not just a general average number of vehicles, but average numbers of vehicles for any time period of interest, whether that be an average Tuesday evening in springtime or the noise level for a particular hour, day of the week, and date.

By using traffic counts reported at thousands of locations across CONUS, a simple model is created to represent and predict traffic volume. This uses Fourier analysis to find temporal patterns in traffic counts at each site individually, and the principal component analysis to find the most common combinations of temporal patterns across sites. The model requires only nine coefficients to represent the hourly-dynamic nature of traffic volume for most locations.

This simplified model not only creates a concise way to represent traffic volume patterns, but also enables simple prediction of traffic volume when counts are unknown. Because only nine coefficients are needed, further methods can be created to predict these coefficients for locations where traffic counts are unknown. This remains a topic of interest and will be explored further.

By better representing and predicting traffic volume, further improvements in the prediction of road traffic sound levels can be made. While annual average expected traffic noise levels are important, increasing the

temporal variability to enable hourly-expected noise levels, without drastically increasing complexity, can greatly increase accuracy and reliability in predicting sound levels caused by road traffic.

Future research will include not just temporal variability of traffic volume as a whole, but also the temporal variability of different traffic class types, such as large trucks, which have different expected spectral characteristics and sound levels than do smaller vehicles. This increased traffic variability model can then be used to predict sound levels and spectral characteristics of traffic noise across the continent on hourly, instead of average, time scales.

ACKNOWLEDGMENTS

This work was supported by a U. S. Army Small Business Innovation Research contract to Blue Ridge Research and Consulting, LLC, with Dr. James Stephenson as the technical monitor.

REFERENCES

[1] E. Öhrström, A. Skånberg, H. Svensson, A. Gidlöf-Gunnarsson, "Effects of road traffic noise and the benefit of access to quietness," Journal of Sound and Vibration, Volume 295, Issues 1-2, August 2006, pp. 40-59.

[2] G. Shannon, L. M. Angeloni, G. Wittemyera, K. M. Fristrup, K. R. Crooks, "Road traffic noise modifies behaviour of a keystone species," Animal Behaviour, Volume 94, August 2014, pp. 135-141.

[3] K. M. Parris and A. Schneider, "Impacts of Traffic Noise and Traffic Volume on Birds of Roadside Habitats, Ecology and Society, Vol. 14, No. 1, June 2009.

[4] D. R. Johnson and E. G. Saunders, "The evaluation of noise from freely flowing road traffic," Journal of Sound and Vibration, Volume 7, Issue 2, March 1968, pp. 287-288, IN1, 289-309.

[5] S. K. Tang and K. K. Tong, "Estimating traffic noise for inclined roads with freely flowing traffic," Applied acoustics, Volume 65, Issue 2, February 2004, pp. 171-181.

[6] National Transportation Noise Map by the Bureau of Transportation Statistics, https://www.bts.gov/geospatial/national-transportation-noise-map, accessed January 2021.

[7] A. D. May, "Traffic Flow Fundamentals," Prentice-Hall Incorporated, 1990.

[8] F. Kessels, "Introduction to Traffic Flow Modelling," Springer Link, 2018.

[9] H. Xiao, H. Sun, B. Ran, and Y. Oh, "Fuzzy-Neural Network Traffic Prediction Framework with Wavelet Decomposition," Transportation Research Record 1836, no.1 (2003), pp. 16-20.

[10] D. S. Dendrinos, "Urban Traffic Flows and Fourier Transforms," Geographical analysis, Volume 26, Issue 3, July 1994, pp. 261-281.

[11] Y. Xie, Y. Zhang, and Z. Ye, "Short-Term Traffic Volume Forecasting Using Kalman Filter with Discrete Wavelet Decomposition," Computer-aided Civil and Infrastructure Engineering, Volume 22, Issue 5, July 2007, pp. 326-334.

[12] W. Min and L. Wynter, "Real-time road traffic prediction with spatio-temporal correlations," Transportation Research Part C: Emerging Technologies, Volume 19, Issue 4, August 2011, pp. 606-616.

[13] L. Li, S. He, J. Zhang, and B. Ran, "Short-term highway traffic flow prediction based on a hybrid strategy considering temporal-spatial information," Journal of Advanced Transportation, Volume 50, Issue 8, December 2016, pp. 2029-2040.

[14] K. Pedersen, M. K. Transtrum, K. L. Gee, S. V. Lympany, M. M. James, and A. R. Salton, "Validating two geospatial models of continental-scale environmental sound levels," JASA Express Letters 1, 122401 (2021).

[15] P. Sun, N. AlJeri and A. Boukerche, "A Fast Vehicular Traffic Flow Prediction Scheme Based on Fourier and Wavelet Analysis," 2018 IEEE Global Communications Conference (GLOBECOM), 2018, pp. 1-6.

[16] MATLAB function "nufft", Natick, Massachusetts, The MathWorks Inc., copyright 2019.

[17] M. Fu, J. A. Kelly, and J. P. Clinch, "Estimating annual average daily traffic and transport emissions for a national road network: A bottom-up methodology for both nationally-aggregated and spatially-disaggregated results," Journal of Transport Geography, Vol 58, 2017, pp. 186-195.

Chapter 5

Toward a dynamic national transportation noise map: Modeling temporal variability of traffic volume

5.1 Introduction

This article describes the basic aspects of the traffic volume model, and gives expected model errors, comparing them to expected errors when using the annual average daily traffic. It shows the utility of VROOM, the Vehicular Reduced-Order Observation-based Model, which predicts dynamic road traffic volume and road traffic noise, and shows how VROOM predictions are much more accurate than using average vehicle numbers in predicting traffic volume.

5.2 Required Copyright Notice

The following article was submitted to the Journal of the Acoustical Society of America on May 23, 2023, under the title "Toward a dynamic national transportation noise map: Modeling temporal variability of traffic volume". It is reproduced in its original submission format here by rights granted in the Acoustical Society of America Transfer of Copyright document.

https://asa.scitation.org/pb-assets/files/publications/jas/jascpyrt-1485379914867.pdf

I hereby confirm that the use of this article is compliant with all publishing agreements.

5.3 Submitted Article

Toward a dynamic national transportation noise map: Modeling temporal variability of traffic volume

Mylan R. Cook,[1] Kent L. Gee,[1] Mark. K. Transtrum,[1] and Shane V. Lympany[2]

[1] *Department of Physics and Astronomy, Brigham Young University, Provo, Utah 84602, USA*

[2] *Blue Ridge Research and Consulting, LLC, Asheville, North Carolina 28801, USA*

The National Transportation Noise Map (NTNM) gives time-averaged traffic noise across the continental United States (CONUS) using annual average daily traffic. However, traffic noise varies significantly with time. This paper outlines the development and utility of a traffic volume model which is part of VROOM, the Vehicular Reduced-Order Observation-based Model, which, using hourly traffic volume data from thousands of traffic monitoring stations across CONUS, predicts nationwide hourly-varying traffic source noise. Fourier analysis finds daily, weekly, and yearly temporal traffic volume cycles at individual traffic monitoring stations. Then, principal component analysis uses denoised Fourier spectra to find the most widespread cyclic traffic patterns. VROOM uses nine principal components to represent hourly traffic characteristics for any location, encapsulating daily, weekly, and yearly variation. The principal component coefficients are predicted across CONUS using location-specific features. Expected traffic volume model sound level errors—obtained by comparing predicted traffic counts to measured traffic counts—and expected NTNM-like errors, are presented. VROOM errors are typically within a couple of decibels, whereas NTNM-like errors are often inaccurate, even exceeding 10 decibels. This work details the first steps towards creation of a temporally and spectrally variable national transportation noise map. [Work supported by U.S. Army SBIR.]

I. INTRODUCTION

Road noise comprises a significant component of total anthropogenic noise in many developed areas and can have a large impact on diverse acoustic environments. Increased noise levels are correlated with anything from mild annoyance to an increase in violent crime.[1] Not only are humans adversely affected by loud road noise,[2,3] but so are many other species.[4,5] Road noise cannot be effectively measured along every roadside in the country, and long-time-averaged levels are seldom accurate for particular times of day, so accurate modeling of road noise is necessary for improving road noise characterization.

Because overall road traffic noise is directly related to traffic volume—the number of vehicles per time period—road traffic noise characterization depends heavily on characterization of traffic volume itself, along with other parameters such as vehicle class mix, vehicle speed, pavement type, and road inclination.[6,7] The National Transportation Noise Map published by the Bureau of Transportation Statistics uses annual average daily traffic (AADT) counts to predict annually-averaged A-weighted 24-hr equivalent sound levels near major roads across the continental United States (CONUS).[8] While this map is useful for determining average sound levels, it lacks temporal and spectral variability, and so may not reflect the actual sound level for a particular time period.

Traffic volume can show large variation, not only diurnally, but also from weekday to weekend and from summer to winter. Characterizing the dynamic nature of traffic volume is not only useful for determining the changes in sound levels at locations where traffic counts are known but can also lead to a model for predicting variable traffic volume at other locations, and therefore to predicting sound levels across CONUS for particular time periods.

Traffic volume can be modeled in various ways, though a simplified model can be made using vehicle count data at various locations across CONUS.[9,10] The Federal Highway Administration tabulates hourly traffic counts recorded at thousands of traffic monitoring stations

across the United States. While hourly counts give a detailed representation of hourly traffic volume for individual stations, this representation requires thousands of individual hourly counts for each location, and using vehicle counts to predict traffic volume at other times or at other locations is not straightforward. Other methods such as wavelet decomposition[11,12] can be used to model temporal variability. In this paper, the first part of an original model is introduced. This model is called VROOM, which stands for the Vehicular Reduced-Order Observation-based Model. VROOM predicts hourly traffic noise for roads across CONUS. The first part of VROOM, which is the focus of this paper, predicts vehicle numbers—used synonymously with traffic volume—across CONUS.

Treating traffic volume as a time-dependent signal enables application of signal processing techniques. VROOM was developed using Fourier analysis[13] and principal component analysis, PCA, to characterize traffic patterns common across CONUS. VROOM requires only nine values—which are predictable from geospatial and road-specific feature values—at a location to fully represent hourly traffic volume for any time period.

VROOM was developed using hourly-resolution vehicle counts, and does not consider shorter-term traffic volume behavior, though it may be possible to adapt this approach for shorter timescales.[14-16] VROOM predicts hourly traffic volume at any location using geospatial or location-specific features. While predicting traffic counts is itself a useful result, VROOM is also able to predict traffic noise across the continent on hourly, rather than time-averaged, timescales.[17]

To create a temporally and spectrally varying national transportation noise map, the following steps are needed:

- Predict traffic volume along roads
- Predict time-varying traffic class mix along roads, e.g. heavy trucks vs smaller vehicles
- Calculating traffic noise emissions along roads based on vehicle class numbers
- Propagate source vehicle noise to other locations to create noise maps

Figure 1 shows a schematic of these steps. The user inputs include road data and geospatial data. Road data includes values such as the number of through lanes, the speed limit along road segments, the f-system—or type of road, such as interstate, principal arterial, or local road—and whether the location is urban or rural. Geospatial data[18] can include features such as nighttime light brightness, land cover, urban population, etc.

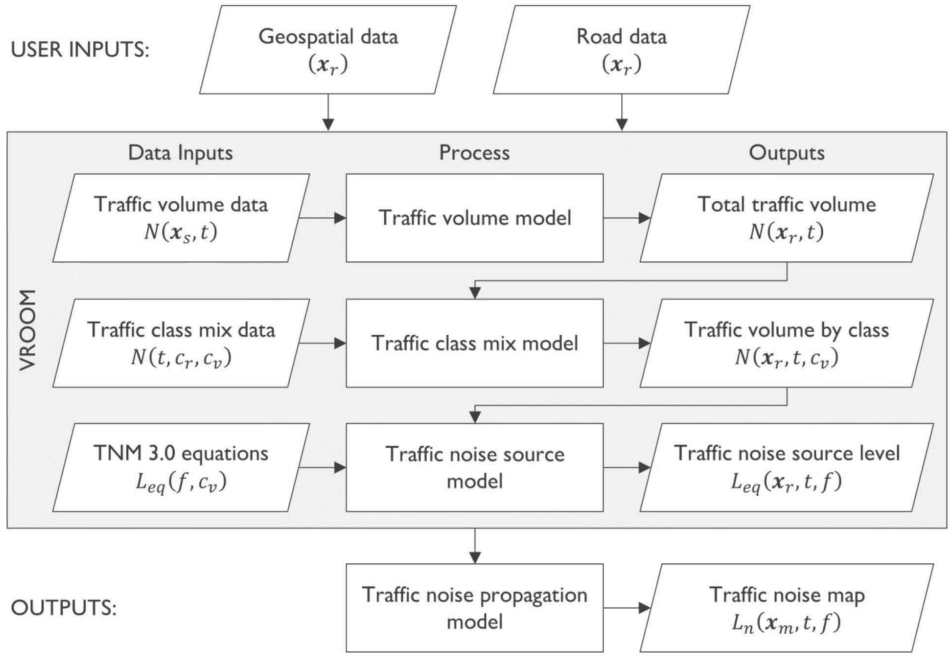

Figure 1. Flowchart outlining the steps towards creating a dynamic national road traffic noise map.

This paper considers only the traffic volume model part of VROOM—the first line of VROOM as shown in Figure 1—and does not consider the traffic class mix model or the traffic noise source model parts of VROOM. Instead of considering the full model, a simplified error metric for the traffic volume model is presented, which gives predicted decibel errors for VROOM-predicted traffic volume. Predicted errors when using yearly averaged vehicle numbers are also presented, which would be similar to expected errors in the Bureau of Transportation Statistics' National Transportation Noise Map near roads. Errors are calculated by comparing predicted vehicle numbers to reported vehicle numbers.

II. FOURIER ANALYSIS AND PRINCIPAL COMPONENT ANALYSIS OF TRAFFIC VOLUME

Fourier analysis can be used to find repeating temporal cycles or patterns in data. Reported hourly vehicle counts from 2015-2018 from by thousands of traffic monitoring stations located across CONUS[19] were used; by investigating the Fourier spectra produced, strong temporal patterns were found that represent daily, weekly, and yearly variation in traffic volume at individual stations. Repeatable temporal cycles were isolated by removing noise from the Fourier spectra. For further details, see "Toward improving road traffic noise characterization: A reduced-order model for representing hourly traffic volume dynamics" by Cook et al, Proc. Mtgs. Acoust. **45**, 055001 (2021).[20]

While using a denoised Fourier spectrum does create a simplified model for temporal variability of traffic volume at a particular location, PCA was also used to create a generalized model that can predict traffic volume at other locations. Fourier spectra were split into separate weekly and yearly cycles, and principal components were found to represent the most common combinations of

cyclic weekly and yearly traffic patterns found across stations. Because data from all stations were not equally reliable, a weighted PCA was used. See Cook et al. for further details.[20] Each resulting principal component represents a linear combination of several Fourier amplitudes or, by using an inverse Fourier transform, a specific traffic volume pattern. The principal component coefficients, which are simply numeric values, give the combination of these traffic volume patterns.

The first principal component vectors, one for the weekly data and another for the yearly data, are shown in temporal space in Figure 2, and give the weighted average traffic volume pattern seen across all stations. The yearly pattern shows little variation across the course of a year. The weekly pattern shows the weighted average hourly traffic pattern found across CONUS during the course of a week; weekends show a smooth hourly variation during daytime hours, while weekdays show an increase in morning and evening hours higher than that during the middle of the day (during rush hours), with less traffic activity during the nighttime hours. This type of traffic pattern is common for urban locations and is similar to data shown in Fu et al. (2017).[21]

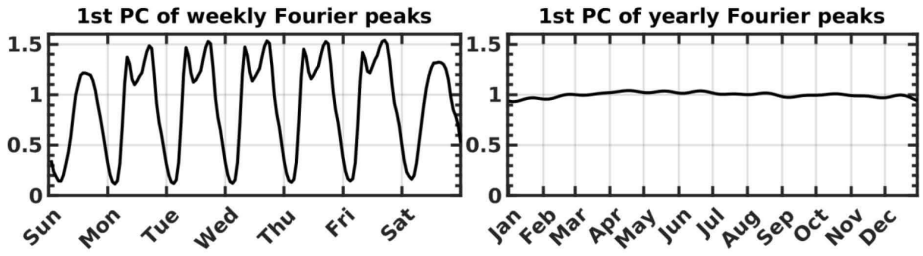

Figure 2. Normalized principal components which represent the most common normalized traffic patterns found across CONUS.

By using a normalized approach, VROOM was created to model hourly traffic volume, and requires just nine total coefficients to represent hourly traffic volume for any location. Eight of the

values are the principal component coefficients and are used to calculate the variation of traffic volume from the average traffic pattern. The other coefficient is the annual average daily traffic, AADT, which scales the total traffic pattern to give the correct average number of vehicles and is often known for any particular road. The methods for predicting VROOM coefficients are considered in the following section.

III. PREDICTION OF VROOM COEFFICIENTS

VROOM predicts dynamic traffic volume by predicting nine coefficients—or eight coefficients when the AADT is known. These coefficients can be predicted along any road by using location-dependent features. Pedersen el. al.[22] showed that several features (slope, distance to railroads, land cover, etc.) for a location can be represented using a non-linear basis, called diffusion coordinates (DCs). Because these DCs characterize locations, they can also be used to predict traffic volume for that location by predicting VROOM coefficients. For the current analysis, the first 12 DCs are used, along with road data, including features such as speed limit and the number of through lanes. Together these comprise the VROOM predictors.

Using the VROOM predictors and the known VROOM coefficients at traffic monitoring stations, a weighted least-squares method is used to find a best-fit linear transformation from predictors to coefficients. This yields a best-fit multiplying matrix X_0 so that VROOM predictors at arbitrary locations can be used to predict VROOM coefficients and therefore traffic volume at arbitrary locations. Using P as a matrix containing the VROOM predictors at each traffic monitoring station, W as a diagonal matrix for the station weightings, and C as a matrix containing the coefficients at each, the matrix X_0 can then be obtained and used to predict coefficients for

arbitrary locations. The coefficient matrix for arbitrary locations $\tilde{C}_{loc}$ is given by multiplying the matrix P_{loc}, which contains the VROOM predictors for those locations, by X_0.

$$X_0 = \min_X ||PWX - C|| = (P^T W P)^{-1}(P^T W C), \qquad \tilde{C}_{loc} = P_{loc} X_0. \tag{1}$$

The predicted coefficients $\tilde{C}_{loc}$ can then be used to obtain predicted traffic volume for any hour desired using the VROOM traffic volume model.

Figure 3 shows the normalized weekly and yearly VROOM predictions for stations in Idaho, Wyoming, and Oklahoma, known respectively as Site A, B, and C. Also shown are the average normalized traffic counts and the AADT representation, which uses the average value for all time periods. The average normalized traffic counts across a year are obtained by using the mean number of traffic counts for each week of the year, rather than each hour or day of the year. This is necessary because with only four years of data (2015-2018), average daily or hourly counts across a year would be heavily impacted by the days of the week for which data were available (at most 4 different days of the week). This approach removes this bias; unfortunately, it can also mask some of the benefit of predicting hourly values when looking at yearly predictions but is necessary for accurate comparison. Thus, comparisons show 168 hourly values for weekly results, and 52 weekly values for yearly results.

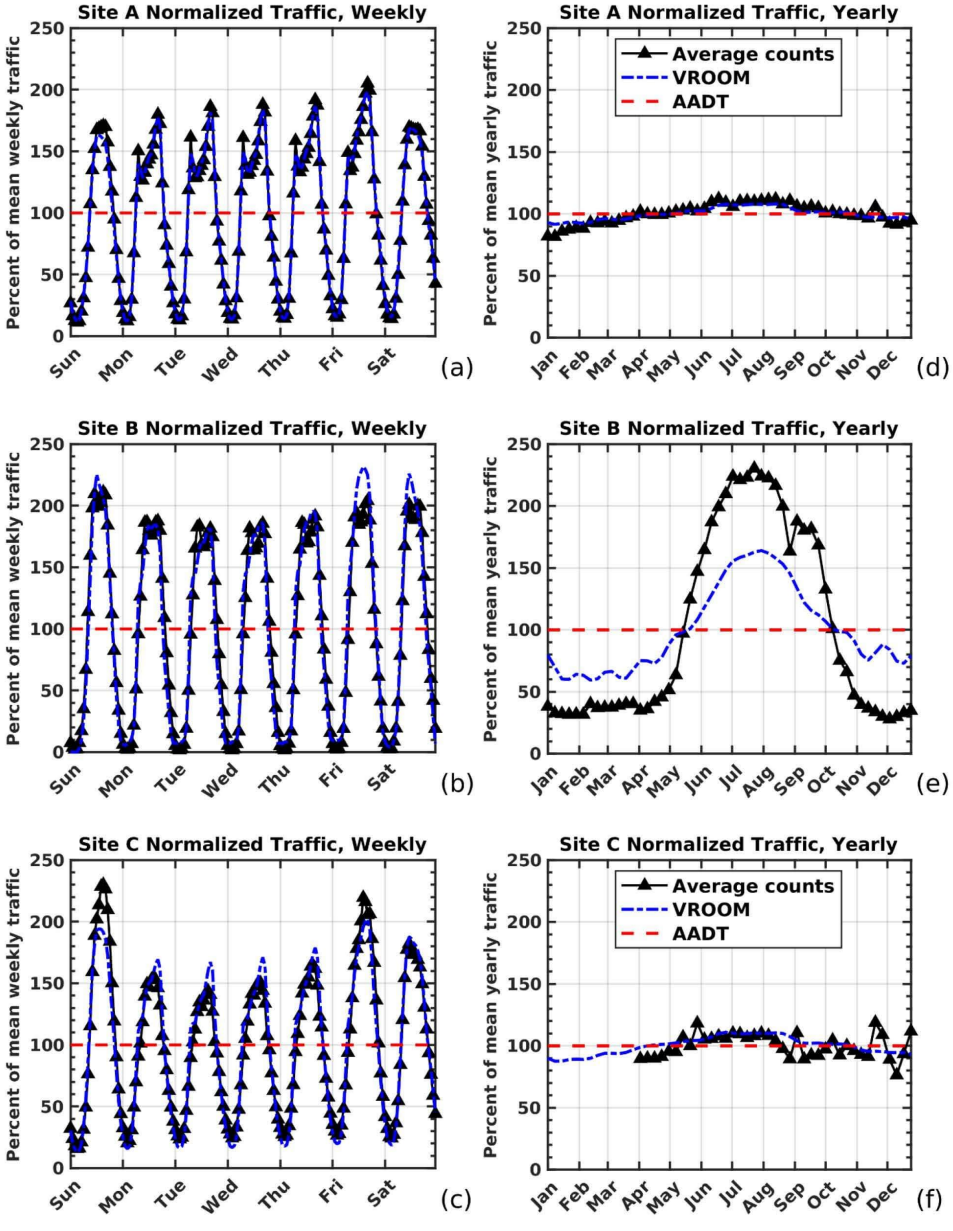
Site A Normalized Traffic, Weekly
Percent of mean weekly traffic
Sun
Mon
Tue
Wed
Thu
Fri
Sat
(a)
Site A Normalized Traffic, Yearly
Percent of mean yearly traffic
Average counts
VROOM
AADT
Jan
Feb
Mar
Apr
May
Jun
Jul
Aug
Sep
Oct
Nov
Dec
(d)
Site B Normalized Traffic, Weekly
(b)
Site B Normalized Traffic, Yearly
(e)
Site C Normalized Traffic, Weekly
(c)
Site C Normalized Traffic, Yearly
(f)

141

142

143

9

144 Figure 3. (Color online). For three sites, the weekly traffic patterns (left) and the yearly traffic
145 patterns (right) are shown. The average traffic counts can be compared with the VROOM
146 prediction.

147

148 Figure 3(a) shows the weekly patterns for site A, located in southern Idaho, with the
149 corresponding yearly patterns shown in Figure 3(d). There is high agreement between the averaged
150 data and the VROOM prediction. This site is typical of several locations across CONUS where the
151 VROOM prediction faithfully approximates reported vehicle counts.

152 Site B, which is located in northwest Wyoming and is shown in Figure 3(b) and Figure 3(e),
153 has a very different traffic pattern than Site A. The average reported traffic counts increase
154 dramatically in the summer and are higher on weekends than on weekdays, without any sort of rush
155 hour. This behavior, while not uncommon for seasonal roads like those near ski resorts or some
156 national parks, as this site is, is found in only a few locations across CONUS. While the VROOM
157 prediction is unable to fully capture the variability of the reported traffic counts, differing by up to
158 25%, it is still an improvement over the AADT approach, which can differ up to 57%.

159 Site C, located in Oklahoma and shown in Figure 3(c) and Figure 3(f), reported only counts
160 for April through December for a single year. As such, yearly errors cannot be calculated from
161 January through March. Though errors cannot be calculated for this time period, VROOM can still
162 predict the traffic volume despite the missing traffic counts. This shows an example of how
163 VROOM predictions can be made not just where and when counts are reported, but at roads across
164 all of CONUS for any time period.

165 While looking at results for a few individual locations is insightful, it is infeasible to show an
166 adequate number of locations individually, since there are millions of road segments across the
167 country. Multimedia 1 shows the relative VROOM predicted weekly traffic volume and Multimedia

168 2 shows the relative VROOM predicted yearly traffic volume at roads across the country, alongside
169 average traffic counts at traffic monitoring stations. Normalized traffic volumes are shown, and so
170 do not indicate total number of vehicles, but rather whether each location has more or less traffic
171 than it does on average. Differences between interstates and other roads can be seen, as well as
172 behaviors such as rush hours in cities. The AADT approach is not shown here, as it would give a
173 value of 100% for all time periods and locations.
174
175 Multimedia 1. Relative VROOM-predicted weekly traffic volume for locations across CONUS. Each
176 location is shown relative to its average weekly value of 100%.
177 Multimedia 2. Relative VROOM-predicted yearly traffic volume for locations across CONUS. Each
178 location is shown relative to its average yearly value of 100%.
179
180 **A. Sound level error metric**
181 Model prediction accuracies of both the VROOM and the AADT approaches can be calculated by
182 comparing average reported normalized traffic counts $N_{reported}$ to the predicted normalized traffic
183 volume $N_{predicted}$ at traffic monitoring stations. The 'prediction' for the AADT approach is simply
184 the average number of vehicles. A normalized approach is taken so that errors are a result of the
185 model prediction, and not caused by differences between the reported AADT and reported hourly
186 counts. From an acoustics viewpoint, a useful error metric is a sort of expected sound level error in
187 decibels. Because different vehicles can be considered to be uncorrelated sound sources, the
188 expected sound level error, E_{dB}, at a site can be determined at a particular time by
189
190 $$E_{dB} = 10\,log_{10}\left(\frac{N_{predicted}}{N_{reported}}\right) \quad (2)$$

191

192 With this metric, an error of +3 dB means that the number of vehicles predicted is double the
193 average reported number of vehicles, and an error of -3 dB means that the prediction is half the
194 average reported value.[6] This error metric gives expected model sound level errors based solely on
195 the traffic volume representation and reported vehicle numbers, without considering things such as
196 vehicles types or vehicle speed, and as such assumes no temporal change in vehicle class mix or road
197 conditions. While incomplete, this error metric is still viable to show relative errors between
198 VROOM and the AADT approach because everything except total traffic volume is assumed to be
199 the same for both methods. The AADT errors are at least partially indicative of possible expected
200 errors of the National Transportation Noise Map at the locations and times considered.
201

202 **B. Prediction accuracy**

203 While the prediction accuracy cannot be obtained for all locations, the weekly and yearly errors for
204 predictions of both methods can be calculated at traffic monitoring stations. Errors for sites A, B,
205 and C are shown in Figure 4. VROOM prediction errors are much smaller than AADT prediction
206 errors for most time periods, more noticeably for hours across a week and most drastically during
207 nighttime hours. The largest consistent VROOM prediction errors occur near midnight on weekdays
208 at sites with low traffic volume and are a result of either the predicted normalized traffic volume or
209 the normalized reported traffic counts being close to zero. Errors for each station are shown
210 geographically and temporally in Multimedia 3, which shows the weekly errors, and in Multimedia 4
211 which shows the yearly errors.
212

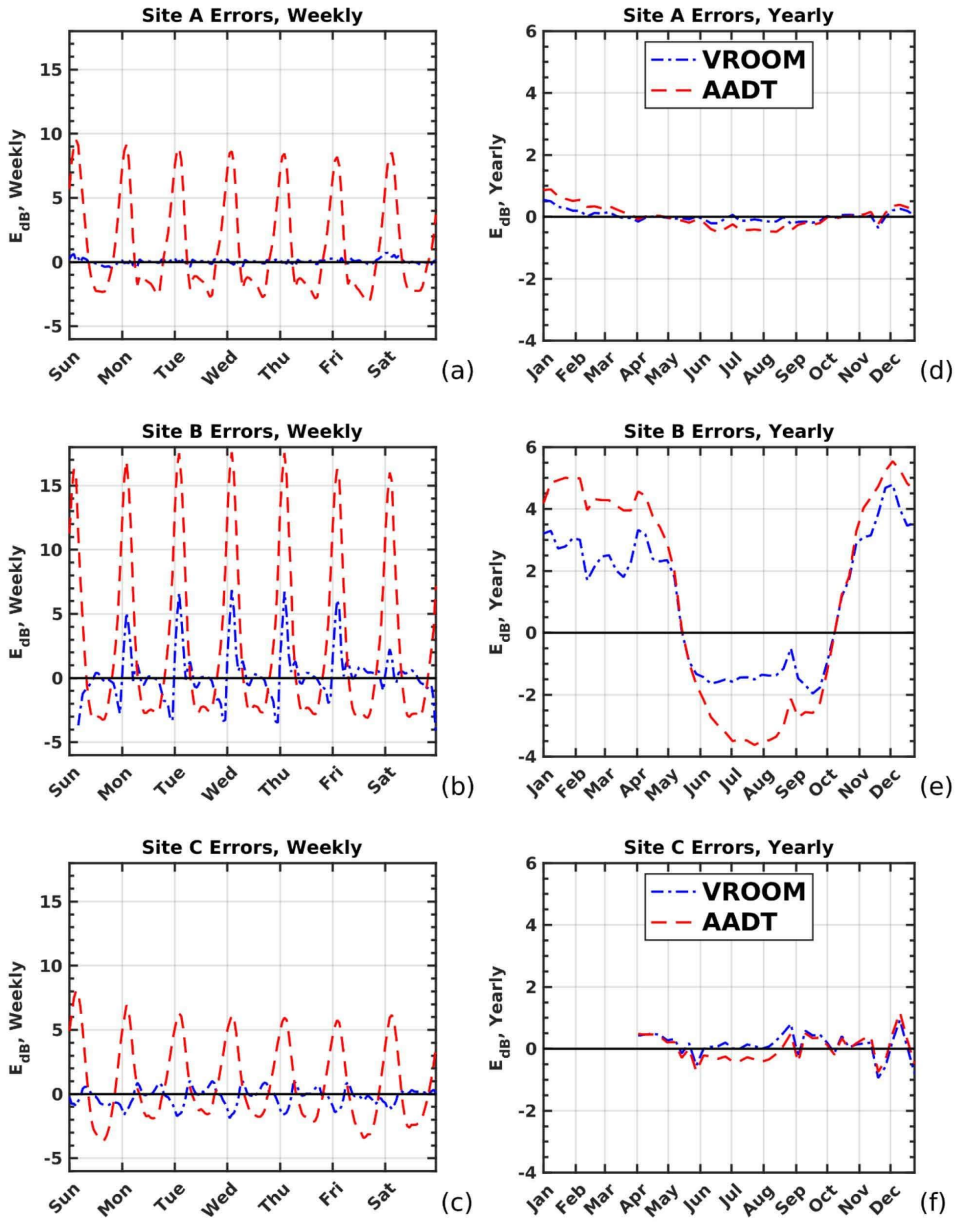

Figure 4. (Color online). Predicted model errors, both weekly (left) and yearly (right), for three sites.

Multimedia 3. VROOM weekly errors are shown alongside AADT weekly errors, shown geographically and temporally. VROOM gives much smaller errors than the AADT method for weekly errors.

Multimedia 4. VROOM yearly errors are shown alongside AADT yearly errors, shown geographically and temporally. VROOM gives slightly smaller errors than the AADT method for yearly errors, though differences are not as extreme as the weekly errors.

While errors vary across both time and space, and so are shown in video format, median absolute decibel errors, $|E_{dB}|_{50}$, averaged across either time or space, can be shown in static figures. The absolute value is needed so that positive and negative errors don't unjustly cancel one another out. The median errors across all locations can be calculated for each time period and are shown in Figure 5. The VROOM prediction errors are much smaller errors than the AADT prediction errors, again most noticeably across the hours of a week. While the absolute error does not show the sign, AADT errors are generally positive during nighttime hours and during the winter months, and negative during daytime hours and the summer months. VROOM errors may be either positive or negative. The largest errors occur during nighttime hours for both methods, and median AADT errors can exceed 10 decibels.

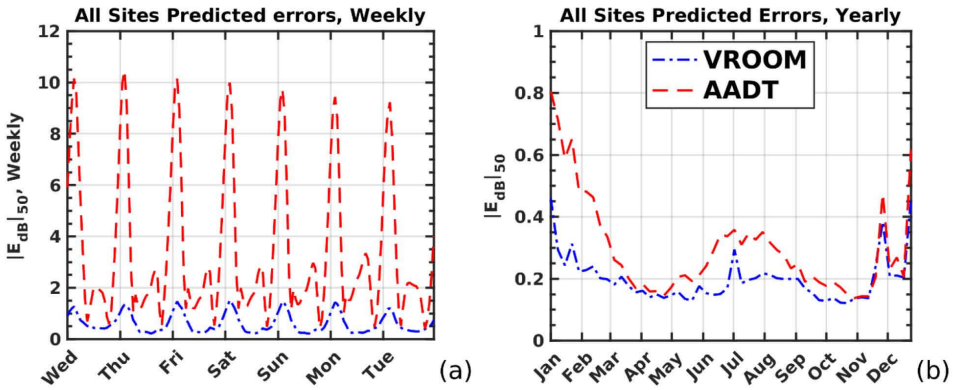

Figure 5. (Color online). Median location-averaged absolute VROOM and AADT errors, shown both weekly and yearly. The VROOM prediction errors are clearly smaller than AADT prediction errors, most especially for weekly errors. Median nighttime AADT prediction errors can exceed 10 dB, and median daytime errors can exceed 3 dB.

Figure 6 shows the median absolute errors when, instead of averaging across location, the absolute errors are averaged across time. The yearly expected errors for both methods are typically within 1 dB. This is because traffic volume does not change drastically by week of the year for most locations, with some notable exceptions, primarily in the northwest. While the VROOM prediction errors are generally slightly smaller, the AADT approach is a valid representation for most locations. The largest yearly errors for both methods can occur at sites near seasonal roads, like site B, which is in Jackson, Wyoming. While the VROOM prediction does not always reproduce that amount of variation faithfully, VROOM is still more accurate than the AADT method for nearly all locations.

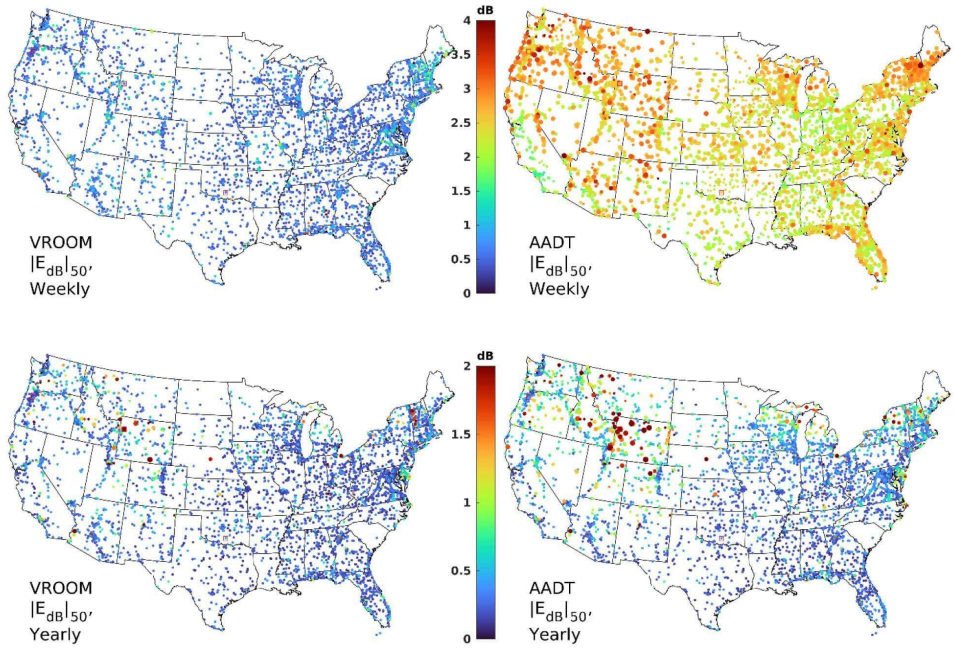

Figure 6. (Color online). Median time-averaged absolute VROOM and AADT errors, shown both weekly and yearly. The VROOM prediction errors are clearly smaller than AADT predictions, most especially for weekly errors. Notably, AADT weekly errors exceed 1.5 dB for 98.4% of locations VROOM weekly errors are less than 1.5 dB for 98.4% of locations.

A large difference between the methods is seen when considering the temporally averaged weekly errors. The AADT prediction errors exceed 1.5 dB for 98.4% of locations and exceed 3 dB for 4.3% of locations. In contrast, the VROOM prediction errors exceed 1.5 dB for only 1.6% of locations and exceed 3 dB for only 0.2% of locations. By predicting traffic volume for each hour with VROOM, errors are dramatically reduced across CONUS, with few significant errors.

Further insight can be gained by viewing the full distribution of errors, without using absolute median errors. Figure 7 shows histograms for both methods' errors, both for weekly and yearly time periods. The yearly errors for both methods, seen in Figure 7(b), are typically within ±1 dB, as was seen previously, with the AADT errors forming a slightly wider distribution with larger tails.

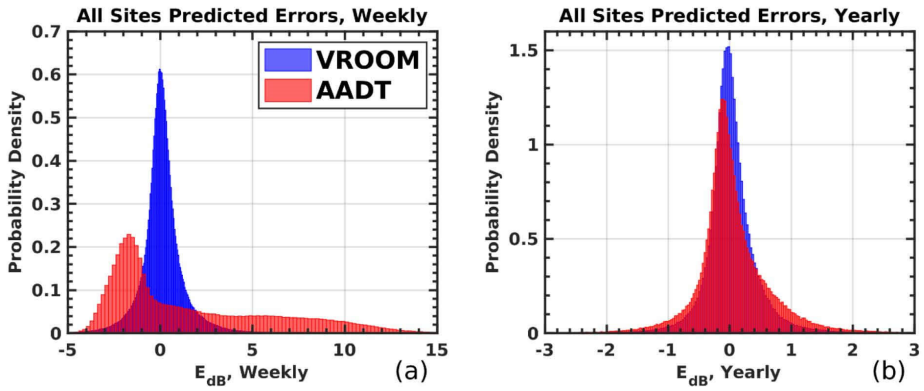

Figure 7. (Color online). Histogram of expected errors in decibels for the AADT approach and for VROOM. Weekly errors in particular are significantly reduced using VROOM.

The weekly errors tell a more interesting story. The weekly VROOM errors form a tight distribution, as do the yearly errors. However, the AADT error distribution is much different, peaking around -2 dB with a long, flat tail of positive errors. This indicates that hourly-averaged traffic volumes very poorly represent reported hourly traffic volumes. Expected errors evidence that average sound levels are seldom indicative of actual sound levels across the hours of a week. Modeling hourly traffic volume with VROOM can vastly improve expected hourly sound level predictions.

IV. CONCLUSION

The hourly-dynamic nature of traffic volume in its variety across CONUS can be represented in a concise manner using VROOM, which also enables prediction of traffic volume. Requiring just nine values—predictable from geospatial and road data—vehicle counts can be accurately represented and predicted with full temporal variability. By improving representation of traffic volume, road traffic sound levels can be better represented and predicted.

While using annual average daily traffic counts can give a decently accurate representation of traffic volume for most days of the year, daily and yearly averaged traffic counts do not accurately represent particular hourly traffic volumes. This means that annual average daily sound levels do not accurately portray what the actual sound level would be for most hours—not just during nighttime hours, where errors can often exceed 10 dB—but also for many daytime hours. By instead modeling traffic volume using reported hourly traffic counts with VROOM, sound levels can be more accurately predicted.

The approach outlined in this paper is the first step towards a dynamic national transportation noise map. In future, advancements towards predicting hourly road traffic noise can be made by accounting for dynamic differences in different vehicle classes, such as medium or heavy trucks, as different vehicle classes have different characteristic sound emission spectra. By accounting for differences in vehicle classes, both spectral and temporal variability of traffic noise can be better modeled and is a topic of ongoing analysis.

ACKNOWLEDGMENTS

This work was supported by a U. S. Army Small Business Innovation Research contract to Blue Ridge Research and Consulting, LLC, with Dr. James Stephenson as the technical monitor.

REFERENCES

[1] T. Hener, "Noise pollution and violent crime," Journal of Public Economics, Volume 215, November 2022, 104748. https://doi.org/10.1016/j.jpubeco.2022.104748.

[2] E. Öhrström, A. Skånberg, H. Svensson, A. Gidlöf-Gunnarsson, "Effects of road traffic noise and the benefit of access to quietness," Journal of Sound and Vibration, Volume 295, Issues 1-2, August 2006, pp. 40-59.

[3] C. Chin, Z. Y. Thang, and S. Saju, "Study on impact of noise annoyance from highway traffic in Singapore City," Proc. Mtgs. Acoust. **39**, 015001 (2019); doi: 10.1121/2.0001116

[4] G. Shannon, L. M. Angeloni, G. Wittemyera, K. M. Fristrup, K. R. Crooks, "Road traffic noise modifies behaviour of a keystone species," Animal Behaviour, Volume 94, August 2014, pp. 135-141.

[5] K. M. Parris and A. Schneider, "Impacts of Traffic Noise and Traffic Volume on Birds of Roadside Habitats, Ecology and Society, Vol. 14, No. 1, June 2009.

[6] D. R. Johnson and E. G. Saunders, "The evaluation of noise from freely flowing road traffic," Journal of Sound and Vibration, Volume 7, Issue 2, March 1968, pp. 287-288, IN1, 289-309.

[7] S. K. Tang and K. K. Tong, "Estimating traffic noise for inclined roads with freely flowing traffic," Applied acoustics, Volume 65, Issue 2, February 2004, pp. 171-181.

[8] Information on the National Transportation Noise Map by the Bureau of Transportation Statistics available at https://www.bts.gov/geospatial/national-transportation-noise-map (accessed April 2023).

[9] A. D. May, "Traffic Flow Fundamentals," Prentice-Hall Incorporated, 1990.

[10] F. Kessels, "Introduction to Traffic Flow Modelling," Springer Link, 2018.

[11] H. Xiao, H. Sun, B. Ran, and Y. Oh, "Fuzzy-Neural Network Traffic Prediction Framework with Wavelet Decomposition," Transportation Research Record 1836, no.1 (2003), pp. 16-20.

[12] P. Sun, N. AlJeri and A. Boukerche, "A Fast Vehicular Traffic Flow Prediction Scheme Based on Fourier and Wavelet Analysis," 2018 IEEE Global Communications Conference (GLOBECOM), 2018, pp. 1-6.

[13] D. S. Dendrinos, "Urban Traffic Flows and Fourier Transforms," Geographical analysis, Volume 26, Issue 3, July 1994, pp. 261-281.

[14] Y. Xie, Y. Zhang, and Z. Ye, "Short-Term Traffic Volume Forecasting Using Kalman Filter with Discrete Wavelet Decomposition," Computer-aided Civil and Infrastructure Engineering, Volume 22, Issue 5, July 2007, pp. 326-334.

[15] W. Min and L. Wynter, "Real-time road traffic prediction with spatio-temporal correlations," Transportation Research Part C: Emerging Technologies, Volume 19, Issue 4, August 2011, pp. 606-616.

[16] L. Li, S. He, J. Zhang, and B. Ran, "Short-term highway traffic flow prediction based on a hybrid strategy considering temporal-spatial information," Journal of Advanced Transportation, Volume 50, Issue 8, December 2016, pp. 2029-2040.

[17] K. Pedersen, M. K. Transtrum, K. L. Gee, S. V. Lympany, M. M. James, and A. R. Salton, "Validating two geospatial models of continental-scale environmental sound levels," JASA Express Letters 1, 122401 (2021).

[18] K. L. Pedersen, "Using Machine Learning to Accurately Predict Ambient Soundscapes from Limited Data Sets," BYU Theses and Dissertations, (2021).

[19] Federal Highway Administration Special Tabulations available at https://www.fhwa.dot/gov/policyinformation/tables/tmasdata/ (accessed April 2023).

[20] M. R. Cook, K. L. Gee, M. K. Transtrum, S. V. Lympany, M. F. Calton, "Toward improving road traffic noise characterization: A reduced-order model for representing hourly traffic volume dynamics," Proc. Mtgs. Acoust **45**, 055001 (2021). https://doi.org/10.1121/2.0001636.

[21] M. Fu, J. A. Kelly, and J. P. Clinch, "Estimating annual average daily traffic and transport emissions for a national road network: A bottom-up methodology for both nationally-aggregated and spatially-disaggregated results," Journal of Transport Geography, Vol 58, 2017, pp. 186-195.

[22] K. L. Pedersen, M. K. Transtrum, K. L. Gee, S. V. Lympany, M. M. James, A. R. Salton, M. F. Calton, "Feature reduction through manifold learning for a geospatial model of ambient soundscapes," J. Acoust. Soc. Am. **146**, 2906 (2019). https://doi.org/10.1121/1.5137083.

PART III: SPATIO-SPECTRO-TEMPORAL DATA MODELING

Chapter 6

Toward a dynamic national transportation noise map: Modeling spectral traffic noise emission levels

6.1 Introduction

This article expands upon the article in Chapter 5, going on to describe the traffic class mix model and how vehicular source noise is obtained from predicted traffic volume by class type. It shows how VROOM, the Vehicular Reduced-Order Observation-based Model, predicts traffic noise with hourly resolution and gives predicted traffic noise nationwide.

6.2 Required Copyright Notice

The following article is being prepared for submission to the Journal of the Acoustical Society of America, under the title "Toward a dynamic national transportation noise map: Modeling traffic class mix dynamics and traffic noise spectral source emission levels". It is reproduced in the format intended for submission, with rights granted in the Acoustical Society of America Transfer of Copyright document.

https://asa.scitation.org/pb-assets/files/publications/jas/jascpyrt-1485379914867.pdf

I hereby confirm that the use of this article is compliant with all publishing agreements.

6.3 Article for submission

Toward a dynamic national transportation noise map: Modeling spectral traffic noise emission levels

Mylan R. Cook,[1] Kent L. Gee,[1] Mark. K. Transtrum,[1] Shane V. Lympany,[2] and Matthew F. Calton[2]

[1] *Department of Physics and Astronomy, Brigham Young University, Provo, Utah 84602, USA*

[2] *Blue Ridge Research and Consulting, LLC, Asheville, North Carolina 28801, USA*

The National Transportation Noise Map predicts time-averaged road traffic noise across the continental United States (CONUS) based on annual average daily traffic counts. However, traffic noise varies temporally. This paper outlines a method for predicting nationwide hourly-varying source traffic sound emissions called VROOM, the Vehicular Reduced-Order Observation-based Model. VROOM includes three models that predict temporal variability of traffic volume, predict temporal variability of different traffic classes, and utilize equations from the Traffic Noise Model (TNM) 3.0 to give traffic noise emission levels based on vehicle numbers and class mix. Location-specific features are used to predict average class mix across CONUS. VROOM then incorporates dynamic traffic class mix data from the Federal Highway Administration's report "Vehicle Volume Distributions by Classification" by Hallenbeck et al (1997) to obtain dynamic traffic class mix. TNM 3.0 equations then give estimated equivalent sound level emission spectra near roads. Important temporal traffic noise characteristics are modeled, including diurnal traffic patterns, rush hours in urban locations, and yearly variation, for which a few examples are considered. Areas of uncertainty are identified. Altogether, VROOM can be used to map national transportation noise with temporal and spectral variability.

I. INTRODUCTION

Road traffic noise comprises a significant component of total anthropogenic noise in many developed areas and can have a large impact on diverse acoustic environments. Increased noise levels are correlated with anything from mild annoyance to an increase in violent crime, and evidences of the negative effects of traffic noise abound.[1-5] Humans are not the only species that is adversely affected by loud road noise, as many other species are also sensitive to noise.[6,7] Road noise cannot be effectively measured along every roadside in the country, and long-time-averaged levels are seldom accurate for particular times of day, so accurate modeling of road noise is necessary for improving road noise characterization.

Because overall road traffic noise is directly related to traffic volume—the number of vehicles per time period—road traffic noise characterization depends heavily on characterization of traffic volume itself, along with other parameters such as vehicle class mix, vehicle speed, pavement type, and road inclination.[8,9] The Federal Highway Administration's (FHWA) National Transportation Noise Map (NTNM) uses annual average daily traffic (AADT) counts to predict annually-averaged A-weighted 24-hr equivalent sound levels near major roads across the continental United States (CONUS).[10] While this map is useful for determining average sound levels, it lacks temporal variability, and so may not reflect the actual sound level for a particular time of the day or night. This is important not only for calculating average traffic noise exposure, but hourly traffic noise exposure, as some areas have higher noise levels at night as well as during the daytime.

In Cook et al (2021),[11] a method to represent traffic volume dynamics was outlined. This traffic volume model is the first part of VROOM, the Vehicular Reduced-Order Observation-based Model, a flowchart of which is shown in Figure 1. By using a combination of road data (e.g., speed limit, through lanes, road classification) and geospatial data (e.g., combinations of features like nighttime light brightness, land cover, and population), the VROOM traffic volume model predicts

dynamic traffic volume across CONUS. Further developments of the traffic volume model, along with expected sound level errors in decibels based on total traffic volume were presented and compared to expected errors when using time-averaged traffic volume in Cook et al. (2023)[12]. The VROOM predictions were shown to have much smaller errors than the errors obtained from using time-averaged traffic volume.

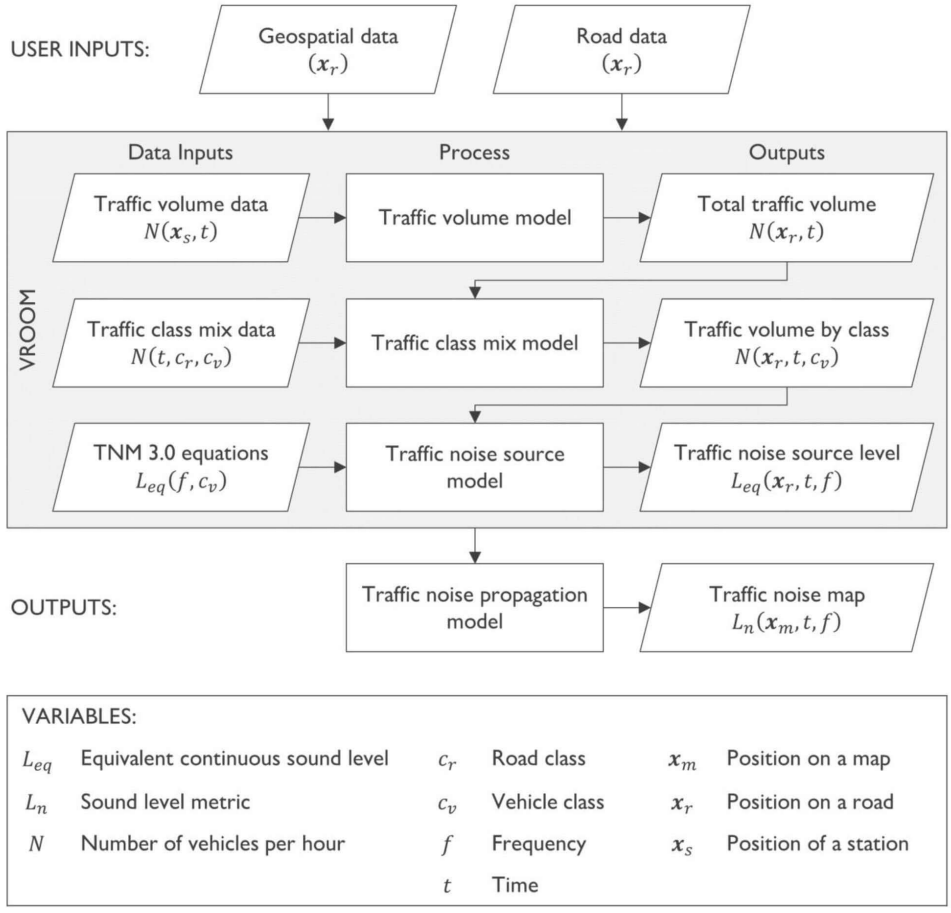

Figure 1. Flowchart outlining the steps towards creating a dynamic national road traffic noise map. For further information on the traffic volume model piece of VROOM, see Cook et al.[12] The traffic class mix model and traffic noise source model are presented in this paper.

While the traffic volume model aspect of VROOM is an important step towards calculating dynamic sound levels characteristic of road traffic, another important step is to characterize traffic

class mix, or the different types of vehicles that compose the total traffic volume. Heavy trucks produce much higher sound pressure levels than smaller vehicles, and their characteristic sound spectra also differ. This paper outlines the traffic class mix model and the traffic noise source model utilized by VROOM, as shown in Figure 1. By combining hourly class mix predictions with total vehicle number predictions, hourly vehicle numbers for each traffic class type are predicted.

When vehicle class numbers are known, either reported or predicted by VROOM, the Federal Highway Administration's (FHWA) Traffic Noise Model (TNM) 3.0 equations can be used to predict hourly spectral traffic noise source levels.[13] Spectral traffic noise source levels, or traffic noise emission levels, are the predicted one-third octave band A-weighted equivalent levels, or LAeq, produced by a given number of vehicles of each traffic class type. As defined by the TNM 3.0 equations,[13] the traffic noise emissions give an estimate of the spectral levels that would be measured 15 m (15 ft) from a road segment at a height of 1.5 m (5 ft), dependent on vehicle traffic class numbers, speed, and road type.

By incorporating the TNM 3.0 equations,[13] given road data and geospatial data, VROOM predicts traffic noise source levels across CONUS. As shown in Figure 1, the predicted traffic noise source levels can then be used in conjunction with traffic noise propagation models to predict traffic noise across the continent with spatial, spectral, and temporal variation. VROOM-predicted noise levels do not include propagation of sound to acoustic receivers at different distances from roadways, but instead give predicted traffic noise source levels for individual road segments. Propagating source levels to get full spatial variability remains a topic of future consideration.

VROOM can be useful for many different applications beyond the noise applications mentioned previously. Urban planning uses traffic congestion, and so can benefit from additional insights into traffic dynamics.[14,15] Similarly, freight analysis framework forecasting could be aided by

62 the VROOM framework.[16-18] Beyond characterizing noise emissions, VROOM could also be helpful
63 for traffic planning in reducing greenhouse gas emissions.[19]
64
65 ## II. GEOSPATIAL AND ROAD DATA
66 VROOM uses a combination of geospatial and road data to predict temporal variability of traffic
67 volume. In this section, these input variables are considered. While the geospatial data values are
68 known everywhere across CONUS, road data may or may not be reported, so VROOM accounts
69 for missing road data by using default values utilized by TNM, and when default AADT values are
70 not available, VROOM predicts road data using known road data at other locations.
71 ### A. Geospatial data
72 The geospatial data used by VROOM comprise 13 values for each location and are known
73 everywhere across CONUS. One is a Boolean value indicating whether or not a location is classified
74 as urban (including suburban), or as rural. The other 12 values are known as Diffusion Coordinates
75 (DCs) and are explained in Pedersen et al. (2021).[20] The DCs are a reduced-order model representing
76 a combination of 51 geospatial features, including brightness of nighttime lights, population density,
77 land use, etc. The values for the first DC are shown across CONUS in Figure 2. For maps of these
78 13 geospatial values at roads across CONUS, see the appendix.

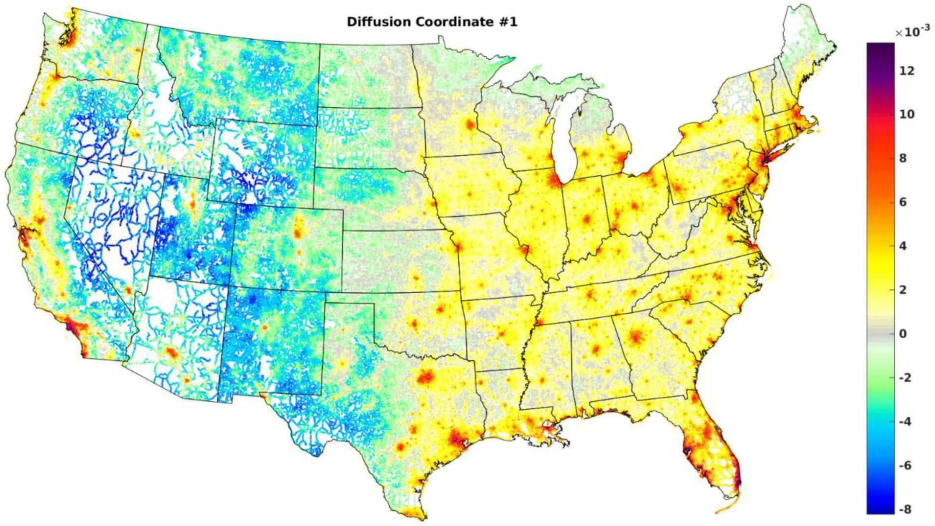

Figure 2. (Color online).Values for the 1st diffusion coordinate are shown geographically. For all 12 DC values, see the appendix.

B. Road data

While hourly traffic counts are only reported at a few thousand locations across CONUS, road data are reported for millions of road segments across CONUS. However, for locations where road data are unknown, TNM default values can be used for the number of through lanes, the f-system, pavement type, and speed limit. Additionally, VROOM limits these values in computation to avoid unnecessary complexity, such as limiting the maximum number of through lanes to be eight. To see the reported values alongside the values used by VROOM, see the appendix.

1. AADT

Dealing with missing AADT values, and also with missing average class mix data, is more difficult, because default values are not available. Instead, values must be predicted. Several methods were investigated for predicting the AADT. Ultimately, separate models were created for different f-

system values (which distinguish interstates, other freeways, etc.), urbanization (urban or rural), and for each individual state, since states tend to have very different AADT values, even when other road and geospatial values are similar. For each model, a least-squares fit of the logarithmic value of the AADT, with the DCs as the predictive variables, was found to give reasonable results. Mathematically, for D_{s_i,u_i,f_i} being the diffusion coordinates for all roads with a particular set of state, urbanization, and f-system values, and A_{s_i,u_i,f_i} being the logarithm of the known AADT, the predicted logarithmic AADT values $\tilde{A}_{s_i,u_i,f_i}$ are given by:

$$\begin{gathered} X_{\mathrm{s_i,u_i,f_i}} = \min_X \left|\left|D_{s_i,u_i,f_i}X - \mathrm{A}_{s_i,u_i,f_i}\right|\right| = \left(D^T_{s_i,u_i,f_i}D_{s_i,u_i,f_i}\right)^{-1}\left(D^T_{s_i,u_i,f_i}\mathrm{A}_{s_i,u_i,f_i}\right) \\ \widetilde{\mathrm{A}}_{s_i,u_i,f_i} = \widetilde{D}_{s_i,u_i,f_i}X_{\mathrm{s_i,u_i,f_i}} \\ u = \{\text{urban, rural}\},\ s = \{\text{US states}\} \\ f = \{\text{Interstate, Other freeway, Principal arterial, Other}\}. \end{gathered} \tag{1}$$

The AADT for all reported locations is shown alongside the AADT used by VROOM in Figure 3. By design, predictions are always positive. While many locations do report AADT values, VROOM can predict the AADT at all roads. The locations with predicted AADT values are better

seen in the western states, where road density is less than in eastern states. Results appear reasonable, and possible prediction biases are considered in Section V.

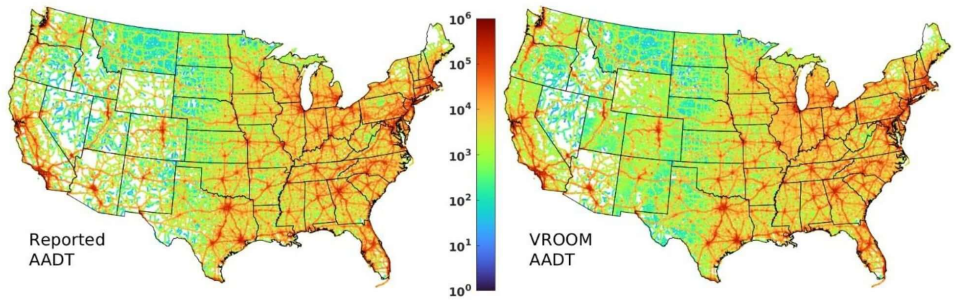

Figure 3. Reported AADT values are shown alongside AADT values used by VROOM. VROOM is able to predict reasonable results at locations where AADT values are not reported.

2. Average traffic class mix

Average traffic class mix, like AADTs value, are not reported along all road segments. Before a dynamic class mix can be predicted, the average class mix must be predicted when it is unknown. A similar method to the AADT prediction method is used, but with a few additional constraints.

To be physically meaningful, individual traffic class mix percentages must always be between 0% and 100%. Additionally, the sum of all traffic class mix predictions must be equal to 100%. While these constraints can be met in various ways, such as ensuring non-negativity and regularizing predictions, another option is to convert traffic class mix percentages into n-dimensional spherical coordinates on a hyperplane.[21] For a particular traffic class mix of the three main traffic class types (combination trucks, single-unit trucks, and other vehicles), this can be represented as a point on the plane $x + y + z = 1$, which is characterized by the two angular coordinates θ_1 and θ_2 where $0 \leq$

123 $\theta_i \leq \frac{\pi}{2}$, as shown in Figure 4. This approach is generalizable to any number of traffic class types, and

124 is not limited to just the main three traffic class types.

125

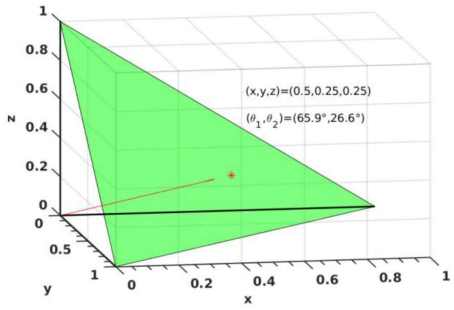

126

127 Figure 4. (Color online). A visual representation of a particular traffic class mix. The sum of the

128 three percentages, represented by x, y, and z, must equal 100% (or a value of 1), and so lie on the

129 plane shown. Any point is uniquely identified by two angular coordinates.

130

131 The average traffic class mix is predicted in the same way as the AADT, but by way of

132 predicting angular coordinates rather than values or percentages directly. The angular coordinates

are then converted to percentages for each traffic class type. Figure 5 shows the reported percentages of both single-unit and combination trucks alongside the percentages used by VROOM.

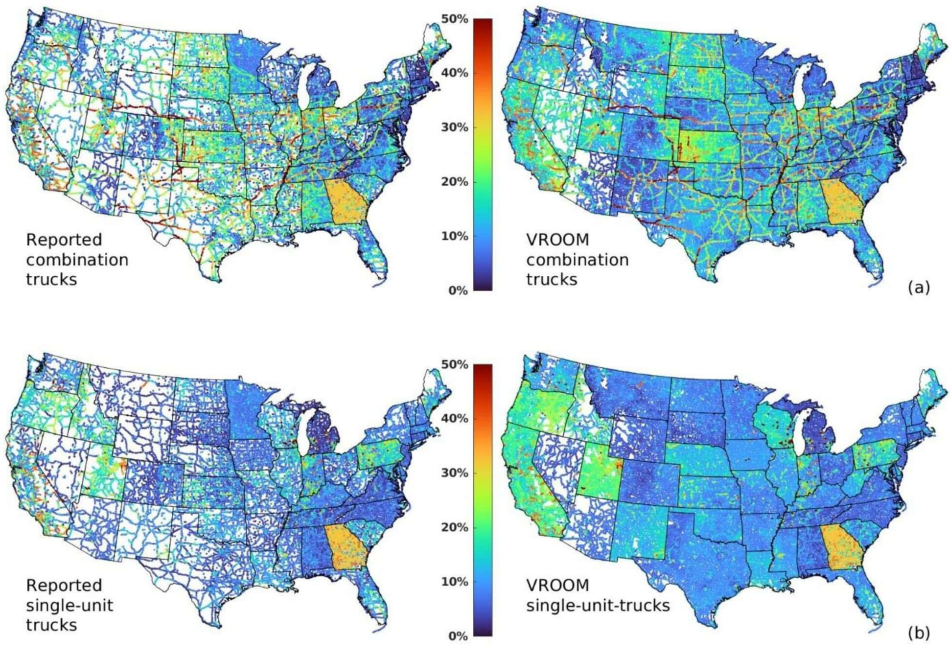

Figure 5. (Color online). Reported percentage of traffic that are combination (a) or single-unit trucks (b) shown alongside the percentages used by VROOM. Predicted percentages are only needed at locations where traffic class mixes are not reported. Differences in reported values by different states explain the need for creating models for each state separately.

III. TRAFFIC CLASS MIX MODEL

With either reported or predicted average traffic class mix values, VROOM can then model temporal variation in traffic class mix numbers. In 1997, a FHWA report was published by

146 Hallenbeck et al.[22] This report includes observed characteristic temporal variation of the three main
147 traffic class types for both urban and rural locations, and, despite its age, is still used by the FHWA
148 for traffic volume by vehicle classification. The results of this report can be used together with
149 VROOM's traffic volume model to predict temporal variation in each traffic class type on roadways
150 across CONUS. Yearly variation is predicted separately from weekly variation, as outlined below.
151
152 **A. Yearly variation**

153 Observed yearly traffic characteristics of different traffic class types from Hallenbeck et al.
154 (1997)[22] are reported on a month-by-month basis for both urban and rural locations (see Table 7 in
155 the report). The monthly resolution reported is a discreet representation of just twelve values.
156 However, using VROOM's traffic volume model, smooth yearly traffic variation can be represented
157 with just three values. For further details, see Cook et al. (2021).[11] The three coefficients to represent
158 the relative amount of combination trucks across a year (and three to represent single-unit trucks,
159 and three more to represent other vehicles), are found by using an optimization method, yielding the
160 coefficients which create the yearly traffic flow pattern which most closely matches the step-wise
161 reported yearly traffic variation of each traffic class type in the Hallenbeck data.

162 The Hallenbeck data represent the compilation of traffic counts at 99 geographic locations,
163 and the reported values are given for each month of a year. The VROOM representation was
164 obtained from traffic count data at thousands of geographic locations, with values for each hour of a
165 year. By finding a VROOM representation to approximate the Hallenbeck data, a smoothed traffic

pattern based on nationwide reported traffic flow behavior is obtained. The Hallenbeck data are shown together with the fitted pattern in Figure 6.

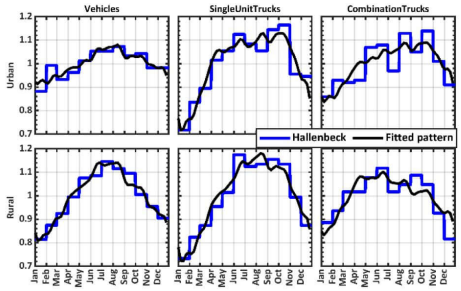

Figure 6. (Color online). Average relative amount of each traffic class type on both urban and rural roads, as seen in Hallenbeck et al. and the fitted pattern using VROOM's yearly traffic volume model representation.

Note that because the mean average relative amount is equal to one, the fitted value can be used as a yearly traffic class multiplier. When multiplied by the average traffic class percentage and the predicted total traffic volume, the product gives the predicted traffic volume for that particular traffic class type (e.g., the number of combination trucks) at that time period.

B. Weekly variation

Observed weekly traffic characteristics of different traffic class types from Hallenbeck et al. (1997)[22] are reported on a day-of-week basis and an hour-of-day basis for both urban and rural locations (see Table 3 and Figure 6, respectively, in the report). By combining the two, a total hour-of-week characteristic variation is obtained. While this makes for a relatively smoothly varying representation, there is some discontinuity when transitioning to and from the weekends, most

184 notably for heavy/combination trucks. Further refinements, such as accounting for the lack of rush
185 hour traffic for urban vehicles on weekends, are made in Hallenbeck et al.[22]

186 Rather than refining each class type and time period, the approach taken in this paper is to
187 use VROOM's traffic volume model to find a similar VROOM representation for weekly traffic
188 patterns of each traffic class type. The same approach outlined to fit the yearly data is used to find
189 five coefficients for vehicles and five coefficients for single-unit trucks.

190 For combination trucks, a five-coefficient VROOM representation does not accurately
191 represent observed patterns. This is because the number of combination trucks does not decrease
192 significantly during nighttime hours. This highlights a potential weakness of the VROOM weekly
193 representation; because observed total traffic volume always decreases during nighttime hours, the
194 VROOM representation cannot accurately represent traffic patterns that do not decrease during
195 nighttime hours. Instead of using the VROOM representation for combination trucks, the transition
196 to and from weekend combination truck numbers is simply smoothed by adjusting the hours around
197 midnight, which removes the large discontinuities in reported numbers.

198 The reported and fitted weekly traffic patterns for each traffic class type are shown in Figure
199 7. The fitted patterns shown approximate the combined patterns of the Hallenbeck data on
200 weekdays for all traffic class types. On weekends for single unit trucks, and more obviously for
201 vehicles, a more smoothly varying pattern is found, which does not include the artificial morning
202 and evening rush hours. While the Hallenbeck data are further refined using additional methods (to
203 remove erroneous rush hour patterns on weekends), the VROOM representation is automatically
204 able to remove such artifacts since the representation was created using observed traffic counts. The

smoothed pattern shown for combination trucks does not entirely vary smoothly, but does account for the temporal variation, and removes discontinuities on weekday/weekend transitions.

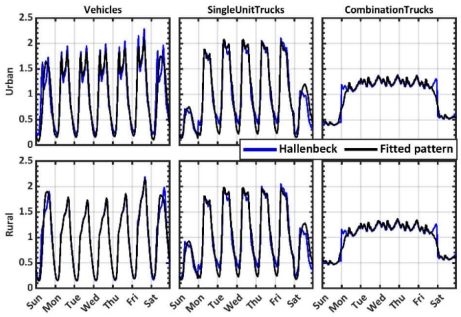

Figure 7. (Color online). Observed and fitted hour-of-week traffic patterns for each of the three major traffic class types.

Figure 5 showed time-averaged reported and modeled traffic class mix percentages without accounting for temporal variation. VROOM predicts the dynamic class mix percentage at any location by multiplying the predicted temporal variation with the average class mix at that location, explained further in the next section. Multimedia 1 shows an example of the temporal variability across the hours of a week by showing the predicted percentage of trucks (the sum of both combination trucks and single-unit trucks). Urban locations often have a low percentage of trucks both day and night, while freeways often have larger percentages, as expected.

Multimedia 1. The predicted percentage of trucks (both combination and single-unit trucks) for hours across a week. Averaged hourly predictions across time match reported time-averaged percentages by design.

C. Combining with average predictions

Because the weekly and yearly traffic class predictions are normalized, combining them with the average traffic class for any time period desired requires only simple multiplication. The predicted number of heavy trucks for a particular time is calculated by multiplying the relative weekly prediction for that time, the relative yearly prediction for that time, the average percentage of combination trucks at that location, and the average predicted traffic volume at that location (the AADT divided by 24). Due to the constraints, the predicted number of vehicles of each class type will always be non-negative, and the sum of vehicles of each class type for any hour will be the total number of vehicles predicted for that hour. In this manner annual average daily traffic values are maintained.

IV. SOUND EMISSION SPECTRA

With the predicted number of vehicles of each class type for any time period, calculating the predicted sound emission spectra requires use of the Traffic Noise Model or TNM 3.0 equations (see Appendix A in the technical manual, particularly Equation 5),[13] as was outlined in Figure 1. With these equations, the predicted number of vehicles of each class, the speed limit (whether or not this is a good indication of how fast vehicles are actually going), and pavement type at each location, sound emission spectral levels can be predicted for any time period, with up to hourly resolution. The predicted overall sound pressure levels give a predicted 1-hour A-weighted equivalent sound level, LAeq, at a distance 15 m (50 ft) from each road at a height of 1.5 m (5 ft), which is the predicted traffic noise source level.

Figure 8 shows the time-averaged predicted 1-hr LAeq across CONUS. Interstates and other freeways are seen to be the dominant sources of traffic noise across the country, and on several

247 freeways sound levels exceed 85 dBA, while smaller roads are much quieter, some with sound levels
248 below 35 dBA.
249

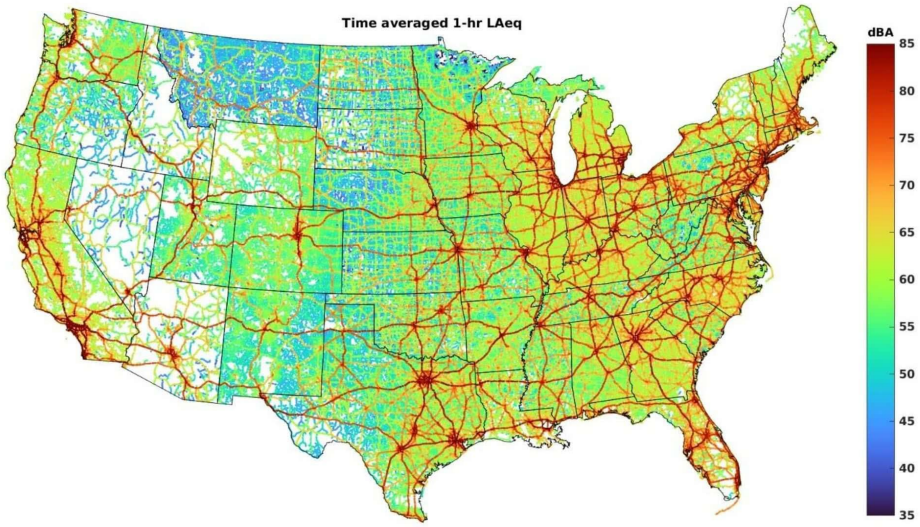

250
251 Figure 8. (Color online). Time-averaged predicted traffic noise source levels across CONUS.
252
253 While the VROOM-predicted average sound levels are useful, the NTNM already gives
254 time-averaged levels for geographic locations.[10] The utility of VROOM is that it can predict source
255 levels for any time period and frequency of interest. VROOM-predicted sound levels are more easily
256 understood using multimedia, so that results can be seen both spatially and temporally. Subsection A
257 shows the weekly and yearly temporal variability of VROOM-predicted sound levels across CONUS

using multimedia. Subsection B shows VROOM predictions for two specific time periods, and Subsection C explains spectral variability of VROOM predictions.

A. Temporal variability

Multimedia 2 shows the predicted levels for each hour across a week, with the time given being the local time for each location. Most locations, especially more rural locations, have a significant decrease in sound level during nighttime hours (see Subsection B below for specific examples). For most locations, weekends show smooth increases and decreases in overall level. Rural weekday locations show a similar pattern, while urban weekdays show rush hours both morning and afternoon, rather than smooth increases and decreases over the day. Friday evenings also show a more protracted decrease in sound levels.

Multimedia 2. Predicted sound levels at locations across CONUS for each hour across a week, in local time for each location.

In general, sound levels do not change as drastically across days of a year as they do across the hours of week. Instead of showing the predicted sound levels across the days of a year, Multimedia 3 shows the predicted yearly levels relative to the time-averaged sound level for each location. A value of 3 dBA means that for that particular location, the noise level for that time period is 3 dBA louder than the time-averaged level at that location. Note that since some locations have higher sound levels than others on average, a location with a value of -5 dBA may still have a higher overall level than a location with a value of -2 dBA. The differences should not be confused with absolute levels. With this in mind, the changes across the year in different parts of the country are more easily seen in this manner. In the west, especially in locations where national and state parts are common, large changes can be observed from the summer to the winter. In more urban

282 locations, there is less variation across the year. Adjacent locations show similar trends, with smooth
283 spatio-temporal variation.
284
285 Multimedia 3. Predicted sound levels at locations across CONUS for each day across a year, shown
286 relative to the average sound level for each location.

287 **B. Examples of specific time periods**

288 Predictions for two different time periods are given in this subsection. Note that in all
289 results, local time is used for all locations. Additionally, as was done in Multimedia 3, levels are
290 shown relative to the time-averaged LAeq (which was given in Figure 8), and so two locations with
291 the same difference value do not necessarily have the same total level.

292 For the first example, Figure 9 shows relative predicted levels for a weekday nighttime in
293 December. Results therefore show a combination of the weekly behavior and the yearly behavior for
294 a location. Sound levels are seen to be lower than average for all locations, which is a result of the
295 hourly variation across a week, as well as the absence of weekday traffic. There is more variation in
296 the western states, as was seen in Multimedia 3, and so is likely a result of decreased traffic in
297 December. While some urban areas show more variation than surrounding areas, cities generally still
298 have higher sound levels at all times since they have much higher time-averaged levels. This shows

299 that sound level variability is not equal, and some locations exhibit large changes in sound level while
300 others show only small changes.
301

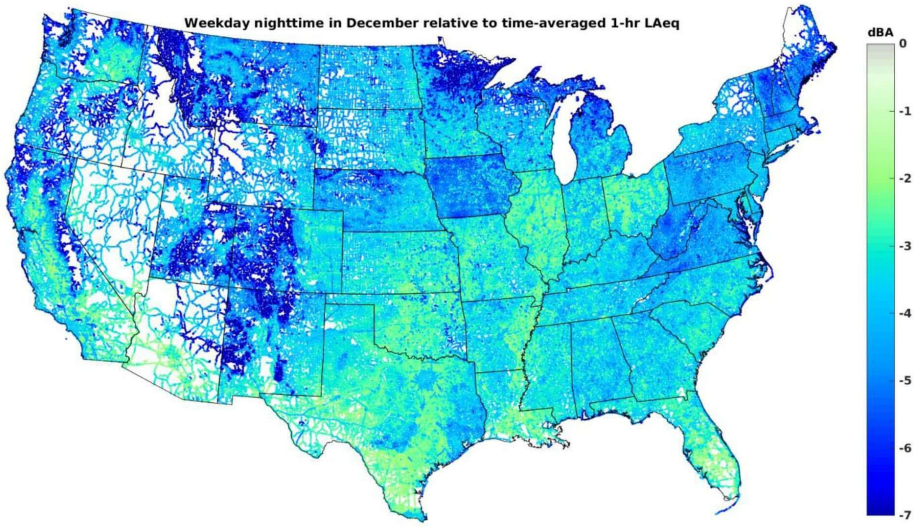

302
303 Figure 9. (Color online). VROOM predicted sound levels for a weekday nighttime in December
304 relative to the time-averaged levels for each location.

305 For the second example, Figure 10 shows the relative predicted levels for a weekend
306 afternoon in July. For many locations sound levels are higher than average, most notably in the
307 Rocky Mountain areas from Montana to New Mexico, as the mountainous areas are much more
308 popular destinations during summer weekends than during wintertime. For some of the larger cities,

sound levels are lower than on average. This could be a result of less traffic in cities due to more people being outside of cities for summer vacations.

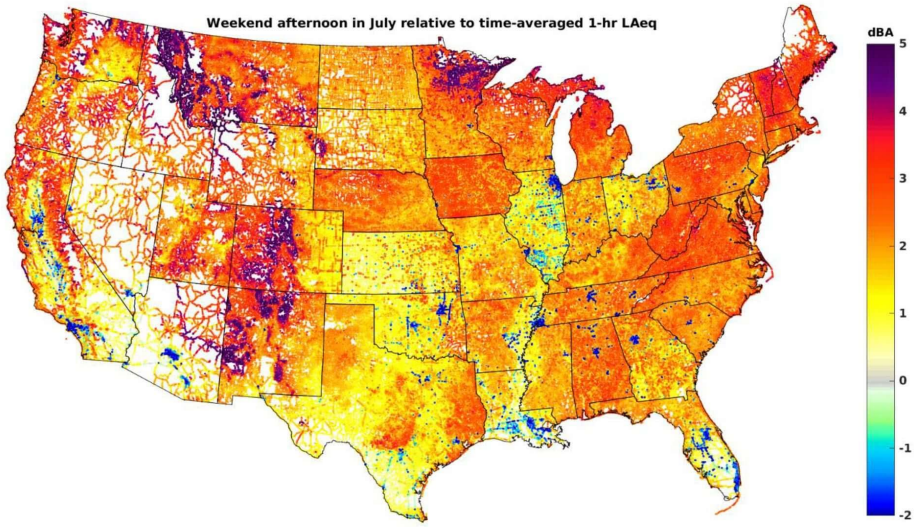

Figure 10. (Color online). VROOM predicted sound levels for a weekend afternoon in July relative to the time-averaged levels for each location.

C. Spectral variation

Consideration has been given thus far primarily to the temporal variability of traffic noise. The spectral variability of traffic noise is also important to consider. Not only do combination trucks produce higher sound levels than smaller vehicles, but they also have fundamentally different spectral characteristics. Predicted time-averaged spectral characteristics are seen in Multimedia 4, which shows differences from the overall sound pressure level for each location and frequency. Differences in spectral characteristics seen between interstates and small roads are primarily a result of different percentages of the vehicle class types, though the speed limit does contribute to spectral

differences as well. This primarily shows that spectral shapes of noise from interstates differs from the spectral shape of noise from smaller roads. Multimedia 4 shows only the time-averaged spectral characteristics, while in reality VROOM predicts spectral characteristics in a dynamic manner.

Multimedia 4. Characteristic spectral differences from the overall sound pressure level for each location across third-octave bands.

V. UNCERTAINTY QUANTIFICATION

The National Transportation Noise Map (NTNM) gives a 24-hr LAeq for road noise across CONUS. VROOM was created to address the temporal and spectral variability of road traffic noise, and so gives a 1-hr LAeq traffic noise source level for individual road segments. To truly create a temporally and spectrally varying traffic noise map, source levels would need to be mapped to physical locations using sound propagation methods (see Figure 1). Additional adjustments due to objects like sound barriers should also be considered. Thus, a direct comparison of NTNM to VROOM-predicted noise levels is not useful at this time. However, the time-averaged 1-hr LAeq shown in Figure *8* was calculated directly using the TNM 3.0 equations, and as such gives the source levels like those used to create the NTNM.

Instead of comparing predicted vehicle emission levels to time-averaged levels, the uncertainty of VROOM is considered in regard to the location of traffic monitoring stations (TMSs). The VROOM traffic volume model was created using hourly vehicle counts from TMSs across CONUS. The locations of these stations are shown in Figure 11. The VROOM coefficients which represent the weekly and yearly traffic flow variability for any location are calculated using the DCs for that location, and values are shown spatially in the appendix. Much of the uncertainty in VROOM comes from the dissimilarity of geospatial and road data values at traffic monitoring stations compared to value found across CONUS.

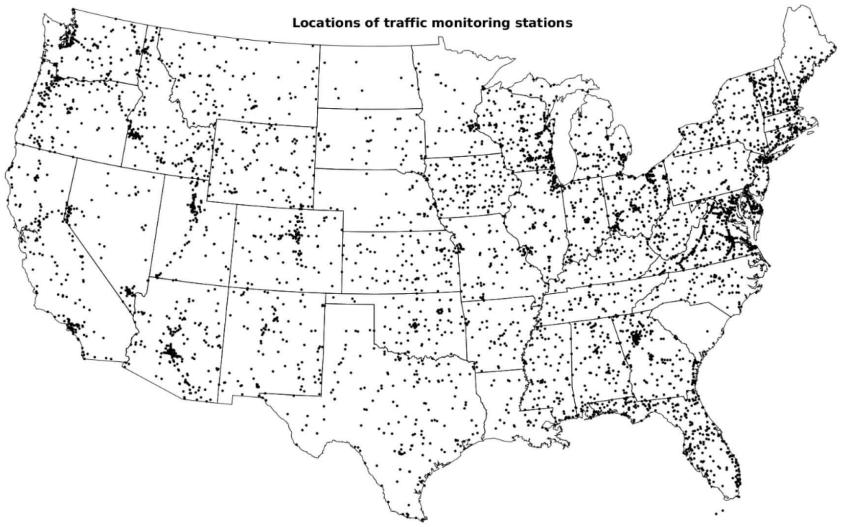

Figure 11. TMS locations across CONUS.

A. Uncertainty based on road data

One form of uncertainty is caused by the bias of TMS locations relative to road data. Ideally, the distribution of any road data at TMS locations should match the distribution seen across CONUS. If the TMS distribution is more weighted towards a particular value than the CONUS distribution, then that value will have more impact on VROOM, and other locations will be underrepresented. For categorical road data such as urbanization, f-system, and pavement type, the distributions can be characterized simply by comparing what percentage of locations are in each category. These results are tabulated in Table 1.

Table 1. Comparisons of the distributions of urbanization, f-system, and pavement type across TMS locations and across roads throughout all of CONUS.

Distribution of urbanization				
TMS	46.2% urban		53.8% rural	
CONUS	38.8 % urban		61.2% rural	
Distribution of f-system				
TMS	26.6% Interstate	9.3% Other freeway	31.7% Principal arterial	32.4% Other
CONUS	4.0% Interstate	1.7% Other freeway	13.0% Principal arterial	81.3% Other
Distribution of pavement type				
TMS	29.6% Average	60.1% Asphalt	10.3% Concrete	
CONUS	66.7% Average	30.2% Asphalt	3.1% Concrete	

These results show that there is some bias towards urban traffic patterns because TMS locations are more common in urban locations than there are urban roads across CONUS. To reduce bias, more TMSs could be placed along rural roads. Similarly, TMS locations are much more heavily weighted towards interstates, freeways, and principal arterial roads than CONUS, and so smaller roads are underrepresented, as stations are often more interested in intercity travel rather than intracity travel. There are also some differences in pavement type distribution.

Other types of road data are numeric rather than categorical, such as the number of through lanes. Since VROOM uses a maximum number of only eight through lanes, this could still be summarized in table format. However, when moving to a variable with more possible values like the speed limit, a probability density plot can be used to show results more concisely. Therefore, comparisons for through lanes, speed limit, and logarithmic AADT are shown as probability densities in Figure 12.

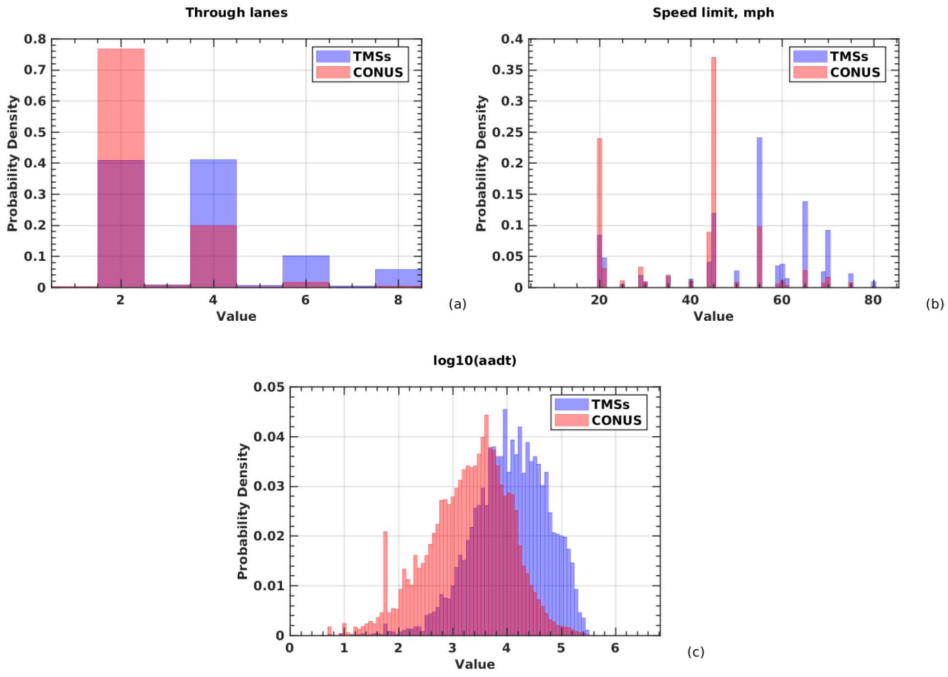

Figure 12. (Color online). Comparisons of the distributions of through lanes (a), speed limit (b), and logarithmic AADT (c) for TMS locations and all roads across CONUS. TMS locations are more heavily weighted towards a greater number of through lanes, higher speed limits, and higher AADT values than the CONUS distributions.

These distributions show that there is a bias towards a greater number of through lanes, higher speed limits, and higher AADT values. While not surprising, as TMS locations are more likely to be located where there is more traffic, this does show that VROOM could be improved, and uncertainty reduced, by obtaining hourly traffic volume for locations where there is less total traffic.

386 **B. Uncertainty based on DCs**

387 VROOM's traffic volume model uses DCs to predict the temporal variability of traffic volume
388 and is based on hourly counts taken at TMSs across CONUS. Therefore, in addition to comparing
389 road data distributions at TMS locations to CONUS, the DC distributions should be considered.
390 For maps of all DC values, see the appendix.

391 If certain DC values were not represented at TMS locations, then predictions for locations
392 with those diffusion coordinate values would have large uncertainty, as with road data. Fortunately,
393 despite being sparse in some geographic locations like South Carolina, TMS locations span the range
394 of, and have similar distributions to, the DC distributions across CONUS. Figure 13 shows the
395 distribution of the first DC value at TMS locations together with the distribution of the first DC
396 value at roads across CONUS. Distributions for the other DCs are similar and are given in the
397 appendix.

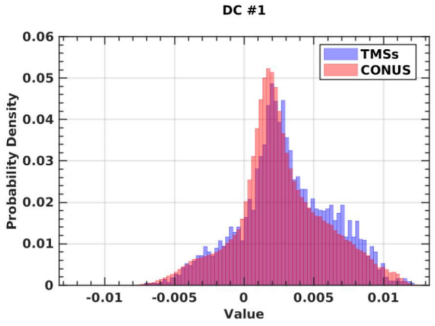

398

399 Figure 13. (Color online). A comparison of the distributions of the first diffusion coordinate at TMS
400 locations compared to across CONUS. The distributions show high agreement. A spatial map of the
401 first DC is shown in Figure 2, and maps for all DCs are shown in the appendix.

402

403 In addition to comparing distributions for individual DCs, an uncertainty measure for an
404 individual location in CONUS can be obtained by calculating the standard deviance, or the root-
405 mean-square distance, between that location's DC values and the DC distributions across TMS
406 locations. This is calculated mathematically for a location l by using the mean (μ_i) and standard
407 deviation (σ_i) of the DC values at all N traffic monitoring stations, with DC_i being the value of the
408 i^{th} diffusion coordinate, as:
409
410 $$\epsilon_l = \sqrt{\frac{1}{12}\sum_{i=1}^{12}\left(\frac{DC_{i,l}-\mu_i}{\sigma_i}\right)^2},\ \mu_i = \frac{1}{N}\sum_{s=1}^{N} DC_{i,s},\ \sigma_i = \sqrt{\frac{1}{N-1}\sum_{s=1}^{N}\left|DC_{i,s}-\mu_i\right|^2}. \quad (2)$$
411
412 The values of ϵ_l can be calculated for each road segment across CONUS, and values are
413 plotted geographically in Figure 14. The value is the RMS standard deviation, and so a value of 3
414 means that the DCs for that location are on average 3 standard deviations away from the
415 distribution of DC values represented at TMS locations. VROOM has lower uncertainty at locations
416 with a lower RMS standard deviation. While there is some moderate uncertainty at locations such as
417 southern Florida and northern Minnesota, RMS standard deviation values are generally relatively
418 low, which shows that VROOM is likely to have low uncertainty for most geographic locations
419 across CONUS.
420

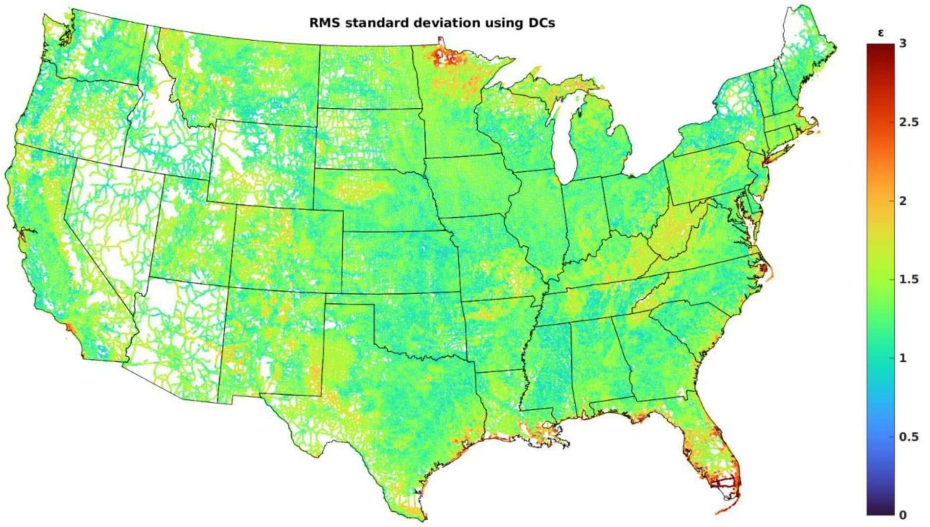

Figure 14. RMS standard deviation of the DCs for each location relative to the distribution across TMS locations are shown geographically. Most locations have small RMS standard deviations, with the most uncertainty seen in locations such as northern Minnesota and southern Florida.

C. Additional uncertainty

Additional uncertainty in VROOM can be caused not just by TMS locations relative to input data, but by uncertainty in the reported data. To mitigate this uncertainty, TMS locations with unreasonable data (e.g., traffic volume that showed strange shifts in reported values so that traffic volume was larger during nighttime hours at irregular intervals) were given a lower weight when creating VROOM coefficients. For more details, see Cook et al (2021).[11] Values for and distributions of VROOM coefficients are shown in the appendix along with the temporal patterns of VROOM components.

434 Other forms of uncertainty that are not included but could be considered are the locations at
435 which the Hallenbeck dynamic traffic class mix data were taken,[22] and uncertainty in the source
436 traffic noise emission equations in TNM 3.0.[13] Additionally, modern changes can also create
437 uncertainty. Accounting for the increase in numbers of electric vehicles and especially electric trucks
438 in recent years, could be made to improve reliability of predicted sound emission levels. Adding new
439 housing developments could change the diffusion coordinates for a location, which would also
440 change the VROOM predictions.
441 Further modifications could be made to account for changes in vehicle speed with traffic
442 volume, rather than just using reported or predicted speed limits. Road segments are also considered
443 separately, so treating locations as a network rather than individual points would improve reliability
444 of predictions. Adding other parameters beyond the road data and the geospatial data considered
445 could likewise improve reliability.
446

447 **VI. CONCLUSION**

448 The hourly-dynamic nature of traffic noise across CONUS can be predicted using VROOM.
449 The included traffic volume model was first shown in Cook et al. (2021),[11] and using geospatial and
450 road data, VROOM predicts total traffic volume with hourly resolution. Expected errors based on
451 total traffic volume were shown in Cook et al. (2023).[12] The traffic class mix model shown in this
452 paper expands upon previous results to include prediction of traffic volume by vehicle class, which
453 is necessary to account for differences in emitted sound spectra and levels produced by different

454 types of vehicles. Using TNM 3.0 equations, the traffic noise source model is used to predict traffic
455 noise source levels with hourly resolution.

456 Without a major nationwide validation study, either recording the traffic volume by class or
457 recording sound levels 50 feet/15 meters from roads, expected model errors cannot be obtained
458 directly. Instead, this paper shows locations of highest uncertainty, as related to geospatial and road
459 data bias in traffic monitoring stations. While not a fully robust way of calculating expected sound
460 level errors, the results illustrate how VROOM predicts temporal and spectral variability of traffic
461 noise with relatively low uncertainty for most locations. The VROOM-predicted sound levels should
462 not be seen as a fully comprehensive analysis of traffic noise predictions, but rather as a way to
463 account for temporal variability—and by using the TNM noise emission spectra equations, spectral
464 variability—of traffic noise near roads.

465 VROOM-predicted noise source levels give expected spectrally varying sound levels near
466 roads, and all VROOM predictions shown in this paper give results in the form of predicted source
467 noise levels, which are valid 50 feet/15 meters from roads. To create true sound maps, the emitted
468 spectral sound levels would need to be used as inputs in a traffic noise propagation model, and other
469 types of noise levels beyond an equivalent noise level, such as percentile exceedance levels, would
470 need to be considered. These are topics of future research.

471 While not without its limitations, VROOM is a powerful tool for predicting temporal and
472 spectral variability of traffic noise. Predictions are based on observed traffic volume across CONUS
473 and on TNM 3.0 traffic noise source emission equations. Expected errors, based on predicted and
474 observed traffic volume where available, are smaller than errors obtained using time-averaged traffic
475 volume, and model uncertainty is low for most locations. By accounting for the temporal variability

476 of traffic volume, VROOM is able to predict traffic noise, not just for an averaged time period, but
477 with hourly resolution.
478
479 **ACKNOWLEDGMENTS**
480 This work was supported by a U. S. Army Small Business Innovation Research contract to
481 Blue Ridge Research and Consulting, LLC, with Dr. James Stephenson as the technical monitor.
482

APPENDIX

This appendix includes additional figures, both spatial maps and distributions, which give a greater understanding of the underlying values used in VROOM. These figures include reported road data alongside VROOM road data, diffusion coordinate values, urbanization status, and VROOM components and coefficient values.

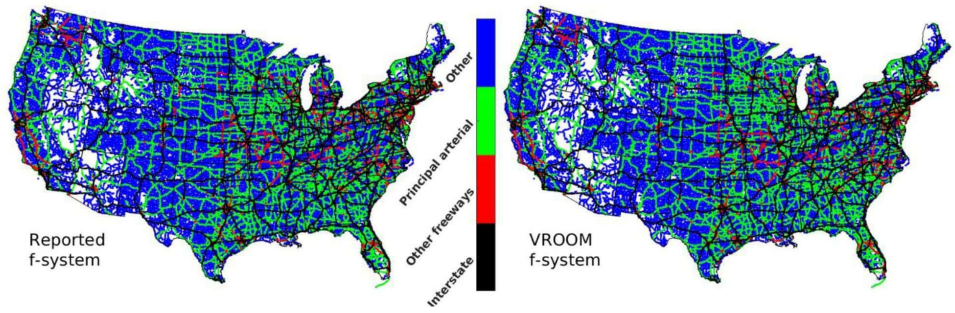

Figure 15. (Color online). Reported f-system values alongside f-system values used by VROOM.

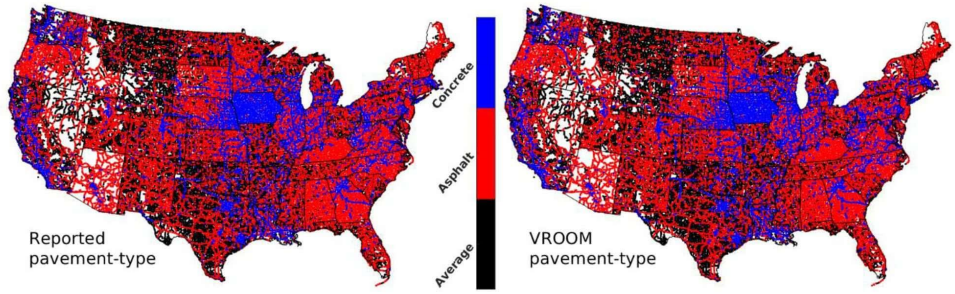

Figure 16. (Color online). Reported pavement type alongside pavement types used by VROOM.

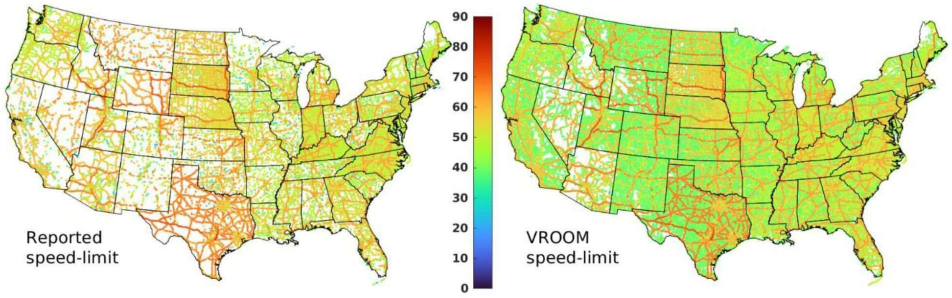

Figure 17. (Color online). Reported speed limit alongside speed limits used by VROOM.

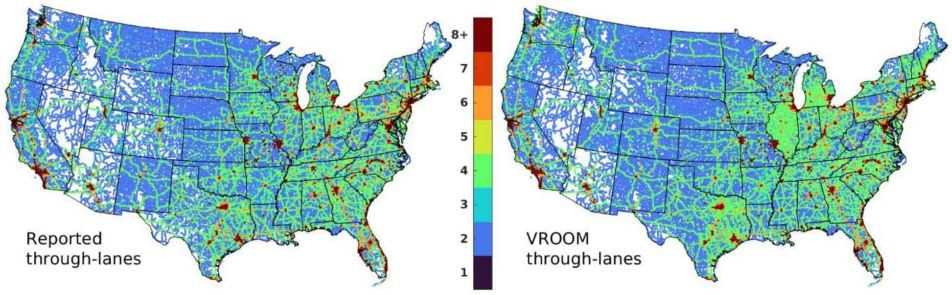

Figure 18. (Color online). Reported number of through lanes alongside number of through lanes used by VROOM.

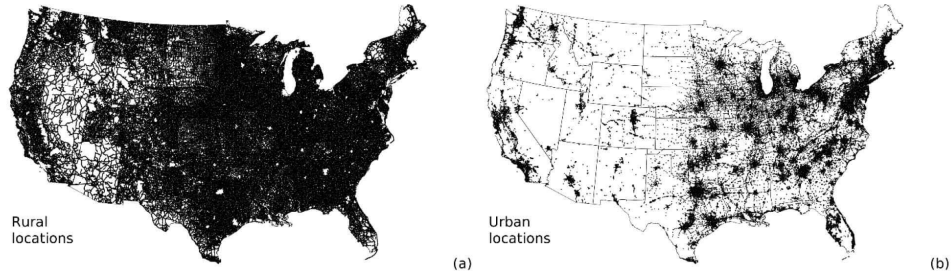

Figure 19. Road locations which are classified as rural (a) and urban (b). This comes from results of clustering analyses explained in Pedersen et al. (2021).[20]

500

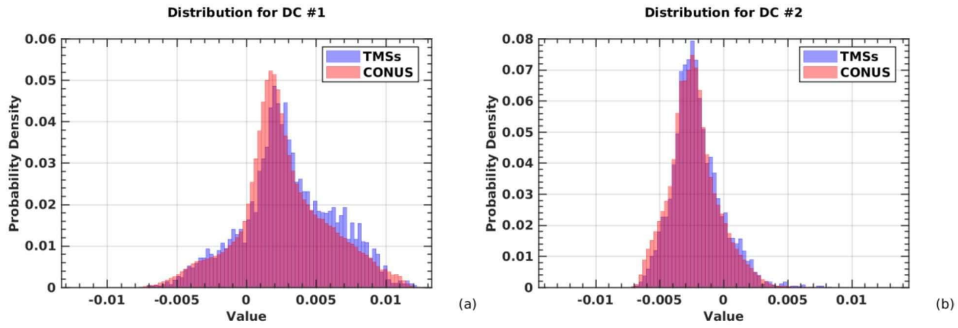

501

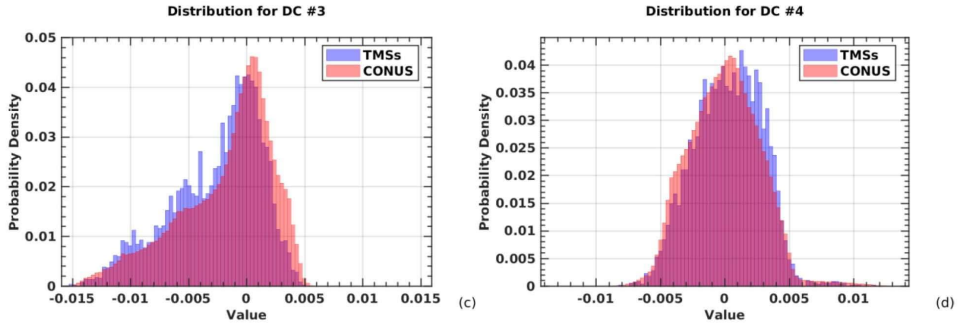

502

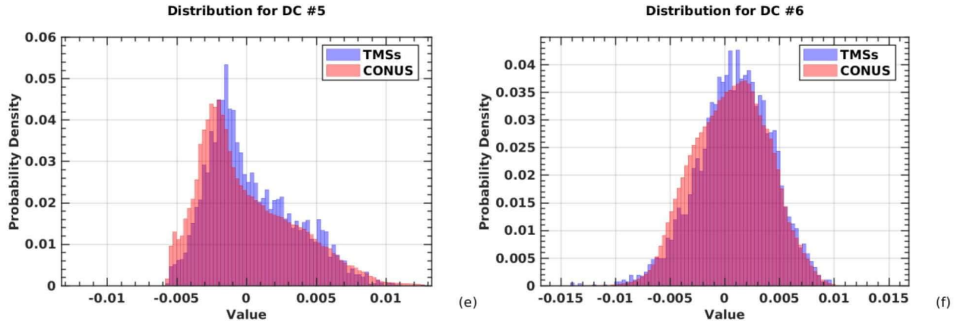

34

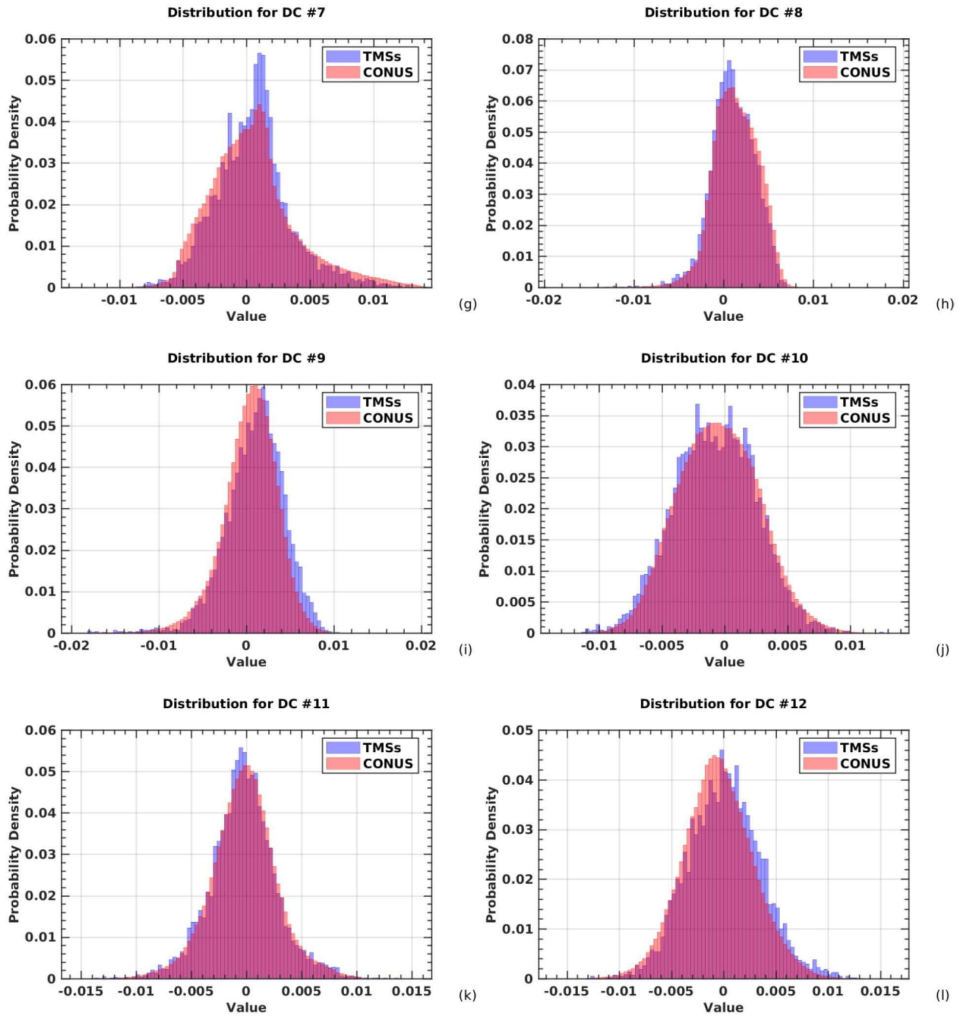

Figure 20. (Color online). Distributions of diffusion coordinates at TMS locations and across CONUS.

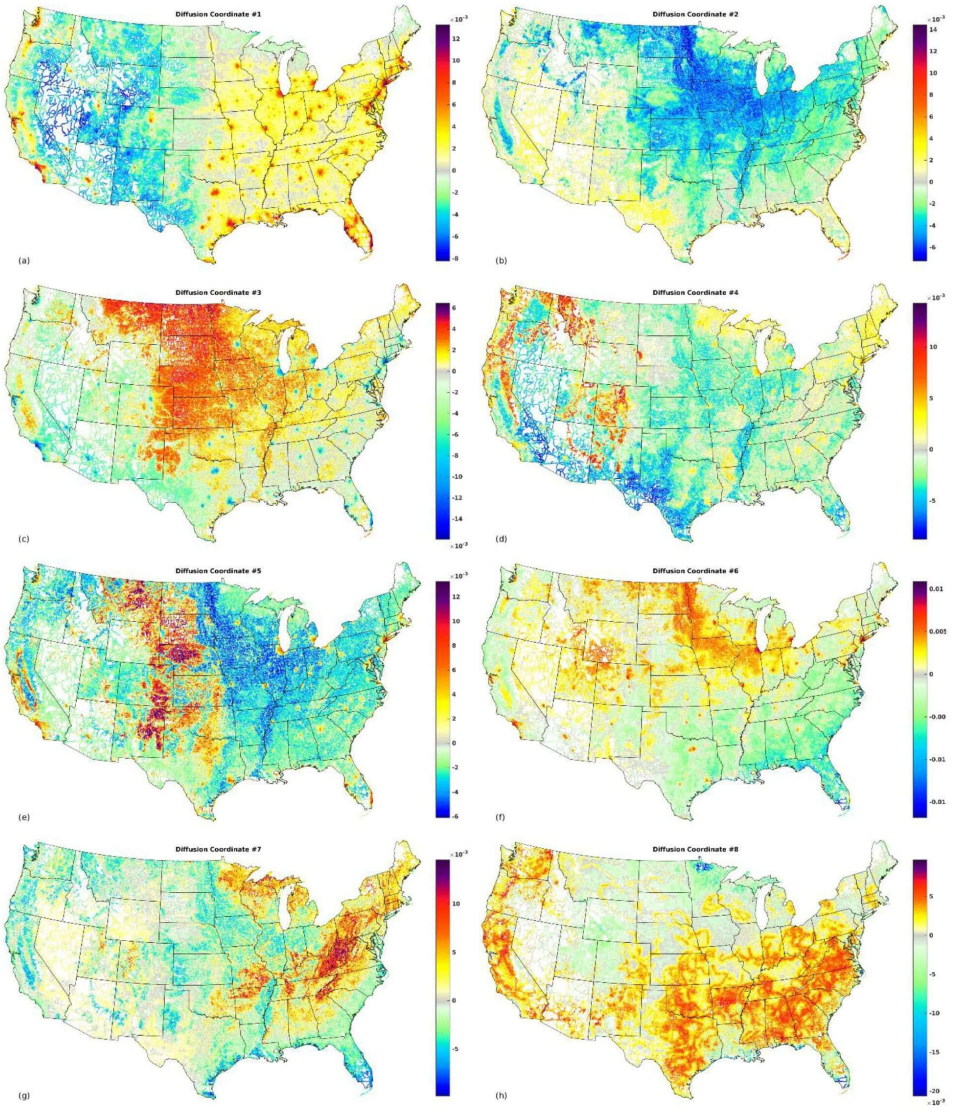

508

509

510

511

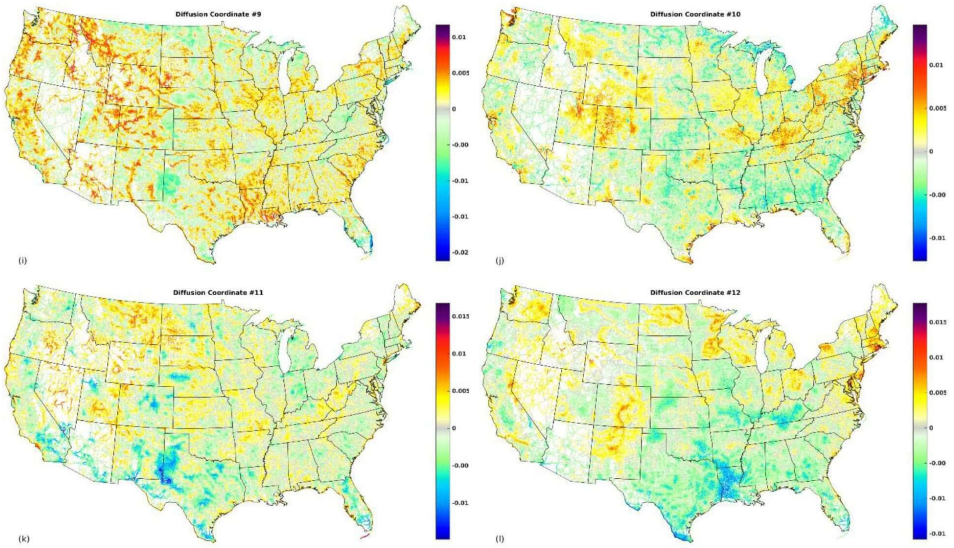

Figure 21. (Color online). Spatial maps of diffusion coordinate values across CONUS.

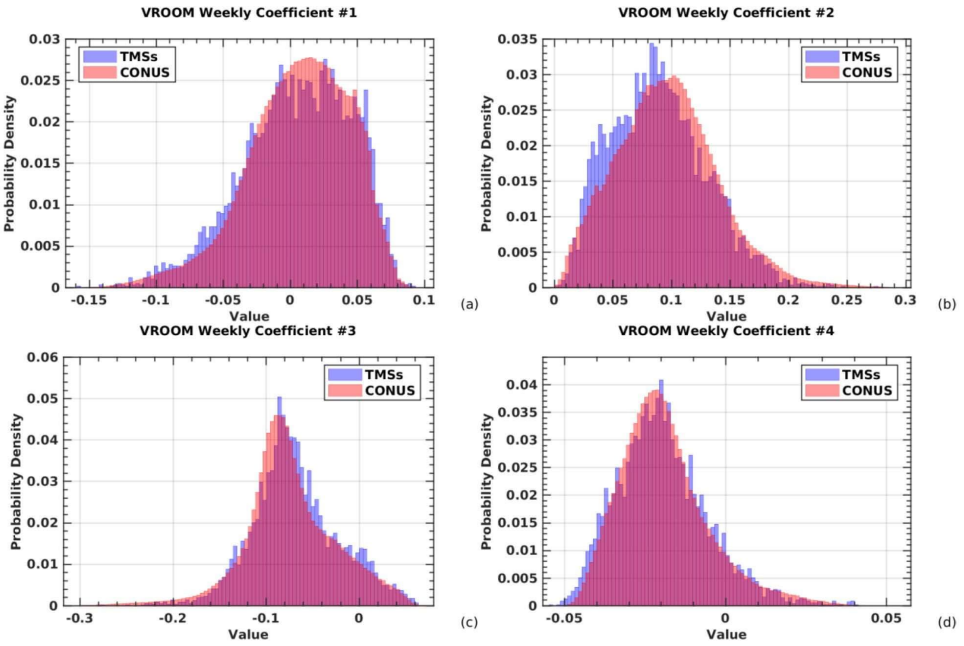

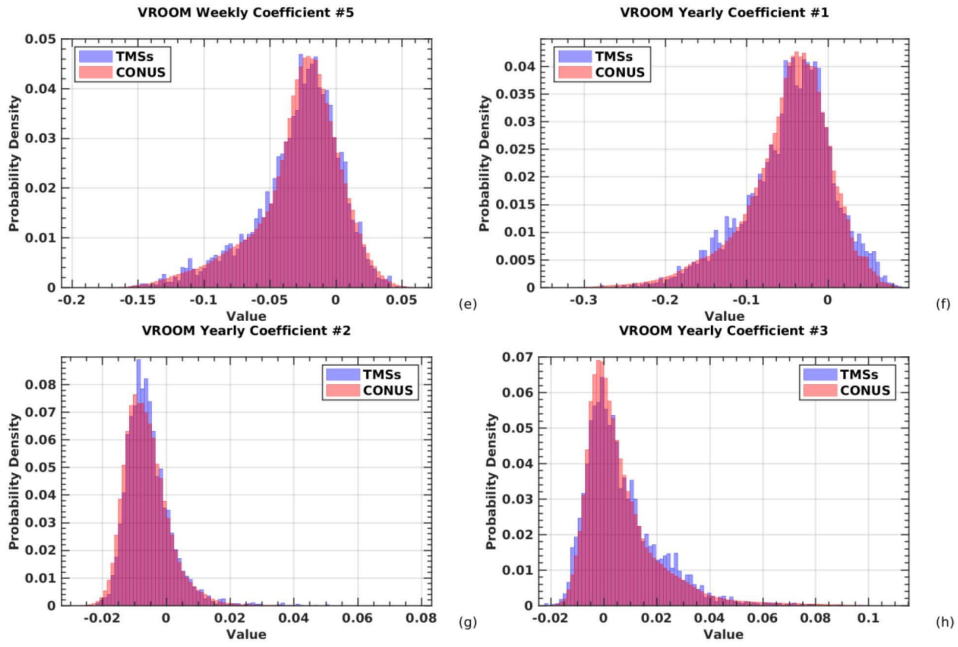

Figure 22. (Color online). Distributions of VROOM coefficient values at TMS locations and across CONUS.

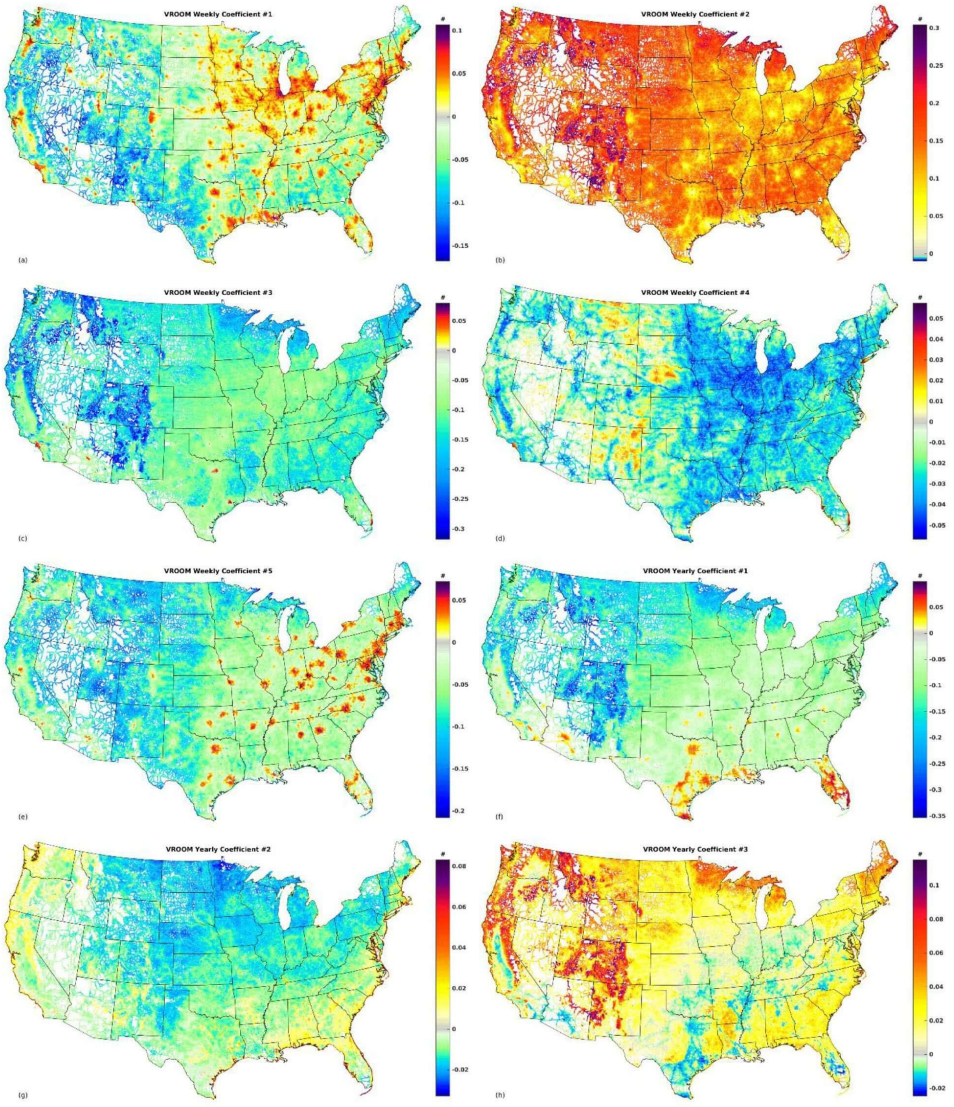

Figure 23. (Color online). Spatial maps of VROOM coefficients across CONUS.

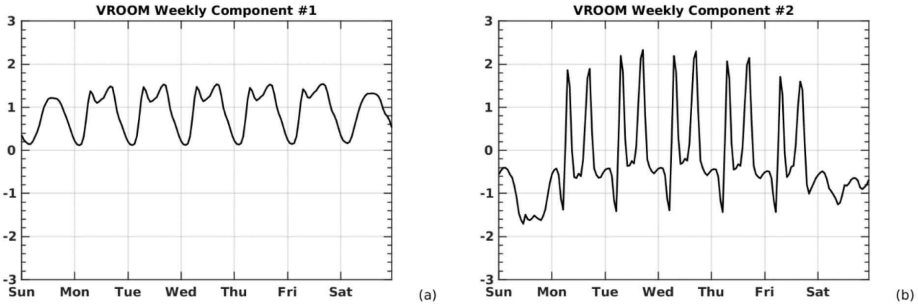
VROOM Weekly Component #1
VROOM Weekly Component #2
3
2
1
0
-1
-2
-3
Sun
Mon
Tue
Wed
Thu
Fri
Sat
(a)
(b)

526

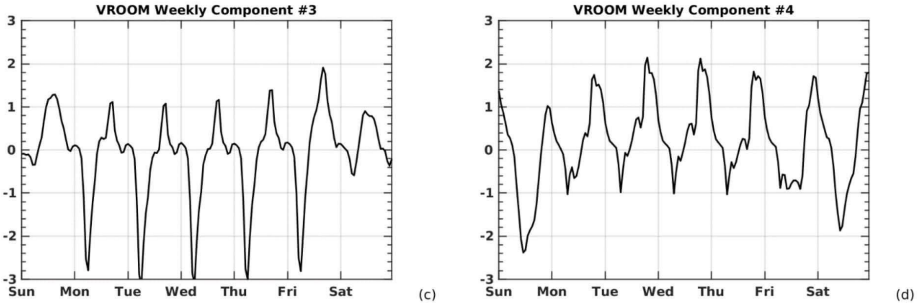
VROOM Weekly Component #3
VROOM Weekly Component #4
3
2
1
0
-1
-2
-3
Sun
Mon
Tue
Wed
Thu
Fri
Sat
(c)
(d)

527

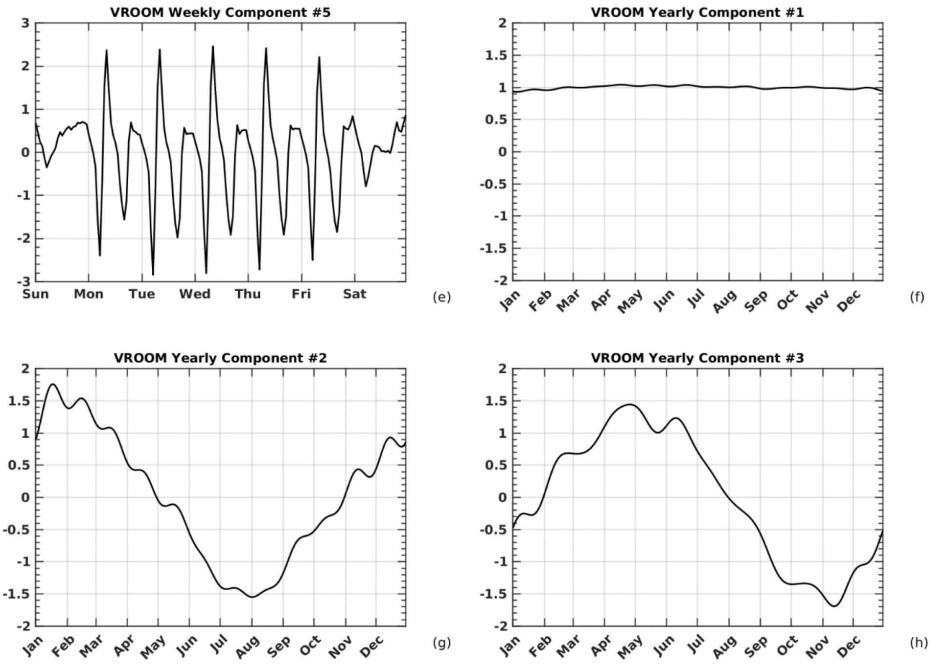

528

529

530 Figure 24. Temporal variability incorporated by VROOM components.

531

REFERENCES

[1] T. Hener, "Noise pollution and violent crime," Journal of Public Economics, Volume 215, November 2022, 104748. https://doi.org/10.1016/j.jpubeco.2022.104748.

[2] S. Stansfeld and C. Clark, "Health Effects of Noise Exposure on Children," Curr. Envir. Health Rpt **2**, 171-178 (2015). https://doi.org/10.1007/s40572-015-0044-1.

[3] H. Ising and B. Kruppa, "Health effects caused by noise: Evidence in the literature from the past 25 years," Noise and Health Vol 6. No 22, pp 5-13 (2004).

[4] E. Öhrström, A. Skånberg, H. Svensson, A. Gidlöf-Gunnarsson, "Effects of road traffic noise and the benefit of access to quietness," Journal of Sound and Vibration, Volume 295, Issues 1-2, August 2006, pp. 40-59.

[5] C. Chin, Z. Y. Thang, and S. Saju, "Study on impact of noise annoyance from highway traffic in Singapore City," Proc. Mtgs. Acoust. **39**, 015001 (2019); doi: 10.1121/2.0001116

[6] G. Shannon, L. M. Angeloni, G. Wittemyera, K. M. Fristrup, K. R. Crooks, "Road traffic noise modifies behaviour of a keystone species," Animal Behaviour, Volume 94, August 2014, pp. 135-141.

[7] K. M. Parris and A. Schneider, "Impacts of Traffic Noise and Traffic Volume on Birds of Roadside Habitats, Ecology and Society, Vol. 14, No. 1, June 2009.

[8] D. R. Johnson and E. G. Saunders, "The evaluation of noise from freely flowing road traffic," Journal of Sound and Vibration, Volume 7, Issue 2, March 1968, pp. 287-288, IN1, 289-309.

[9] S. K. Tang and K. K. Tong, "Estimating traffic noise for inclined roads with freely flowing traffic," Applied acoustics, Volume 65, Issue 2, February 2004, pp. 171-181.

[10] Information on the National Transportation Noise Map by the Bureau of Transportation Statistics available at https://www.bts.gov/geospatial/national-transportation-noise-map (accessed April 2023).

[11] M. R. Cook, K. L. Gee, M. K. Transtrum, S. V. Lympany, M. F. Calton, "Toward improving road traffic noise characterization: A reduced-order model for representing hourly traffic volume dynamics," Proc. Mtgs. Acoust. 45, 055001 (2021). https://doi.org/10.1121/2.0001636.

[12] M. R. Cook, K. L. Gee, M. K. Transtrum, and S. V. Lympany, "Toward a dynamic national transportation noise map: Modeling temporal variability of traffic volume," submitted for publication to J. Acoust. Soc. Am. (2023).

[13] ederal Highway Administration's Traffic Noise Model 3.0 Technical Manual, https://www.fhwa.dot.gov/environment/noise/traffic_noise_model/old_versions/tnm_v30/tnm3_tech_manual.cfm (accessed May 2023).

[14] J. R. Kenworth, P. W. G. Newman, and T. J. Lyons, "Urban Planning and Traffic Congestion," Urban Policy and Research Vol. 7, (1989). https://doi.org/10.1080/08111148908551389.

[15] G. Carlier and F. Santambrogio, "A variational model for urban planning with traffic congestion," ESAIM: COCV, Vol. 11, No. 4, pp. 595-613 (2005). https://doi.org/10.1051/cocv:2005022.

[16] R. Fullenbaum and G. Christopher, "Freight Analysis Framework Inter-Regional Commodity Flow Forecast Study: Final Forecast Results Report," IHS Global Incorporated (2016). http://www.ops.fhwa.dot.gov/publications/fhwahop16043/fhwahop16043.pdf.

[17] C. H. Yang, A. C. Regan, and Y. T. Son, "Another view of freight forecasting modeling trends," KSCE Journal of Civil Engineering, **14**, 237-242 (2010).

[18] J. H. K. Boerkamps, A. J. van Binsbergen, and P. H. L. Bovy, "Modeling behavioral aspects of urban freight movement in supply chains." Transportation Research Record: Journal of the Transportation Research Board, No. 1725, Transportation Research Board of the National Academies, Washington, D.C., pp. 17–25 (2000).

[19] P. Patil, "Sustainable Transportation Planning: Strategies for Reducing Greenhouse Gas Emissions in Urban Areas," Empirical Quests for Management Essences IT, Vol 1. No. 1 (2021).

[20] K. Pedersen, M. K. Transtrum, K. L Gee, S. V. Lympany, M. M. James, and A. R. Salton, "Validating two geospatial models of continental-scale environmental sound levels," JASA Express Lett 1, 122401 (2021). https://doi.org/10.1121/10.0007368.

[21] C. R. Stanley, "Descriptive statistics for N-dimensional closed arrays: A spherical coordinate approach," Math Geol 22, 933–956 (1990). https://doi.org/10.1007/BF00890118.

[22] M. Hallenbeck, M. Rice, B. Smith,. C. Cornell-Martinez, J. Wilkinson, "Vehicle Volume Distributions by Classifications," United States Federal Highway Administration (1997). https://rosap.ntl.bts.gov/view/dot/48834.

Chapter 7

An app for nationwide dynamic traffic noise prediction

7.1 Introduction

This article describes the VROOM (Vehicular Reduced-Order Observation-based Model) app, which was developed using the techniques and models described in Chapter 4, Chapter 5, and Chapter 6. The app allows for real-time prediction of traffic noise and utilizes user inputs to predict traffic noise with the spatial, spectral, and temporal resolution desired. It was accepted for the INTER-NOISE and NOISE-CON Congress and Conference Proceedings, with the publication forthcoming.

7.2 Required Copyright Notice

The following is the author-submitted version of an article for the INTER-NOISE and NOISE-CON Congress and Conference Proceedings, entitled “An app for nationwide dynamic traffic noise prediction”. It is reproduced in its original author-submitted format here by rights granted in https://www.ieee.org/publications/rights/#author-posting-policy.

I hereby confirm that the use of this article is compliant with all publishing agreements.

7.3 Accepted Article

An app for nationwide dynamic traffic noise prediction

Mylan R. Cook[1], Kent L. Gee[2], Mark K. Transtrum[3]
Brigham Young University
N283 ESC, Provo, UT 84602

Shane V. Lympany[4]
Blue Ridge Research and Consulting, LLC
29 N Market St #700, Asheville, NC 28801

ABSTRACT

Despite being so pervasive, road traffic noise can be difficult to model and predict on a national scale. Detailed road traffic noise predictions can be made on small geographic scales using the US Federal Highway Administration's Traffic Noise Model (TNM), but TNM becomes infeasible for the typical user on a nationwide scale because of the complexity and computational cost. Incorporating temporal and spectral variability also greatly increases complexity. To address this challenge, physics-based models are made using reported hourly traffic counts at locations across the country together with published traffic trends. Using these models together with TNM equations for spectral source emissions, a streamlined app has been created to efficiently predict traffic noise at roads across the nation with temporal and spectral variability. This app, which presently requires less than 700 MB of stored geospatial data and models, incorporates user inputs such as location, time period, and frequency, and gives predicted spectral levels within seconds.

1. INTRODUCTION

Noise from road traffic contributes heavily to ambient noise levels in urban and even rural areas. Increased noise levels are correlated with anything from mild annoyance to an increase in violent crime.[1] Noise can also negatively impact other species.[2-5] Characterizing road traffic noise levels is therefore important for anything from urban planning to species conservation and human wellbeing.

Despite being so pervasive, even when they are known or predicted, road traffic noise levels on a national scale are reported only for large-period average time scales, such as a yearly averaged 24-hr LAeq (A-weighted equivalent overall sound pressure level), like in the National Transportation Noise Map.[8] Noise levels and spectra vary with traffic volume and traffic class composition, as well as with other factors such as vehicle speed, pavement type, road inclination, and land cover.[6,7] Temporal changes can be drastic, particularly from daytime to nighttime, though also by day of week and time of year.

[1] mylan.cook@gmail.com
[2] kentgee@byu.edu
[3] mktranstrum@byu.edu
[4] shane.lympany@blueridgeresearch.com

Using hourly traffic counts across the continental United States (CONUS) together with reported temporal variation of traffic classes, the Vehicular Reduced-Order Observation-based Model, or VROOM, has been developed to predict hourly-varying spectral source road traffic noise.[9-10] VROOM uses a concise set of location-specific features and developed models to allow for fast and efficient prediction of source noise levels for roads across CONUS. The VROOM app enables user inputs such as specific location, time period, and frequency, and can calculate and geographically plot source noise emissions within seconds.

2. PREDICTING TRAFFIC WITH VROOM

To predict temporally varying traffic noise, temporally varying traffic volume must be predicted. Additionally, the traffic class mix must also be predicted, as different types of vehicles can produce very different spectral sounds. VROOM predicts total hourly traffic volume using reported hourly vehicle counts from thousands of traffic monitoring stations across CONUS, and hourly traffic class mix is predicted using published traffic class mix characteristics. Traffic noise emissions are then calculated using TNM source noise emission equations for each vehicle class.

2.1. Predicting hourly traffic volume

The Federal Highway Administration tabulates reported hourly vehicle counts from thousands of traffic monitoring stations across CONUS. Using data from 2015-2018, Fourier analysis was used to find weekly and yearly patterns.[11] Principal component analysis was then used on the denoised Fourier spectra. This resulted in a simplified representation for traffic volume dynamics at traffic monitoring stations, which includes a set of traffic volume representative coefficients and principal component vectors. For further details, see "Toward improving road traffic noise characterization: A reduced-order model for representing hourly traffic volume dynamics" by Cook et. al.[12]

To enable prediction of traffic volume at other locations, regression was used to find a transformation from location-specific values to coefficients. The location-specific features include 12 diffusion coordinates,[13] urban or rural designation, and road features such as road classification (interstate, principal arterial, etc.), through lanes, speed limit, and the annual average daily traffic (AADT). The resulting predictive traffic volume model, which is the first part of VROOM, uses location-specific features to predict coefficients, and therefore traffic volume, anywhere across CONUS.

2.2. Predicting hourly traffic volume of each traffic class

Like average annual sound levels, average annual traffic class mix is known for many locations across CONUS. However, where the class mix is unknown, it must be predicted. This is done using regression with the same location-specific features as are used to predict traffic volume representative coefficients. Due to physical constraints, there is some additional nuance. Each traffic class mix percentage must be between 0% and 100%, and the sum of each class mix percentage must equal 100%. One way to ensure this is by using angular coordinates. This approach is generalizable to any number of traffic classes, though most often three traffic classes—vehicles, medium trucks, and heavy trucks—are used.

Regression on the angular coordinates where traffic class mix is known yields a transformation from location-specific features to angular traffic class mix. This enables VROOM to predict traffic class anywhere using location-specific features, much the same as VROOM predicts traffic volume dynamics by predicting traffic volume representative coefficients.

Average annual class mix is necessary to determine traffic noise characteristics, but, as with traffic volume, traffic class mix varies temporally. Traffic class mix is not reported with temporal variation at thousands of traffic monitoring stations, and so published trends of national temporal variability of traffic classes from a Federal Highway Administration report by Hallenbeck, et al. are used.[14]

Average temporal variability of individual traffic classes is reported for different types of road designations (such as freeways or local roads) in either urban or rural locations across hours of the day, days of the week, and months of the year. By combining and normalizing the temporal variation, temporal multipliers for the traffic class mix are obtained.

VROOM predicts the total number of vehicles of a particular traffic class for any particular hour by multiplying the following values:

- The annual average total hourly traffic volume (AADT/24)
- The predicted normalized hourly traffic volume
- The average traffic class mix percentage
- The predicted hourly traffic class mix percentage

The product is calculated for each traffic class individually and gives the predicted number of vehicles of that class type. With the number of vehicles of each class type, the noise emissions for each class can be calculated.

2.3. Calculating noise emissions

For a known number of vehicles of a particular vehicle class type, the spectral noise emissions are calculated using equations from the Traffic Noise Model (TNM). These equations give the noise emissions at 50 feet from the road at a height of 5 feet based on traffic class numbers, pavement type, and vehicle speed. These equations can be found in Appendix A of the TNM Technical Manual.[15]

For any time period greater than one hour, average hourly noise emissions are calculated by averaging the relevant hourly VROOM-predicted vehicle numbers. The TNM equations are then used on the average numbers of vehicles of each class type, which results in the predicted spectral levels for the desired time period. Figure 1 shows the predicted 1-hr LAeq for a fully averaged time period, without regard for the time of day, day of week, or time of the year. This can be compared to TNM-predicted average sound levels and the National Transportation Noise Map's sound levels 50 feet from each road.

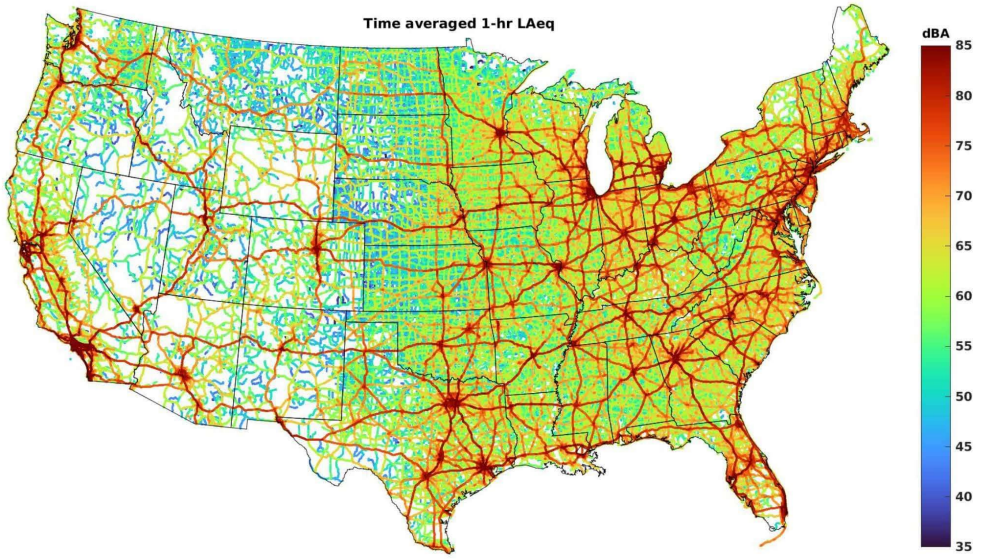

Figure 1. Temporally averaged VROOM-predicted A-weighted 1-hr LAeq.

The average sound levels, while important to know, are given in the National Transportation Noise Map. The utility of VROOM is that it can predict not just time-averaged levels, but levels for any time period and frequency of interest, down to hourly time scales. This is important because sound levels can change drastically across the course of a single day. Predictions for two different time periods are shown in Figure 2 and in Figure 3. Differences of a few decibels are hard to see with a large range, like the 70 dBA range used in Figure 1, and so the figures show not overall levels, but differences from the average sound levels shown in Figure 1. Across the country, sound levels are much lower than average during nighttime hours on weekdays in December, and for many locations sound levels are higher on weekend afternoons in July.

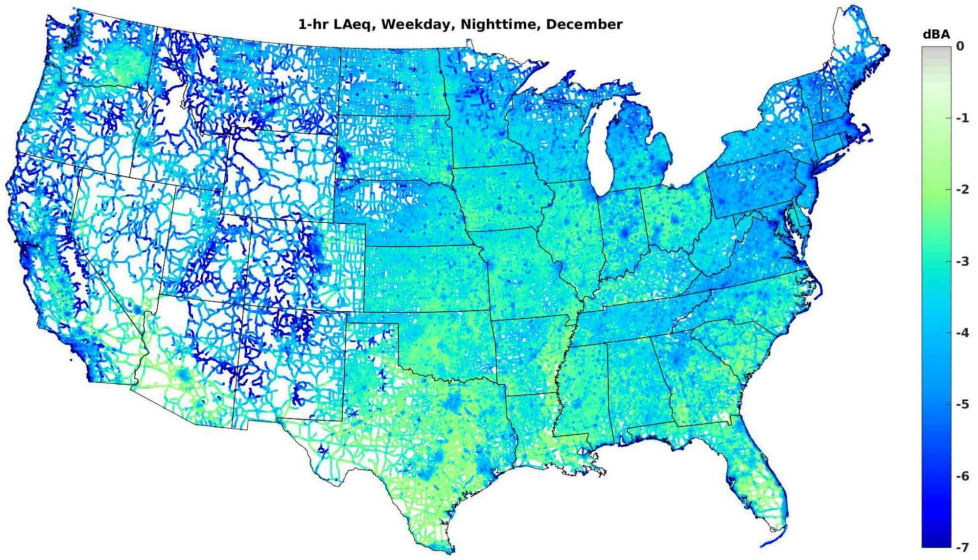

Figure 2. 1-hr LAeq for an average weekday nighttime in December, relative to the average sound level.

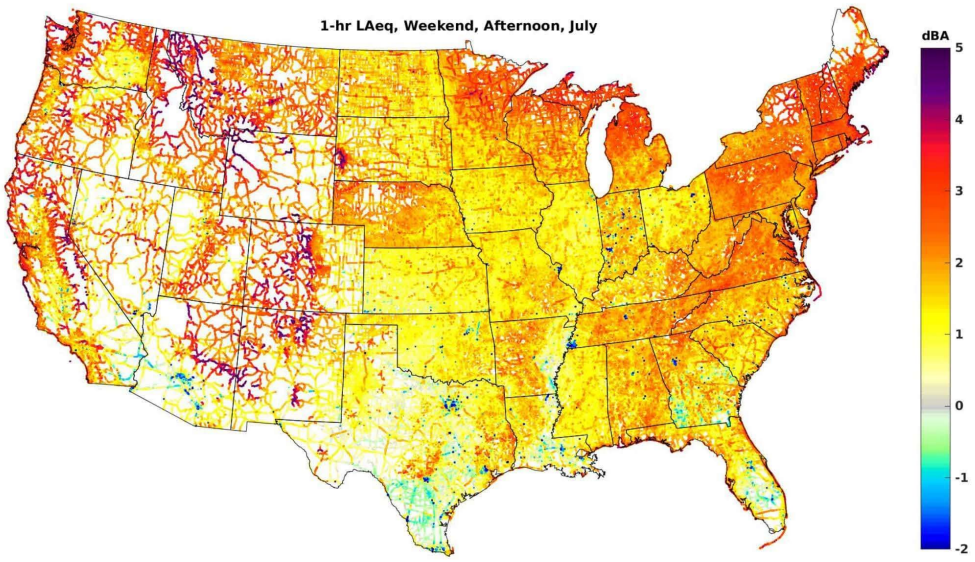

Figure 3. 1-hr LAeq for an average weekend afternoon in July, relative to the average sound level.

3. THE VROOM APP

VROOM can predict hourly sound emissions for roads across the country in a computationally simple manner. By using about 18 features for each location of interest, a few matrix and linear multiplications and additions yield the predicted hourly source noise emissions. While computer RAM and memory can limit the number of parallel computations for millions of road locations—and especially the number of locations for which results can be plotted—using VROOM to calculate and plot results for even state-wide scales can be done in a relatively short amount of time for even a simple laptop computer.

The VROOM app was developed using the methods described in this paper to allow calculation and plotting of source road traffic noise using user inputs. The models consist of a few streamlined codes, and the ~18 location-specific features for millions of locations across CONUS can be stored using less than 700 MB of memory. Thus, predicted sound characteristics for geographic areas as large as individual states can be shown using a simple computer.

The VROOM app performs calculations and plots results in real time. Because of the speed of calculation, user inputs can be utilized. Figure 4 shows a snapshot of the user interface for the VROOM app, together with the predicted sound levels in Grand Rapids, Michigan at 5:00 pm on a spring weekday. Users can input the location by state, county, and city, or by latitude and longitude. When a state is selected, the county options are updated automatically. Likewise, the cities options are updated when the county is selected. Alternatively, the user can select latitude and longitude limits, which are automatically updated when states, counties, or cities are selected.

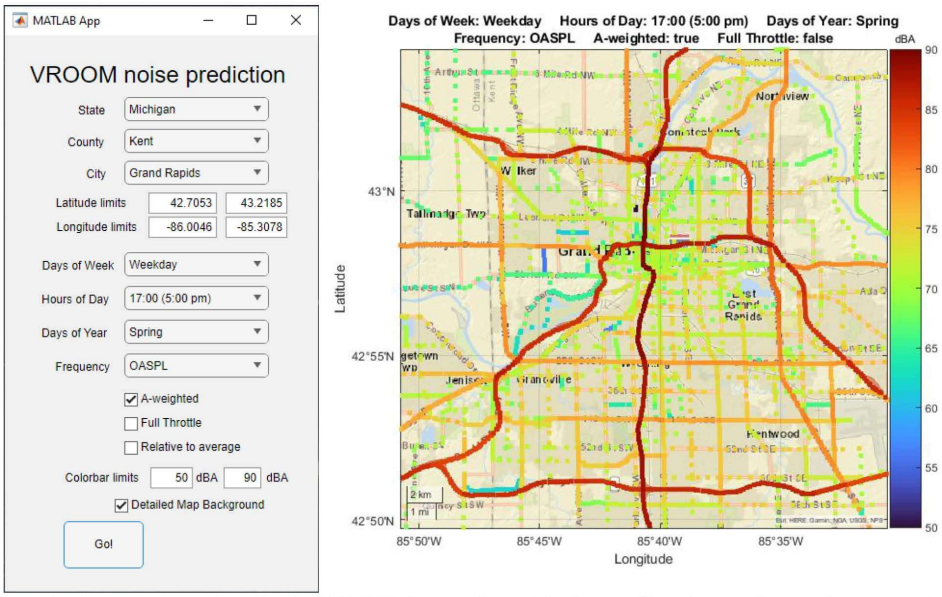

Figure 4. The user interface for the VROOM app, alongside the predicted overall sound pressure level for roads near Grand Rapids, Michigan on a spring weekday at 5:00 pm.

Users can also input the desired time period, which can be as specific as a particular hour of the day, day of the week, and month or season of the year. Individual one-third octave band frequencies or overall sound pressure levels can likewise be selected, along with flat or A-weighted levels. Additional inputs, such as vehicle throttle—which indicates whether or not vehicles are accelerating—and additional mapping preferences are also incorporated.

The VROOM app is a powerful tool that allows users to predict source traffic noise emissions quickly and efficiently for roads across CONUS. The versatility and simplicity for the user make this app useful for a variety of applications.

4. CONCLUSIONS

The VROOM app allows users to input parameters such as location, time period, and frequency, and predicts and plots predicted traffic noise along roads throughout the country. The app uses a concise set of location-specific features and physics-guided, observation-based models totaling less than 700 MB to efficiently predict traffic noise for the user-defined inputs.

While predicted average sound levels agree with national average levels, and the models used were made with reported vehicle numbers and traffic class mix, noise emission error validations have yet to be performed. Improvements to the VROOM app, such as incorporating minor roads and reducing overhead computation and memory storage, are being made. Work is also being done to propagate source noise levels to surrounding areas, as well as to predict noise characteristics such as median or percentile-based noise emissions in addition to equivalent sound levels.

While standard national traffic noise levels are only given for average time scales, the VROOM app can predict noise levels with hourly resolution, and can do so in real time. With a simple user interface, desired temporal and spectral characteristics can be highlighted. VROOM is a powerful tool for predicting traffic noise across the country.

ACKNOWLEDGEMENTS

Development of traffic noise predictive models was supported in part by a U. S. Army Small Business Innovation Research contract to Blue Ridge Research and Consulting, LLC, with Dr. James Stephenson as the technical monitor. Development of the VROOM app described in this paper was supported by the Department of Physics and Astronomy at Brigham Young University.

REFERENCES

1. T. Hener, "Noise pollution and violent crime," Journal of Public Economics, Volume 215, November 2022, 104748. https://doi.org/10.1016/j.jpubeco.2022.104748.
2. E. Öhrström, A. Skånberg, H. Svensson, A. Gidlöf-Gunnarsson, "Effects of road traffic noise and the benefit of access to quietness," Journal of Sound and Vibration, Volume 295, Issues 1-2, August 2006, pp. 40-59.
3. C. Chin, Z. Y. Thang, and S. Saju, "Study on impact of noise annoyance from highway traffic in Singapore City," Proc. Mtgs. Acoust. 39, 015001 (2019); doi: 10.1121/2.0001116.
4. G. Shannon, L. M. Angeloni, G. Wittemyera, K. M. Fristrup, K. R. Crooks, "Road traffic noise modifies behaviour of a keystone species," Animal Behaviour, Volume 94, August 2014, pp. 135-141.
5. K. M. Parris and A. Schneider, "Impacts of Traffic Noise and Traffic Volume on Birds of Roadside Habitats, Ecology and Society, Vol. 14, No. 1, June 2009.
6. D. R. Johnson and E. G. Saunders, "The evaluation of noise from freely flowing road traffic," Journal of Sound and Vibration, Volume 7, Issue 2, March 1968, pp. 287-288, IN1, 289-309.
7. S. K. Tang and K. K. Tong, "Estimating traffic noise for inclined roads with freely flowing traffic," Applied acoustics, Volume 65, Issue 2, February 2004, pp. 171-181.
8. National Transportation Noise Map by the Bureau of Transportation Statistics, https://www.bts.gov/geospatial/national-transportation-noise-map, accessed January 2021.
9. A. D. May, "Traffic Flow Fundamentals," Prentice-Hall Incorporated, 1990.
10. F. Kessels, "Introduction to Traffic Flow Modelling," Springer Link, 2018.
11. D. S. Dendrinos, "Urban Traffic Flows and Fourier Transforms," Geographical analysis, Volume 26, Issue 3, July 1994, pp. 261-281.
12. M. R. Cook, K. L. Gee, M. K. Transtrum, S. V. Lympany, and M. F. Calton, "Toward improving croad traffic noise characterization: A reduced-order model for representing hourly traffic volume dynamics," Proc. Mtgs. Acoust. **45**, 055001 (2021); https://doi.org/10.1121/2.0001636.
13. K. L. Pedersen, "Using Machine Learning to Accurately Predict Ambient Soundscapes from Limited Data Sets," BYU Theses and Dissertations, 2018.
14. M. E. Hallenbeck, M. Rice, B. Smith, C. Cornell-Martinez, J. Wilkinson, "Vehicle Volume Distributions by Classification," FHWA-PL-97-025, (1997); https://rosap.ntl.bts.gov/view/dot/48834.
15. Federal Highway Administration's Traffic Noise Model, Version 1.0 – Technical Manual, Appendix A Vehicle Noise Emissions, accessed March 2023, https://www.fhwa.dot.gov/environment/noise/traffic_noise_model/old_versions/tnm_version_10/tech_manual/tnm03.cfm#tnma31.

Chapter 8

Conclusions

Physics-guided approaches for modeling spatio-spectro-temporal data allow for more accurate characterization of acoustic environments. By ensuring that spatial, spectral, and temporal relationships are maintained, models are able to not just represent the data, but are better able to give physically meaningful predictions. By using physics-guided approaches, wind noise can be automatically detected and reduced, and both traffic volume and traffic noise are better characterized and predicted on a nationwide scale.

Much of the research performed for this dissertation was done in collaboration with Blue Ridge Research and Consulting, LLC, under a U.S. Army SBIR. Results have been instrumental in furthering characterizing outdoor acoustic environments on a nationwide scale. This research has applications in many areas, including human health and wellness, bioacoustics, wildlife conservation, urban and roadway planning, land development and conservation, noise ordinance legislation, homebuying, and more.

While limitations of the different models were considered in the papers, a few additional notes should be made. With regard to the wind noise classification and reduction method, the classifier can fail for high wind speeds. This is because only above the crossover frequency does the characteristic slope of wind noise approach -26.7 dB per decade. Additional improvements could be made by searching not just for this slope, but by also searching for the crossover frequency itself. This could be further improved by explicitly accounting for the temporal variability of wind

speed. Each time interval was treated independently in the classifier, rather than accounting for spectra that were temporally adjacent.

For VROOM, the Vehicular Reduced-Order Observation-based Model, the major limitation is the lack of experimental validation. Analyses were performed to quantify the uncertainty of the model, though this is not a substitute for experimental validation. Because source traffic noise levels cannot be measured directly, it is necessary to account for sound propagation (as well as for barriers and other obstructions near roadways) to compare model predictions with acoustic measurements. A detailed comparison with measured acoustic data is necessary to validate the VROOM predictions and remains a topic of further research.

Of particular note, as implied by the title of and the paper presented in Chapter 7, an app for nationwide dynamic traffic noise prediction has been developed utilizing VROOM. Since the submission of the article, improvements have been made, and many additional road segments have been included. The app is now approximately 1.5 GB and is being tested for errors. Efforts are being made to develop this app for commercial use, and applications of the methods and models developed are being considered for other private and commercial applications.

VROOM should not be considered as the epitome of traffic noise prediction, but rather as a tool to improve understanding of the temporal variability of road traffic noise. Further improvements, particularly in treating road segments as a network rather than independent points, could improve reliability and accuracy of road traffic noise predictions.

The research and the models presented herein outline some of the present limitations when dealing with limited data, as well as the advantages of using a physics-guided modeling approach. While predictions may or may not be proven correct in future, these models are tools for increasing understanding of some of the most prevalent sources of noise in this present-day world. This

research can be used to assist others in understanding the usefulness of physics-guided modeling of acoustic environments using limited spatio-spectro-temporal data.